2014

SYNTHESIS AND EVALUATION OF AMPHIPHILIC PEPTIDES AS NANOSTRUCTURES AND DRUG DELIVERY TOOLS

Naser Ali Sayeh
University of Rhode Island, nsaeh@yahoo.co.uk

SYNTHESIS AND EVALUATION OF AMPHIPHILIC PEPTIDES AS NANOSTRUCTURES AND DRUG DELIVERY TOOLS

BY

NASER ALI SAYEH

A DISSERTATION SUBMITTED IN PARTIAL FULFILLMENT OF THE

REQUIREMENTS FOR THE DEGREE OF

DOCTOR OF PHILOSOPHY

IN

PHARMACEUTICAL SCIENCES

UNIVERSITY OF RHODE ISLAND

2014

DOCTOR OF PHILOSOPHY DISSERTATION

OF

NASER ALI SAYEH

APPROVED:

Thesis Committee:

Major Professor Keykavous Parang

David.Rowley

Nasser H. Zawia

Aftab Ahmed

Geoffrey Bothun

Nasser H. Zawia

DEAN OF THE GRADUATE SCHOOL

UNIVERSITY OF RHODE ISLAND

2014

ABSTRACT

Intracellular delivery of cell-impermeable compounds in a variety cells using delivery systems have been extensively studied in recent years. Obtaining desirable cellular uptake levels often requires the administration of high quantities of drugs to achieve the expected intracellular biological effect. Thus, improving the translocation process across the plasma membrane will significantly reduce the quantity of required administered drug and consequently minimize the side effects in most of the cases. Efficient delivery of these molecules to the cells and tissues is a difficult challenge. Compounds with low cellular permeability are commonly considered to be of limited therapeutic value. Over the past few decades, several biomedical carriers, such as polymers, nanospheres, nanocapsules, liposomes, micelles, peptides and dendrimers have been widely used to deliver therapeutic and diagnostic agents to the cells. Biomaterials generated from nano-scale compounds have shown some promising data for delivery of many compounds in a number of diseases, such as viral infections, cancer, and genetic disorders. Although much progress has been achieved in this field, many challenges still remain, such as toxicity and limited stability.

Liposomes suffer from poor stability in the bloodstream and leakage during storage. They tend to aggregate and fuse with or leak entrapped drugs, especially highly hydrophilic small molecules. For **solid lipid nanoparticles (SLNs)**, drug expulsion after polymorphic transition during storage, inadequate loading capacity, and relatively high water content of the dispersions have been observed.

Poly lactic-co-glycolic acid (PLGA) degrades in the body producing its original monomers of lactic acid and glycolic acid, which are the by-products of various metabolic pathways. However, this acidic microenvironment that occurs during degradation could negatively affect the stability of the loaded compound. **Dendrimers** can carry drugs as complexes or as conjugates although one limitation lies in the effort of controlling the rate of drug release. The encapsulated or complexed drugs tend to be released rapidly (before reaching the target site) and in the dendrimer–drug conjugates, it is the chemical linkage that controls the drug release. Thus, future studies in this field are urgently required to create more efficient and stable biomaterials.

Peptides are considered as efficient vectors for achieving optimal cellular uptake. The potential use of peptides as drug delivery vectors received much attention by the discovery of several cell-penetrating peptides (CPPs). The first CPPs, discovered in 1988, were sequences from HIV-1 encoded TAT protein, TAT (48–60), and penetrated very efficiently through cell membranes of cultured mammalian cells. CPPs are a class of diverse peptides, typically with 8–25 amino acids, and unlike most peptides, they can cross the cellular membrane with more efficiency. CPPs have also shown to undergo self-assembly and generate nanostructures. The generation of self-assembled peptides and nanostructures occur through various types of interactions between functional groups of amino acid residues, such as electrostatic, hydrophobic, and hydrogen bonding. Appropriate design and functionalization of peptides are critical for generating nanostructures.

Chemically CPPs are classified into two major groups: linear and cyclic peptides. It has been previously reported that linear peptides containing hydrophilic and hydrophobic amino acids could act as membrane protein stabilizers. These compounds are short hydrophilic or amphiphilic peptides that have positively charged amino acids, such as arginine, lysine or histidine, which can interact with the negative charge phospholipids layer on the cell membrane and translocate the cargo into the cells.

Conjugation to cationic linear CPPs, such as TAT, penetratin, or oligoarginine efficiently improves the cellular uptake of large hydrophilic molecules, but the cellular uptake is predominantly via an unproductive endosomal pathway. Therefore, the biological effect is very limited, as the compounds are trapped in these compartments and cannot reach their biological targets in the cytoplasm or the nucleus. Mechanisms that promote endosomal escape or avoid endosomal route are required for improving bioavailability. Highly cationic CPPs preferentially interact with particular cell types, have limited plasma half-life, show toxicity, do not cross multicellular barriers such as vasculature epithelia or the blood-brain barrier, and efficient cargo delivery requires 9-15 arginine residues. Highly cationic CPPs are, therefore not ideal small molecule drug delivery vehicles. Linear CPPs are susceptible to hydrolysis by endogenous peptidases. Conjugation to cationic CPPs, such as TAT, penetratin, or oligoarginine efficiently improves the cellular uptake of large hydrophilic molecules, but the cellular uptake occurs predominantly via an unproductive endosomal pathway. Therefore, the biological effect is very limited, as the compounds are trapped in these compartments and cannot reach their biological targets in the cytoplasm or the nucleus.

Mechanisms that promote endosomal escape or avoid endosomal route are required for improving bioavailability. Highly cationic CPPs preferentially interact with particular cell types, have limited plasma half-life, show toxicity, do not cross multicellular barriers such as vasculature epithelia or the blood-brain barrier, and efficient cargo delivery requires 9-15 arginine residues. Highly cationic linear CPPs are, therefore, have not become optimized as small molecule drug delivery vehicles.

On the other hand, cyclic peptides containing hydrophilic and hydrophobic amino acids have shown greater potential as drug delivery tools due to their enhanced chemical and enzymatic stability. Parang's laboratory has reported that Amphiphilic Cyclic Peptides (ACPs) containing positively charged arginine and hydrophobic tryptophan residues as potential candidates for drug delivery. Cyclic peptides have several benefits compared to linear peptides, such as rigidness of structure and stability against proteolytic enzymes. The rigidity of the structure can enhance the binding affinity of ligands toward receptors by reducing the freedom of possible structural conformations. Cyclic peptides are also present in nature and have been developed as therapeutics. Cyclosporine, gramicidin S, polymoxin B, and daptomycin are well-known examples of cyclic peptide drugs. Parang's laboratory designed amphiphilic cyclic CPPs containing alternative tryptophan and arginine residues as the positively charged and hydrophobic residues, respectively. The peptides were efficient in improving the cellular delivery of anticancer and antiviral drugs.

The cellular uptake mechanism of CPPs into cells is still a matter of some debate. The cellular entry of CPP can be influenced by the type of CPP, the cell line, the nature of the cargo, and the conditions of incubation. As described above, linear CPPs pass through the plasma membrane mostly via an energy-independent or endocytosis pathway.

Moreover, the cellular delivery of CPP-conjugated molecules also occurs through endosomal pathway and a strong enzymatic degradation and an inadequate cytoplasmic release of intact molecules from the conjugates are expected, thus leading to an inefficient transfer into the cytoplasm. The best strategy to overcome this issue is to designing CPP that by pass the endosomal uptake or by increasing the escape rate from the endosome to improve the intracellular delivery of CPP-attached molecules.

Parang laboratory has reported the cellular uptake of a number of cyclic peptides independent of endocytotic pathway. The extraordinary ability of cyclic peptides containing tryptophan and arginine, $[WR]_4$ and $[WR]_5$ to spontaneously translocate across bilayers independent of an energy source is distinctly different from the behavior of the well-known, highly cationic CPPs, such as TAT and Arg_9, which do not translocate across phospholipid bilayers, and enter cells mostly by active endocytosis.

Alternatively, researchers have found that an effective cellular delivery vector can be improved developed by conjugating a CPP with a fatty acid chain. Amphiphilic peptides have also become a subject of major interest as potent antibacterial agents. Antimicrobial peptides (AMPs) are produced naturally by bacteria and are considered as the first line of host defense protecting against microbial infection. Various types of AMPs have been discovered, such as defensins, cecropins, magainins and cathelicidins, with significant different structures and bioactivity profiles.

These peptides are reported to be effectors and regulators of the innate immune system by increasing production and release of chemokines, and enhance wound healing and angiogenesis. They are able to suppress biofilm formation and induce the dissolution of existing biofilms. Thus, design of new AMPs with higher activity are urgently needed.

Although a number of cyclic peptides were discovered and reported as efficient cellular delivery agents and/or antimicrobial agents, a more systematic investigation is required to identify design rules for optimal entrapment, drug loading, and stability.

The balance of many small forces determines the overall morphology, size, and functionality of the structures. A deeper understanding of these factors is required for guiding future research, and for customizing cyclic peptides for drug loading and cellular delivery applications.

Thus, additional amphiphilic cyclic and linear peptides with variable electrostatic and hydrophobic residues were designed here to optimize drug encapsulation. The diversity in ring size, amino acid number, position and sequences, number of rings, net charge, and hydrophobicity of side chains in cyclic peptides will allow us to explore requirements for generating peptides with optimized drug encapsulation and to establish correlations between the structure of peptides with their drug entrapment properties. Thus, the general objective of this dissertation was to design and evaluate additional cyclic or amphiphilic peptides as nanostructures and to compare their efficiency in delivery of small molecules with the previously reported cyclic peptides containing tryptophan and arginine residues. This dissertation consists of three chapters.

Chapter 1. MANUSCRIPT I (*published in Current Organic Chemistry 2014).* The objective of this work was to design amphiphilic linear and cyclic peptides containing hydrophobic tryptophan W residues that were linked through a triazole ring to positively charged arginine (R) and lysine (K) residues. The peptides were synthesized through click chemistry between hydrophobic peptides containing alkyne and positively charged peptides containing azide groups. Their structures were investigated using solubility tests, circular dichorism (CD), and transmission electron microscopy (TEM), cytotoxicity assays. The conjugates showed minimal cytotoxicity in two cell lines. The secondary structures of both peptides were similar to a distorted α-helix as shown by CD spectroscopy. TEM imaging also showed that linear-linear $(WG(triazole\text{-}KR\text{-}NH_2))_3$ and cyclic-linear $[WG(triazole\text{-}KR\text{-}NH_2)]_3$ peptides formed nano-sized structures.

Chapter 2. MANUSCRIPT II (*Submitted to Journal of Molecular Modeling*). In this work, we investigated the structural and dynamical aspects of cyclic-linear peptide ($[WG(triazole\text{-}KR\text{-}NH_2)]_3$ and linear-linear peptide $(WG(triazole\text{-}KR\text{-}NH_2))_3$) formed nanostructures compared to a drug delivery system with $[WR]_4$. While $[WR]_4$ was found to be an efficient molecular transporter for small molecule drugs, such as lamivudine and dasatinib, cyclic-linear peptide $([WG(triazole\text{-}KR\text{-}NH_2)]_3$ was inefficient. Molecular modeling was used to explain the differential behavior of these peptides. We showed how the morphology of these systems can affect the drug delivery efficiency. The result of this work provided insights about optimizing the amphiphilic cyclic-linear trizaolyl peptides with more efficient drug delivery capabilities.

Chapter 3. MANUSCRIPT III. The objective of this Chapter was to synthesize a different series of amphiphilic peptides for different objectives. First, the amphiphilic

trizaolyl peptides in Chapter I were systematically modified by increasing the number of arginine and tryptophan sequence in cyclic and linear peptides. The rationale for the modification was to enhance the possibility of interaction with the cell membrane and therefore improving the cellular uptake process. Moreover, a new class of amphiphilic peptides consisting of tryptophan and glutamic acid were conjugated with a peptide containing arginine and lysine residues using Fmoc-based peptide chemistry. These peptides have an amide bond that generates more flexibility compared to a triazole ring. Finally, additional fatty acids with different length chains were conjugated with positively charged peptides and evaluated as antibacterial agents. Stearic acid (C16) and myristic acid (C14) were conjugated with peptides consisting of arginine azide and lysine amino acids to enhance the antibacterial activity.

In summary, the work in this dissertation provided insights about the synthesis and characterization of a new class of amphiphilic triazolyl peptides as drug delivery carriers and amphiphilic peptides as antibacterial agents. Molecular modeling was used to explain why triazolyl peptides were unable to enhance the delivery of small molecule drugs compared to the previously synthesized cyclic peptides $[WR]_4$ (Chapter 2) Modification of synthesized peptides in Chapter 1, by addition of more positively charged amino acids or reducing the rigidity by incorporating amide bonds instead of triazolyl groups can be used to improve the cell penetrating properties. Finally, we conjugated amphiphilic peptides with different fatty acids (Chapter 3) to investigate their application as antibacterial agents.

ACKNOWLEDGEMENTS

First, my deep gratitude to Allah the Almighty for giving me the knowledge, patience, strength and determination to conduct and complete this degree. Foremost I would like to express my deepest appreciation to my major professor, Dr. Keykavous Parang, for offering me the opportunity to work as a Ph.D. student under his supervision. His patience, motivation, enthusiasm, and immense knowledge helped me during my graduate program. I learned from him in both academic and personal aspects. I started from scratch in medicinal chemistry field and learned many methods and experiments techniques. My sincerest gratitude to every moment. This was a great achievement for me when I worked with him. I hope to continue learning from him and look forward to keeping this friendship and supervision in the future. I would like also to thank my collaborators and coauthors for their great ideas and advices. My sincere thanks also goes to my doctoral dissertation committee members, Dr. David Rowley, Dr. Nasser Zawia, Dr. Geoffrey Bothun, Dr. Aftab Ahmed, Dr. Haney Alashwal, and Dr. Brenton DeBoef for their time and scientific inputs. My laboratory colleagues, Dr. Rakesh Tiwari and Dr. Amir Shirazi were always on time to help and assist me for making a scientific and peaceful environment in the laboratory. I am grateful to the INBRE core facility and the College of Pharmacy, the University of Rhode Island for their support and assistances. I would like to extend my appreciation and thanks to the Ministry of Higher Education and Scientific Research, Libya for their financial support and for giving me this opportunity to continue my studies. Last but not the least, I would like to express my great thanks to all my family, parent, wife and kids for their patience and support till I finish my degree.

PREFACE

This dissertation is written based on the University of Rhode Island "Guidelines for the Format of Thesis and Dissertations" standards for Manuscript format. This dissertation is composed of three Chapters to satisfy the requirements of the department of Biomedical and Pharmaceutical Sciences, College of Pharmacy, University of Rhode Island.

CHAPTER 1: MANUSCRIPT I: **Amphiphilic Triazolyl Peptides: Synthesis and Evaluation as Nanostructure.**

This manuscript was published in "*Current Organic Chemistry*", **2014**, *18*, 2665 2671"

CHAPTER 2: MANUSCRIPT II: Cyclic Peptide Nanostructures as Drug Delivery Systems: Structural Insights and Dynamical Behavior.

This manuscript was submitted to "*Journal of Molecular Modeling*".

CHAPTER 3: MANUSCRIPT III. Synthesis of Derivatives Amphiphilic Peptides.

This manuscript is in process.

TABLE OF CONTENTS

LIST OF FIGURES

CHAPTER 1. MANUSCRIPT I

CHAPTER 2. MANUSCRIPT II

CHAPTER 3. MANUSCRIPT III

LIST OF SCHEMES

LIST OF ABBREVIATIONS

CCRF-CEM, human leukemia carcinoma cell line; CD, circular dichroism; CPPs, cell-penetrating peptides; DCM, dichloromethane; DIPEA, *N*,*N*-diisopropylethylamine; DMF, *N*,*N*-dimethylformamide; Dox, doxorubicin ; F′, fluorescein; FACS, fluorescence activated cell sorter; FBS, fetal bovine serum; Human breast carcinoma cell line; EDT, ethandithiol; HBTU, 2-(1H-benzotriazole-1-yl)-1,1,3,3-tetramethyluronium hexafluorophosphate; HOAt, 1-hydroxy-7-azabenzotriazole; HOBt, hydroxybenzotriazole; ITC, isothermal calorimetry; NMM, *N*-methylmorpholine; AMPs, antimicrobial peptides; PyAOP, 7-azabenzotriazol-1-yloxy tripyrrolidinophosphonium hexafluorophosphate);; TFA, trifluoroacetic acid; TEM, transmission electron microscopy.; MDA-MB-468, human breast adenocarcinoma; PBS, phosphate buffered saline solution; PyBOP, benzotriazol-1-yloxytripyrrolidinophosphonium hexafluorophosphate; SK-OV-3, human ovarian adenocarcino.

CHAPTER 1

Manuscript I

Published in *Current Organic Chemistry*, **2014**, *18*, 2665-2671

Amphiphilic Triazolyl Peptides: Synthesis and Evaluation as Nanostructures

Naser Sayeh,[a] Amir Nasrolahi Shirazi,[a,b] Donghoon Oh,[a] Jiadong Sun,[a] David Rowley,[a] Antara Banerjee,[c] Arpita Yadav,[c] Rakesh Kumar Tiwari,[a,b,*] Keykavous Parang[a,b,*]

[a]Department of Biomedical and Pharmaceutical Sciences, College of Pharmacy, University Rhode Island, Kingston, Rhode Island, 02881, United States; [b]Chapman University School of Pharmacy, Irvine, CA, 92618, United States; [c]Department of Chemistry, University Institute of Engineering and Technology, Chhatrapati Shahuji Maharaj University, Kanpur 208024, India

Abstract

A new class of amphiphilic triazolyl peptides were designed and synthesized from peptide-based building blocks containing alkyne and azide functional groups namely linear $(W(pG))_3$, cyclic$[W(pG)]_3$, and Ac-K(N_3)R-NH_2, where W, R, K, and pG represent tryptophan, arginine, lysine, and propargylglycine residues, respectively. The linear $(W(pG))_3$ and cyclic $[W(pG)]_3$ peptides containing alkyne residues were conjugated with Ac-K(N_3)R-NH_2 functionalized with azide group through click chemistry in the presence of $CuSO_4.5H_2O$, Cu (powder), sodium ascorbate, and *N*,*N*-disopropylethylamine in methanol:water to afford amphiphilic triazolyl linear-linear $(WG(triazole\text{-}KR\text{-}NH_2))_3$ and cyclic-linear $[WG(triazole\text{-}KR\text{-}NH_2)]_3$ peptides, respectively. The secondary structures of both peptides were similar to a distorted α-helix as shown by CD spectroscopy. TEM imaging showed that linear-linear $(WG(triazole\text{-}KR\text{-}NH_2))_3$ and cyclic-linear $[WG(triazole\text{-}KR\text{-}NH_2)]_3$ peptides formed nano-sized structures in the size range of 50-100 nm and 50-80 nm, respectively.

Keywords: Amphiphiles, Click chemistry, Cyclic peptides, Nanoparticles, Peptides, Triazole.

1. Introduction

Design and synthesis of well-defined materials in nano-sized structures have turned into an important field in biomaterials science and biomedicine.[1,2] Different intra and intermolecular forces, such as electrostatic interaction, hydrogen bonding, hydrophobic forces, and aromatic stacking contribute to the formation of organized structures.[3-5]

Peptides have become a subject of major interest because of their unparalleled potential applications as nanomaterials, surfactants, and drug delivery systems.[6-8] Linear and cyclic peptides containing appropriate amino acids have been shown to undergo self-assembly and generate nanostructures.[9] The generation of self-assembled peptides and nanostructures occur through various types of interactions between functional groups of amino acid residues, such as electrostatic, hydrophobic, and hydrogen bonding. Appropriate design and functionalization of peptides are critical for generating nanostructures.

Peptides are divided into two major groups namely linear and cyclic. Linear peptides adopt higher flexibility in a solution compared to their cyclic counterparts. Moreover, peptide cyclization has been used as an effective strategy to decrease the conformational freedom of the peptides and to improve the stability against different proteolytic enzymes, such as trypsin, α-chymotrypsin, and dipeptidyl-peptidase IV.[10] It has been previously shown that linear peptides containing hydrophilic and hydrophobic amino acids could act as membrane protein stabilizers.[11]

However, cyclic peptides containing hydrophilic and hydrophobic amino acids have shown greater potential as stabilizing agents due to their enhanced chemical and enzymatic stability.[12] The self-assembly of peptides has drawn significant attention because of their simple structures and their ability to incorporate multiple inter- and intramolecular forces.[13] Depending on the desired application, various properties including polarity, hydrophobicity, and charge in the structure of peptides can be manipulated by using different numbers of amino acids to find an optimized balance among different forces for self-assembly. Furthermore, the biocompatibility and low toxicity of peptides have made them attractive tools in biomedical investigations.[14] Thus, self-assembled peptide nanostructures have employed as biomaterials,[15] drug delivery systems,[16] protein stabilizers,[17] and antimicrobial agents.[18]

We have previously reported design and synthesis of linear and cyclic peptides containing different L-amino acids with hydrophobic (e.g., W, F, L) and charged residues (e.g., K, R, E) by using 9-fluorenylmethyloxycarbonyl (Fmoc)-based peptide chemistry. Among all the designed peptides, $[WR]_4$ containing alternative tryptophan and arginine residues generated self-assembled nanostructures at room temperature after a specific incubation time through hydrophobic force, hydrogen bonding, and/or the π-π stacking interactions between tryptophan residues.[6] A combination of arginine and tryptophan in the structure of cyclic peptides was also found to be an optimal sequence for drug delivery applications.[7,8] Moreover, the cyclic nature of peptides was critical in their biological activities. For example, cyclic peptides with arginine and tryptophan residues exhibited higher potency in kinase inhibition compared to their linear counterparts.[19]

Additional studies are required to investigate sequence effects on morphologies, and elucidate the fundamental physical interactions that drive their self-assembly in this class of peptides. In continuation of our efforts to explore amphiphilic peptides containing tryptophan and arginine residues as nanostructures, herein we report a novel class of amphiphilic triazolyl peptides containing tryptophan-based cyclic and linear peptides linked through a triazole to positively charged linear peptides. Click chemistry was used to attach the cyclic and linear building block peptides containing alkyne with linear peptides functionalized with azide residues to generate cyclic-linear or linear-linear clicked products.

2. Experimental Section

General

Reactions were carried out in Bio-Rad polypropylene columns by shaking and mixing in Glass-Col small tube rotator under dry conditions at room temperature. Peptides were synthesized by solid-phase synthesis using *N*-(9-fluorenyl) methoxycarbonyl (Fmoc)-based chemistry and employing Fmoc-L-amino acid building blocks. H-Trp(Boc)-2-chlorotrityl resin and/or Rink amide resin were used for the synthesis of cyclic and linear peptides, respectively. For the coupling of amino acids, Fmoc-Trp(Boc)-OH and Fmoc-L-propargylglycine were used alternatively, 2-(1*H*-Benzotriazole-1-yl)-1,1,3,3-tetramethyluronium hexafluorophosphate (HBTU) and *N*,*N*-diisopropylethylamine (DIPEA) in *N*,*N*-dimethylformamide (DMF) were used as coupling and activating reagents, respectively.

Rink amide resin, H-Trp(Boc)-2-chlorotrityl resin, coupling reagents, and Fmoc-amino acid building blocks were purchased from Chempep (Miami, FL). Other chemicals and reagents were purchased from Sigma-Aldrich Chemical Co. (Milwaukee, WI). Fmoc deprotection at each step was carried out using piperidine in DMF (20% v/v). The crude peptides were purified by using a reversed-phase Hitachi HPLC (L-2455) on a Gemini C18 column (250 mm × 21.20 cm, 10 μm) and a gradient system. The peptides were separated by eluting the crude peptides at 10.0 mL/min using a gradient of 0-100% acetonitrile (0.1% trifluoroacetic acid (TFA)) and water (0.1% TFA) over 60 min, and then were lyophilized.

The purity of final products (≥95%) was confirmed by analytical HPLC. The chemical structures of the building block peptides and final products were confirmed by high-resolution MALDI AXIMA performance TOF/TOF mass spectrometer (Shimadzu Biotech) or a high-resolution Biosystems QStar Elite time-of-flight electrospray mass spectrometer.

Synthesis of Linear Peptide $(W(pG))_3$

The linear peptide was assembled on Rink amide resin (0.59 g, 0.4 mmol, 0.68 mmol/g) by solid-phase Fmoc/*t*Bu peptide synthesis strategy using Fmoc-protected amino acids [Fmoc-Trp(Boc)-OH and Fmoc-L-Propargylglycine] (Scheme 1). The linear peptide sequence was assembled on the resin after removing the Fmoc group at the *N*-terminal in the presence of 20% piperidine in DMF (v/v) to obtain the sequence NH_2-(pG)W(Boc)(pG)W(Boc)(pG)W(Boc)-Rink amide resin.

The resin was washed with DMF (3 times, 15 mL) and DCM (3 × 15 mL) to remove any traces of piperdine. The peptidyl resin was dried in vacuum for 24 h. A freshly prepared reagent R cleavage cocktail trifluoroacetic acid (TFA)/thioanisole/ethandithol (EDT)/anisole (90:5:3:2, v/v/v/v, 15 mL) was added to the resin, and the resin was agitated at room tempertuare for 2 h. The resin was collected by filtration and consequently washed with 2 mL of reagent R. The crude peptide was precipitated by adding peptide filterates to cold diethyl ether (200 mL, Et_2O) and centrifuged at 4000 rpm for 5 min followed by decantation to obtain the solid precipitate. The solid material was further washed with cold ether (2 × 100 mL). The peptide was lyophilized and purified by reversed-phase Hitachi HPLC using a gradient system as described above to yield solid white coloured linear peptide $(W(pG))_3$. MALDI-TOF (m/z) $[C_{48}H_{47}N_9O_7]$: calcd, 860.3758; found, 884.3489 $[M + Na + H]^+$.

Synthesis of Cyclic Peptide $[W(pG)]_3$

The linear protected peptide sequence was assembled using H-Trp(Boc)-2-chlorotrityl resin (0.51 g, 0.4 mmol, 0.78 mmol/g). The resin was swelled using DMF (3 × 30 mL, 10 min) followed by coupling with appropriate amino acids (Fmoc-Trp(Boc)-OH and Fmoc-L-propargylglycine) and deprotection cycle with piperidine in DMF (20% v/v). The final *N*-terminal Fmoc group was removed to assemble the sequence on the peptidyl resin, NH_2-(pG)W(Boc)(pG)W(Boc)(pG)W(Boc)-2-chlorotrityl resin (Scheme 2). The resin was washed with DMF (3 × 15 mL) and DCM (3 × 15 mL) to remove any traces of piperdine. Side chain-protected peptides were cleaved from the resins by agitating the peptidyl resin with cleavage cocktail, acetic acid/ 2,2,2-trifluoroethanol

(TFE)/dichloromethane (1:2:7, v/v/v, 50 mL) for 1 h at room temperature followed by filtration and washing the resin with TFE:DCM (2:8 v/v, 20 mL).

The collected filtrate was evaporated to reduce volume residue. Hexane (2 × 25 mL) and DCM (1 × 25 mL) were added to the residue to remove the acetic acid from the residue. The solvents were evaporated to yield a fluffy white solid compound that was dried overnight. The cyclization of the protected crude solid peptide was carried out in the presence of a mixture of coupling reagents, 1-hydroxy-7-azabenzotriazole (HOAt) (162 mg, 0.4 mmol) and *N,N′*-diisopropylcarbodiimide (DIC) (310 µL, 0.4 mmol) in anhydrous DMF:DCM (60/200 mL) for 24 h.

The solvent was evaporated from a sample solution (5 mL) under reduced pressure, and the residue was cleaved with reagent R that confirmed the cyclization by mass spectrometry. Thus, all the solvents were removed under reduced pressure that generated a high viscous liquid. The final peptide cleavage to remove the side chain protection was carried out by shaking the residue with cleavage cocktail, reagent R, TFA/thioanisole/anisole/EDT (90:5:2:3 v/v/v/v, 15 mL) for 2 h at room tempertuare. The crude peptide was precipitated by the addition of cold diethyl ether (200 mL, Et_2O) and centrifuged at 4000 rpm for 5 min followed by decantation to obtain the solid precipitate. The solid material was further washed with cold ether (2 × 100 mL). The crude peptide was lyophilized and purified by reversed-phase Hitachi HPLC (L-2455) as described above to yield cyclic peptide $[W(pG)]_3$. MALDI-TOF (m/z) $[C_{48}H_{45}N_9O_6]$: calcd, 843.3493; found 866.2380 $[M + Na]^+$.

Synthesis of Azide Functionalised Positively Charged Peptide (Ac-K(N_3)R-NH_2)

The peptide was assembled on Rink amide resin (294 mg, 0.2 mmol, 0.68 mmol/g) by solid-phase peptide synthesis using Fmoc-protected amino acids, Fmoc-Arg(Pbf)-OH and Fmoc-Lys(N_3)-OH. The Rink amide resin was swelled with DCM (50 mL, 10 min) and then DMF (50 mL, 2 × 10 min). The Fmoc group on the resin was deprotected by piperidine in DMF (20%, v/v, 25 mL, 2 × 10 min) followed by washing with DMF (3 × 30mL). Fmoc-Arg (pbf)-OH (389 mg, 0.2 mmol/g) was then coupled to the peptidyl resin in the presence of coupling reagents HBTU (228 mg, 0.2 mmol/g) and DIPEA (210 µL) in *N*,*N*-dimethylformamide (DMF, 10 mL). The mixture was agitated at room tempertuare for 1 h. The resin was then washed with DMF (3 × 10 mL) for 5 min. The Fmoc group was deprotected using using piperidine in DMF (20% v/v, 25 mL, 2 × 10 min) followed by washing with DMF (3 × 20 mL). The Fmoc-Lys (N_3)-OH (173 mg, 0.2 mmol) was coupled by using HBTU (228 mg, 0.2 mmol), DIPEA (210 µL) in DMF for 1 h. The resin was washed with DMF (3 × 20 mL), and Fmoc group was deprotected by using piperdine in DMF (20% v/v, 25 mL, 2 × 10 min). The resin was washed with DMF followed by capping the amino group by acetic anhdyride (Ac_2O, 95 µL, 1 mmol) and DIPEA (174 µL, 1 mmol) in anhydrous DMF (3 mL) for 30 min. The resin was washed with DMF (3 × 30 mL), DCM (3 × 30 mL), and was dried in vaccum overnight before the final cleavage. A freshly prepared cleavage cocktail, TFA /triisopropylsilane /water (95:2.5:2.5 v/v/v, 10 mL) was added to the resin and shaken at room temperature for 1.5 h. The resin was filtered and evaporated to reduce the volume under dry nitrogen. The crude peptide was precipitated by adding cold diethyl ether (200 mL, Et_2O) and centrifuged at 4000 rpm for 5 min followed by decantation to obtain the solid precipitate.

The peptide was purified by reversed-phase Hitachi HPLC using a gradient system, and the HPLC fractions were collected, evaporated and lyophilized to obtain dry product. ESI-TOF (m/z) [$C_{14}H_{27}N_9O_3$]: calcd, 369.2237; found, 370.2144 $[M+H]^+$.

Synthesis of Amphiphilic Triazolyl Peptides by Click Chemistry of Peptides (Linear or Cyclic) with an Azide-Functionalized Positively Charged Linear Peptide

The click reaction was carried out in 20 mL glass vial with small magnetic stir bar by adding the alkyne peptide (linear peptide (7.46 mg, 8.68 µmol) or cyclic peptide (7.25 mg, 8.68 µmol)), $CuSO_4.5H_2O$ (6.5 mg, 0.026 mmole), Cu powder (16.5 mg, 0.26 mmol), sodium ascorbate (51.5 mg, 0.26 mmol), and azide-functionalized peptide, Ac-K(N_3)R-NH_2 (10 mg, 0.026 mmol) in methanol:water (2:1, 5 mL) followed by addition of DIPEA (9 µL, 0.052 mmol). The mixture was stirred at room temperature for 24-48 h. The completion of the reaction was confirmed by MALDI mass spectroscopy. The reaction mixture was filtered, and the solvent was evaporated under reduced pressure to afford the crude product. The crude product was further purified by HPLC using a gradient system as described above, and the HPLC fractions were collected, evaporated and lyophilized to obtain solid compounds. Linear-linear (WG(triazole-KR-NH_2))$_3$, MALDI-TOF (m/z) [$C_{90}H_{128}N_{36}O_{16}$]: calcd, 1969.0309; found 1970.2032 $[M+H]^+$; Cyclic-linear [WG(triazole-KR-NH_2)]$_3$ MALDI-TOF (m/z) [$C_{90}H_{126}N_{36}O_{15}$]: calcd, 1951.0203; found 1951.6645 $[M]^+$.

Circular Dichroism

CD spectra were recorded on a JASCO J-810 spectropolarimeter using 1 mm path length cuvettes. The scan speed was 100 nm/min, and spectra were averaged over 8 scans. All experiments on the samples including cyclic-linear $[WG(triazole\text{-}KR\text{-}NH_2)]_3$ and linear-linear $(WG(triazole\text{-}KR\text{-}NH_2))_3$ (1 mM, H_2O) were tested at room temperature. The CD for background reference (H_2O) was measured and subtracted from the sample.

Transmission Electron Microscopy (TEM)

TEM analyses were conducted in JEOL Transmission Electron Microscope (Tokyo, Japan) at an accelerating voltage 80 keV. The stock solution (1 mM) in deionized water incubated for 3 days was used for the sample preparation. TEM samples of cyclic-linear $[WG(triazole\text{-}KR\text{-}NH_2)]_3$ and linear-linear $(WG(triazole\text{-}KR\text{-}NH_2))_3$ were prepared by depositing a droplet of 5 μL of 1 mM solution in H_2O on a carbon-coated Cu support grid of mesh size 300, which was allowed to rest for 2 min. After drop casting of peptide solution, the grids were then stained with uranyl acetate (20 mL) for 2 min. Excess stain was removed, and the grids were allowed to dry overnight.

Molecular Modeling

Cyclic-linear $[WG(triazole\text{-}KR\text{-}NH_2)]_3$ monomer was built using GaussView software and completely optimized without any contraints utilizing Gaussian 03 software. Charge density was plotted and colored according to electrostatic potential.

Dynamic Light Scattering (DLS)

Zeta potential measurements were conducted by dynamic light scattering using a Malvern Instruments Zetasizer Nano ZS (Worcestershire, UK). The machine was calibrated using a 60 nm polystyrene standard. Each sample of $(WG(triazole\text{-}KR\text{-}NH_2))_3$ and $[WG(triazole\text{-}KR\text{-}NH_2)]_3$ (1 mL, of 1 mM) was loaded into a cell, and the particle size and zeta potential were measured simultaneously in triplicate. To determine the size distribution, 1 mL samples were placed in PCS1115 glass cuvettes and DLS was performed at 25 °C at a backscatter angle of 173 with an equilibration time of 120 s. The intensity was based on 11 scans.

Cell Culture

Ovarian adenocarcinoma SK-OV-3 and Human Embryonic Kidney 293 cells HEK-293T cells obtained from American Type Culture Collection (ATCC no CRL-11268). Cells were grown on 75 cm^2 cell culture flasks with EMEM medium, supplemented with 10% fetal bovine serum (FBS), and 1% penicillin-streptomycin solution (10,000 units of penicillin and 10 mg of streptomycin in 0.9 % NaCl) in a humidified atmosphere of 5% CO_2, 95% air at 37 ºC.

Cytotoxicity Assay

SK-OV-3 and HEK-293T cells were plated overnight in 96-well plates with density of 5000 cells per well in 0.1 ml of appropriate medium at 37 ºC prior to the experiment. The old medium (EMEM containing FBS (10%)) were replaced by different

concentrations of linear $R_3(WG)_3$ and cyclic $R_3[WG]_3$ peptides (5, 10, 15, 25, 50, 75, 100, 150 μM) in serum containing medium and incubated for 2 h at 37 °C in a humidified atmosphere of 5% CO_2. Similar experiments were conducted with linear $(WG)_3$ and cyclic $[WG]_3$. Compounds were removed from medium by replacing with fresh medium, and the cells were kept in an incubator for another 72 h. The cells without compounds were incubated in each experiment as control. After 72 h, 20 μl of MTS was added to the cell and incubated for 2 h. The absorbance of the formazan product was calculated with the fluorescence intensity at 490 nm using a SpectraMax M2 microplate spectrophotometer. The percentage of cell survival was calculated as [(OD value of cells treated with the test mixture of compounds) − (OD value of culture medium)]/[(OD value of control cells) − (OD value of culture medium)] × 100%.

3. Results and Discussion

Click chemistry has been previously used to design diverse structures of peptide scaffolds. For instance, different derivatives of a triazole-containing kinase inhibitor cyclo-[Pro-Val-Pro-Tyr] peptide were synthesized through click chemistry.[20] Furthermore, triazoles were found to be an appropriate substituent for the amide bond in peptides with a α-helical structure.[21] Horne *et al.* designed a class of cyclic peptides containing 1,4- or 1,5-disubstituted 1,2,3-triazoles[22] that were found to serve as surrogates for *trans* or *cis* amide bonds, respectively. Synthesis of amphiphilic peptides containing hydrophobic and positively charged residues by click chemistry remains unexplored. To the best of our knowledge, this is the first report of amphiphilic cyclic-linear and linear-linear peptides linked through a triazole spacer.

The synthesis of linear-linear $(WG(triazole\text{-}KR\text{-}NH_2))_3$ and cyclic-linear $[WG(triazole\text{-}KR\text{-}NH_2)]_3$ peptides containing triazole rings were performed in two major steps by synthesizing the building blocks containing alkyne and azide residues. First, linear $(W(pG))_3$ and cyclic $[W(pG)]_3$ building block peptides (where (pG) = propargylglycine) containing alkyne residues were synthesized by Fmoc-based chemistry. Second, a building block containing azide residue, $Ac\text{-}K(N_3)R\text{-}NH_2$, was synthesized. Finally, the building blocks were conjugated with each other through click chemistry. The linear peptide $(W(pG))_3$ was assembled on Rink amide resin (0.4 mmol, 0.68 mmol/g) by solid-phase Fmoc/*t*Bu peptide synthesis strategy using Fmoc-Trp(Boc)-OH and Fmoc-L-propargylglycine (Scheme 1).

The peptide sequence was assembled on the resin followed by removing of the *N*-terminal Fmoc group to obtain the sequence NH_2-(pG)W(Boc)(pG)W (Boc)(pG)W(Boc)-Rink amide resin. The linear peptide was obtained after cleavage of peptidyl resin using reagent R cleavage cocktail (trifluoroacetic acid (TFA)/thioanisole/ethanedithiol (EDT)/anisole (90:5:3:2, v/v/v/v)) by shaking the mixture at room temperature for 2 h, followed by precipitation with cold ether and centrifugation to afford solid crude linear $(W(pG))_3$ peptide, which was further purified by using HPLC.

In contrast with the synthetic procedure for the linear peptide, the cyclic peptide $[W(pG)]_3$ was synthesized by using H-Trp(Boc)-2-chlorotrityl resin (0.4 mmol, 0.78 mmol/g,) (Scheme 2). The resin was swelled using DMF followed by coupling and deprotection cycles using appropriate amino acids and piperidine in DMF (20% v/v). The final *N*-terminal Fmoc group was removed to assemble the sequence on the peptidyl resin, NH_2-(pG)W(Boc)(pG)W(Boc)(pG)W(Boc)-2-chlorotrityl resin.

The side chain protected peptide was cleaved from the resin by agitating the resin with cleavage cocktail, acetic acid/2,2,2-trifluoroethanol (TFE)/dichloromethane (1:2:7, v/v/v) for 1 h at room temperature followed by filtration and evaporation of cocktail liquid to afford the crude side chain protected peptide. The peptide was dried overnight followed by *N*- to *C*-terminal cyclization by using coupling reagents, 1-hydroxy-7-azabenzotriazole (HOAt) and *N,N′*-diisopropylcarbodiimide (DIC) in DMF/DCM under diluted conditions for overnight. The progress of the reaction was monitored by using MALDI-TOF. The solvent was evaporated and Boc protecting groups were removed in the presence of reagent R cleavage cocktail for 2 h followed by precipitation and HPLC purification to afford the cyclic peptide.

The synthesis of azide-functionalized positively charged peptide building block (Ac-K(N_3)R-NH_2) was performed on Rink amide resin (0.2 mmol, 0.68 mmol/g) using building blocks of Fmoc-protected amino acids including Fmoc-Arg(pbf)-OH and Fmoc-Lys(N_3)-OH. The resin was swelled and deprotected to couple arginine followed by deprotection and coupling with Fmoc-Lys(N_3)-OH. The Fmoc group was deprotected, and amino group was further capped using acetic anhydride in DMF. The peptide was cleaved from the resin using a cleavage cocktail containing TFA/TIS/H_2O (95:2.5:2.5, v/v/v) and purified by HPLC to afford Ac-K(N_3)R-NH_2 (Scheme 3).

Finally, the linear-linear and cyclic-linear amphiphilic triazolyl peptides were synthesized by click reaction between the linear or cyclic peptides containing alkyne, $(W(pG))_3$ and $[W(pG)]_3$, and azide-functionalized linear peptide Ac-K(N_3)R-NH_2 in solution phase using $CuSO_4{\cdot}5H_2O$, Cu powder, sodium ascorbate, and *N,N*-diisopropylethylamine (DIPEA) in methanol/water for 24-48 h (Scheme 4).

The azide peptide Ac-K(N_3)R-NH_2 was used in excess (more than 3 equiv) to conjugate with the three alkyne functional groups in the linear or cyclic peptides at room temperature and afford the linear-linear (WG(triazole-KR-NH_2))$_3$ and cyclic-linear [WG(triazole-KR-NH_2)]$_3$ in 33-35% yield (Scheme 5). The formation of the conjugated 1,4 product was confirmed by MALDI-TOF mass spectroscopy. The structure of optimized conformation of cyclic-linear [WG(triazole-KR-NH_2)]$_3$ monomer was evaluated for charge distribution. The modeling exhibited positively charged arginine extending out of the cyclic peptide (Figure 1). The secondary structure of peptides is one of the responsible elements in the self-assembly pattern.

Circular dichroism (CD) was employed to obtain insights about the secondary structure of both peptides. The secondary structures of the majority of peptides are divided into three major classic forms namely β-sheet, α-helix, and random coil. The β-sheet structures get stabilized through available hydrogen bonding between oligopeptide strands. However, intra-chain hydrogen bonds help the α-helix to form a stable coiled structure. The CD results showed that both peptides have a relatively similar structure. CD spectra of the cyclic-linear peptide (1 mM) solution in water at room temperature showed two minima peaks at 226 nm and 199 nm. The linear peptide exhibited a similar CD pattern to the cyclic peptidewith two minima peaks at 226 nm and 202 nm (Figure 2). However, a blue shift from 202 to 199 nm was found for the cyclic peptide as compared to the linear, suggesting that the secondary structure of the cyclic peptide is slightly different. A distinct α-helix structure shows two minima peaks at 222 and 208 nm. Thus, the structures of these peptides did not follow a typical α-helical structure.

The size and morphologies of peptide nanoparticles were monitored by using transmission electron microscopy (TEM). As shown in Figure 3, the cyclic-linear $[WG(triazole\text{-}KR\text{-}NH_2)]_3$ formed spherical nanostructures in the size range of 50-80 nm. However, the linear-linear $(WG(triazole\text{-}KR\text{-}NH_2))_3$ exhibited entirely different morphologies and size compared to that of the cyclic-linear counterpart. The linear peptide showed nanosized network with particles as small as 5-10 nm. Small sized particles showed aggregation by forming larger particles in the size range 50-100 nm (Figure 4). DLS studies showed a monodisperse size distribution for both linear-linear $(WG(triazole\text{-}KR\text{-}NH_2))_3$ and cyclic-linear $[WG(triazole\text{-}KR\text{-}NH_2)]_3$ while the latter showed larger nanoparticles (Figures 5 and 6).

Although linear-linear and cyclic-linear peptides share the equal number of similar amino acids, they form different types of particles presumably because of the difference in the orientation of positively charged guanidine groups in arginine and hydrophobic tryptophan residues.

Cytotoxicity of both linear-linear $(WG(triazole\text{-}KR\text{-}NH_2))_3$ and cyclic-linear $[WG(triazole\text{-}KR\text{-}NH_2)]_3$ peptides were evaluated in SK-OV-3 and HEK-293T cells (Figures 7 and 8). In general, the peptides did not show significant toxicity at concentration of <25 μM in HEK-293T cells. While cyclic-linear $[WG(triazole\text{-}KR\text{-}NH_2)]_3$ did not exhibit any significant toxicity in SK-OV-3 cells at a concentration of 75 μM, linear-linear $(WG(triazole\text{-}KR\text{-}NH_2))_3$ reduced the cell proliferation by 20% at this concentration. Similar results were obtained when comparing linear $(W(pG))_3$ (Figure 9) and cyclic $[W(pG)]_3$ (Figure 10) building blocks, showing the cyclic peptide less cytotoxic than the linear counterpart.

4. Conclusion

In conclusion, a new class of amphiphilic peptides containing arginine and tryptophan, linear-linear $(WG(triazole\text{-}KR\text{-}NH_2))_3$ and cyclic-linear $[WG(triazole\text{-}KR\text{-}NH_2)]_3$, was synthesized by using click chemistry. CD spectroscopy exhibited that the secondary structures of both peptides have a similar pattern. Cyclic-linear $[WG]_3$ and linear-linear $(WG)_3$ showed nano-sized structures in a range size of 50-100 nm.

Acknowledgments

We thank National Center for Research Resources, NIH, and Grant Number 1 P20 RR16457 for sponsoring the core facility.

Notes

The authors declare no competing financial interest

References

1. Zhang, S. Fabrication of novel biomaterials through molecular self-assembly. *Nat. Biotechnol*. **2003**, *21*, 1171–1178. b) Krishna, R.; Mayer, D. *Eur. J. Pharm. Sci*. **2000**, *11*, 265-283.

2. Krishna, R.; Mayer, D. Multidrug resistance (MDR) in cancer. Mechanisms, reversal using modulators of MDR and the role of MDR modulators in influencing the pharmacokinetics of anticancer drugs. *Eur. J. Pharm. Sci*. **2000**, *11*, 265-283.

3. Whitesides, G. M.; Mathias, J. P.; Set, C. T. Molecular self-assembly and nanochemistry: a chemical strategy for the synthesis of nanostructures. *Science.* **1991**, *254*, 1312–1319.

4. Bryson, J. W.; Betz, S. F.; Lu, H. S.; Suich, D. J.; Zhou, H. X.; O'Neil.; K. T.; DeGrado.; W. F. Protein design: a hierarchic approach. *Science.* **1995**, *270*, 935–941.

5. Dill, K. A. Dominant forces in protein folding. *Biochemistry.* **1990**, *29*, 7133–7155.

6. Brooks, C. L. Protein and peptide folding explored with molecular simulations. *Acc. Chem. Res*. **2002**, *35*, 447–454.

7. Mandal, D.; Tiwari, R.; Nasrolahi Shirazi, A.; Oh, D.; Ye, G.; Banerjee, A.; Yadav, A.; Parang, K. Self-Assembled Surfactant Cyclic Peptide Nanostructures as Stabilizing Agents. *Soft Matter*. **2013**, *9*, 9465-9475.

8. Mandal, D.; Nasrolahi Shirazi, A.; Parang, K. Cell-penetrating homochiral cyclic peptides as nuclear-targeting molecular transporters. *Angew. Chem. Int. Ed*. **2011**, *50*, 9633−9637.

9. Nasrolahi Shirazi, A.; Tiwari, R. K.; Chhikara, B. S.; Mandal, D.; Parang, K. Design and biological evaluation of cell-penetrating peptide-doxorubicin conjugates as prodrugs. *Mol. Pharm.* **2013**, *10*, 488−499.

10. Nasrolahi Shirazi, A.; Mandal, D.; Tiwari, R. K.; Guo, L.; Lu, W.; Parang, K. Cyclic peptide-capped gold nanoparticles as drug delivery systems. *Mol. Pharm*. **2013**, *10*, 500–511.

11. Mandal, D.; Nasrolahi Shirazi, A.; Parang, K. Self-assembly of peptides to nanostructures. *Org. Biomol. Chem*. **2014**, *12*, 3544-61.

12. Vlieghe, P.; Lisowski, V.; Martinez, J.; Khrestchatisky, M. Synthetic therapeutic peptides: science and market Drug. *Discov. Today*. **2010**, *15*, 40–56.

13. Yeh, J.; Du, S.; Tordajada, A.; Paulo, J.; Zhang, S. Peptergents: peptide detergents that improve stability and functionality of a membrane protein, glycerol-3-phosphate dehydrogenase. *Biochemistr*. **2005**, *44*, 16912–16919.

14. Katsara, M.; Selios, T.T.; Deraos, S.; Deraos, G.; Matsoukas, M. T.; Lazoura, E.; Matsoukas, J.; Apostolopoulos, V. Round and round we go: cyclic peptides in disease. *Curr. Med. Chem*. **2006**, *13*, 2221–2232.

15. Lehn, J. M. Toward complex matter: supramolecular chemistry and self-organization. *Proc. Natl. Acad. Sci. USA.* **2002**, *99*, 4763-4768.

16. Bellomo, E. G.; Wyrsta, M. D.; Pakstis, L.; Pochan, D. J.; Deming, T. J. Stimuli-responsive polypeptide vesicles by conformation-specific assembly. *Nat. Mater.* **2004**, *3*, 244-248.

17. Nasrolahi Shirazi, A.; Oh, D.; R. K. Tiwari, Sullivan, B, Gupta, A.; Bothun, G. D.; Parang, K. Peptide amphiphile containing arginine and fatty acyl chains as molecular transporters. *Mol. Pharm.* **2013**, *10*, 4717−4727.

18. Kogan, M. J.; Olmedo, I.; Hosta, L.; Guerrero, A. R.; Cruz, L. J.; Albericio, F. Peptides and metallic nanoparticles for biomedical applications. *Nanomedicine.* **2007**, *2*, 287-306.

19. Kyle, S.; Aggeli, A.; Ingham, E.; McPherson, M. J. Recombinant self-assembling peptides as biomaterials for tissue engineering. *Biomaterials*. **2010**, *31*, 9395-9405.

20. Nasrolahi Shirazi, A.; R. K. Tiwari, Oh, D.; Banerjee, A.; Yadav, A.; Parang, K. Efficient delivery of cell impermeable phosphopeptides by a cyclic peptide amphiphile containing tryptophan and arginine. *Mol. Pharm.* **2013**, *10*, 2008−2020.

21. Nasrolahi Shirazi, A.; Tiwari, R. K.; Chhikara, B. S.; Mandal, D.; Parang, K. Design and biological evaluation of cell-penetrating peptide-doxorubicin conjugates as prodrugs. *Mol. Pharm.* **2013**, *10*, 488−499.

22. Zelzer, M.; Ulijn, R. V. Next-generation peptide nanomaterials: molecular networks, interfaces and supramolecular functionality. *Chem. Soc. Rev.* **2010**, *39*, 3351-3357.

23. Rica, R. D. L.; Matsui, H. Applications of peptide and protein-based materials in bionanotechnology. *Chem. Soc. Rev.* **2010**, *39*, 3499-3509.

24. Jenssen, H.; Hamill, P.; Hancock, R. E. Peptide antimicrobial agents. *Clin. Microbiol. Rev.* **2006**,*19*, 491-511.

25. Nasrolahi Shirazi, A.; Tiwari, R. K.; Brown, A.; Mandal, D.; Sun, G.; Parang, K. Cyclic peptides containing tryptophan and arginine as Src kinase inhibitors. *Bioorg. Med. Chem. Lett*. **2013**, *23*, 3230−3234.

26. Bock, V.D.; Speijer, D.; Hiemstra, H.; van Maarseveen, J.H. 1,2,3-Triazoles as peptide bond isosteres: synthesis and biological evaluation of cyclotetrapeptide mimics. *Org. Biomol. Chem.* **2007**, *5*, 971–975.

27. Horne, W.S.; Yadav, M.K.; Stout, C.D.; Ghadiri, M.R. J. Heterocyclic peptide backbone modifications in an alpha-helical coiled coil. *Am. Chem. Soc.* **2004**, *126*, 15366–15367.

28. Horne, W.S.; Olsen, C.A.; Beierle, J.M.; Montero, A.; Ghadiri, M.R. Probing the bioactive conformation of an archetypal natural product HDAC inhibitor with conformationally homogeneous triazole-modified cyclic tetrapeptides. *Angew. Chem. Int. Ed.* **2009**, *48*, 4718–4724.

Figure Legends:

Figure 1. Molecular electrostatic potential surface of $[WG(triazole\text{-}KR\text{-}NH_2)]_3$.

Figure 2. CD spectra of linear-linear $(WG(triazole\text{-}KR\text{-}NH_2))_3$ and cyclic-linear $[WG(triazole\text{-}KR\text{-}NH_2)]_3$.

Figure 3. TEM images of cyclic-linear $[WG(triazole\text{-}KR\text{-}NH_2)]_3$.

Figure 4. TEM images of linear-linear $(WG(triazole\text{-}KR\text{-}NH_2))_3$.

Figure 5. Dynamic light scattering (DLS) of linear-linear $(WG(triazole\text{-}KR\text{-}NH_2))_3$.

Figure 6. Dynamic light scattering (DLS) of cyclic-linear $[WG(triazole\text{-}KR\text{-}NH_2)]_3$.

Figure 7. Cytotoxicity of linear-linear $(WG(triazole\text{-}KR\text{-}NH_2))_3$ and cyclic-linear $[WG(triazole\text{-}KR\text{-}NH_2)]_3$ in HEK-293T cells after 2 h.

Figure 8. Cytotoxicity of linear-linear $(WG(triazole\text{-}KR\text{-}NH_2))_3$ and cyclic-linear $[WG(triazole\text{-}KR\text{-}NH_2)]_3$ in SK-OV-3 cells after 2 h.

Figure 9. Cytotoxicity of linear $(WG)_3$ in SK-OV-3 cells after 2 h.

Figure 10. Cytotoxicity of cyclic $[WG]_3$ in SK-OV-3 cells after 2 h.

Figure 1.

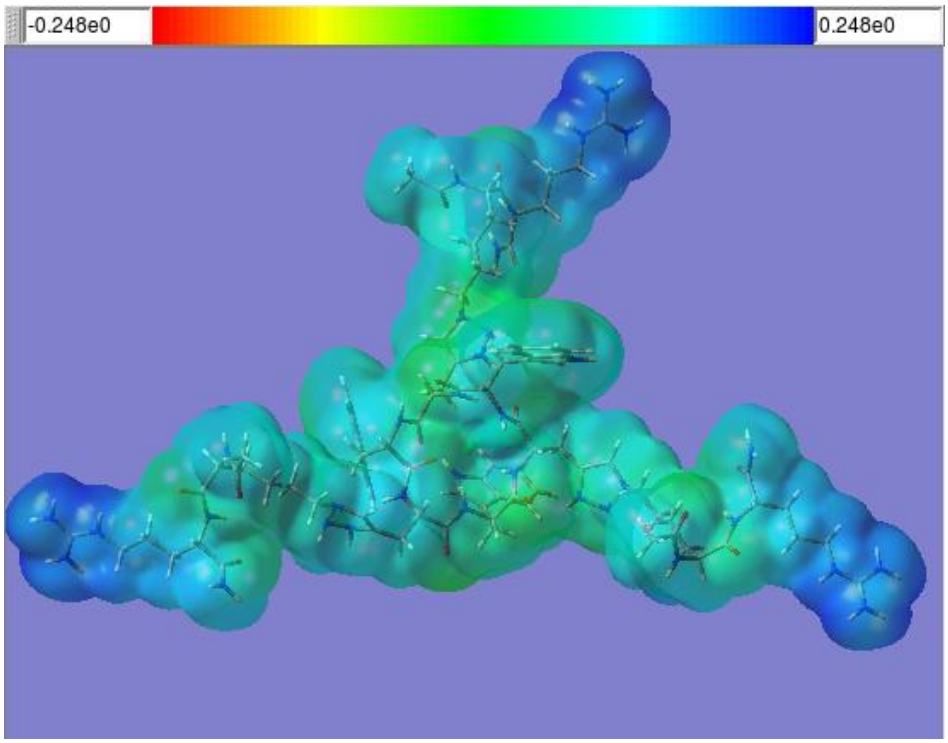

Figure 2.

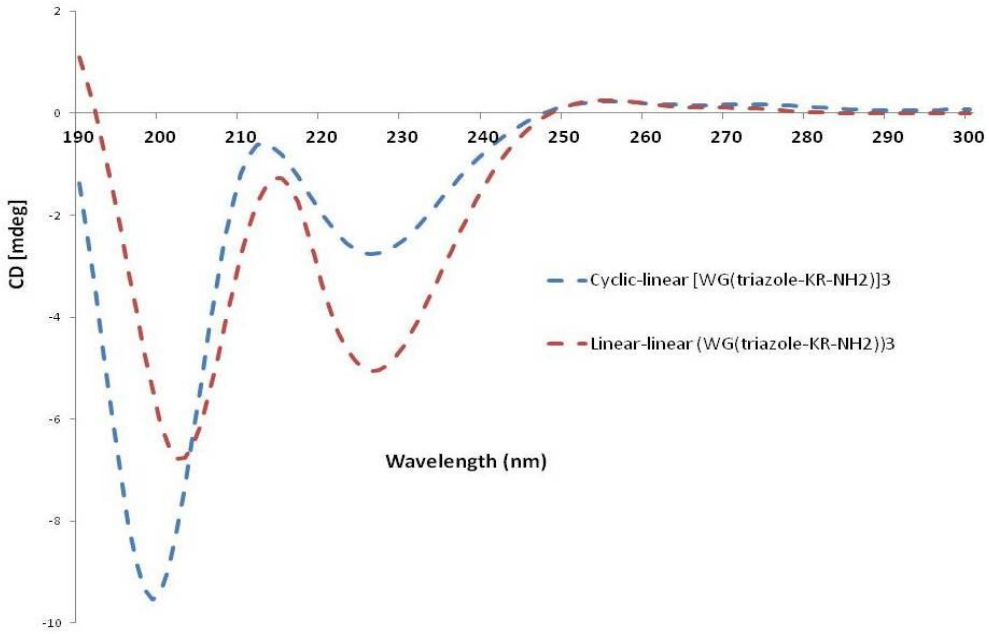
2
0
-2
-4
-6
-8
-10
190
200
210
220
230
240
250
260
270
280
290
300
CD [mdeg]
Wavelength (nm)
Cyclic-linear [WG(triazole-KR-NH2)]3
Linear-linear (WG(triazole-KR-NH2))3

Figure 3.

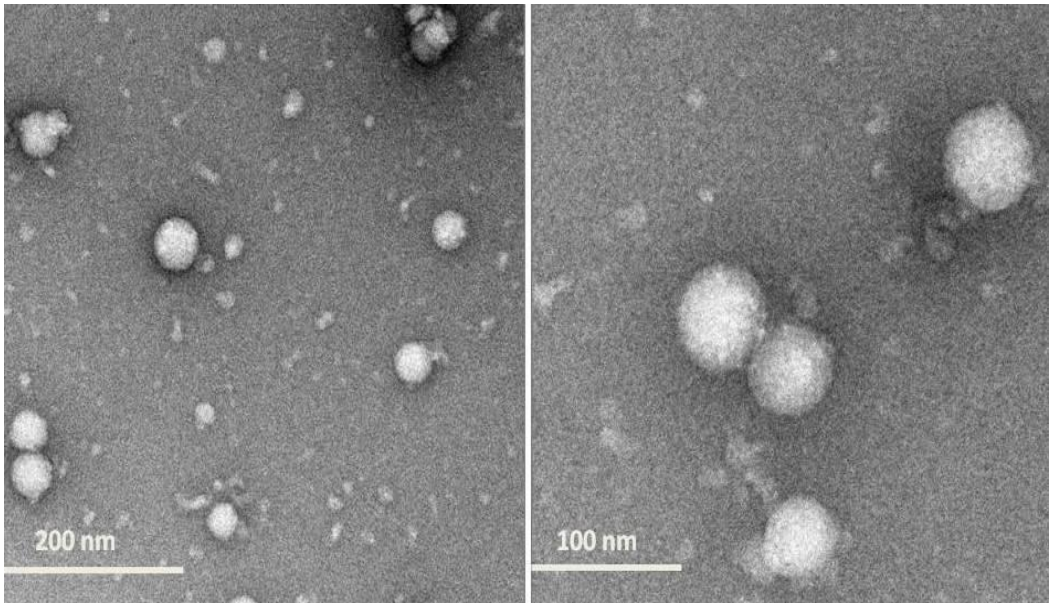

Figure 4.

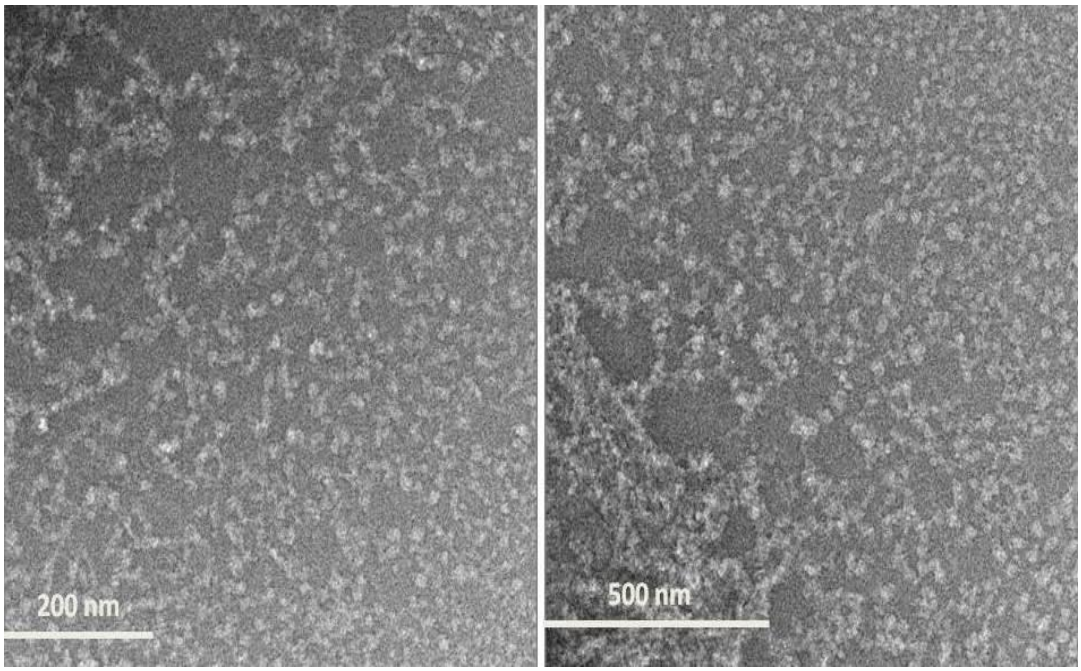

Figure 5.

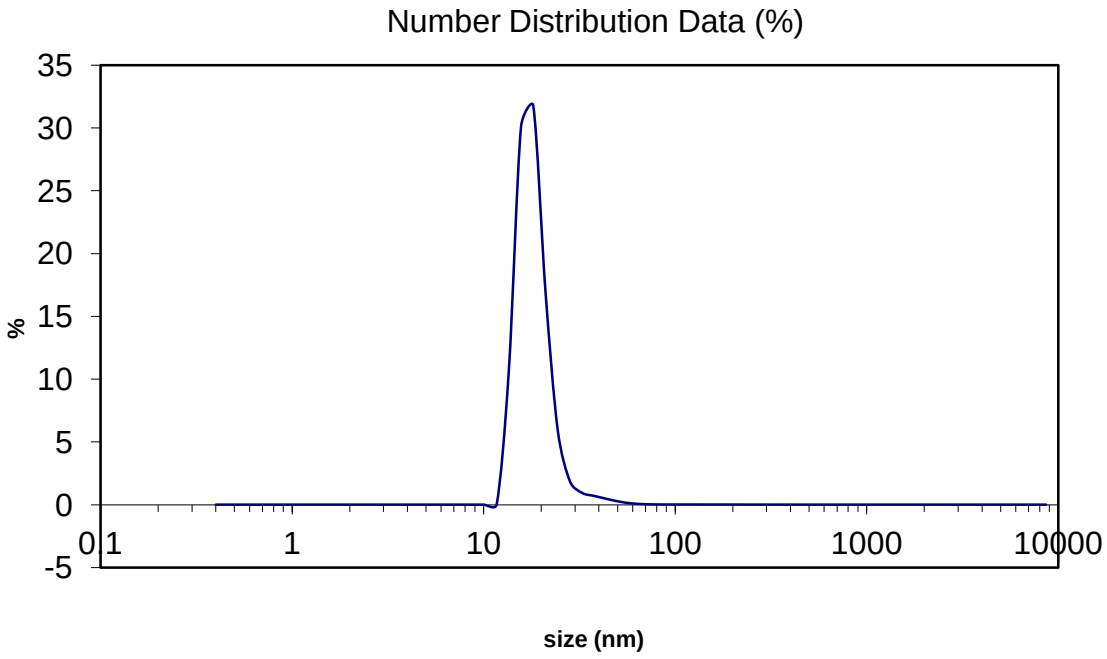
Number Distribution Data (%)
35
30
25
20
15
10
5
0
-5
%
0.1
1
10
100
1000
10000
size (nm)

Figure 6.

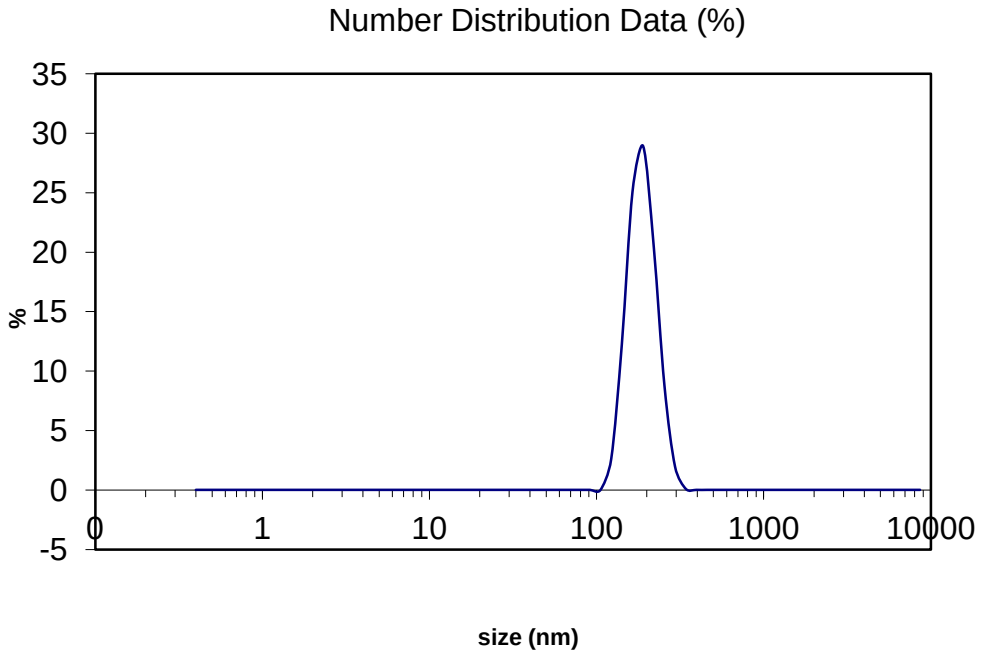
Number Distribution Data (%)
35
30
25
20
15
10
5
0
-5
%
0
1
10
100
1000
10000
size (nm)

Figure 7.

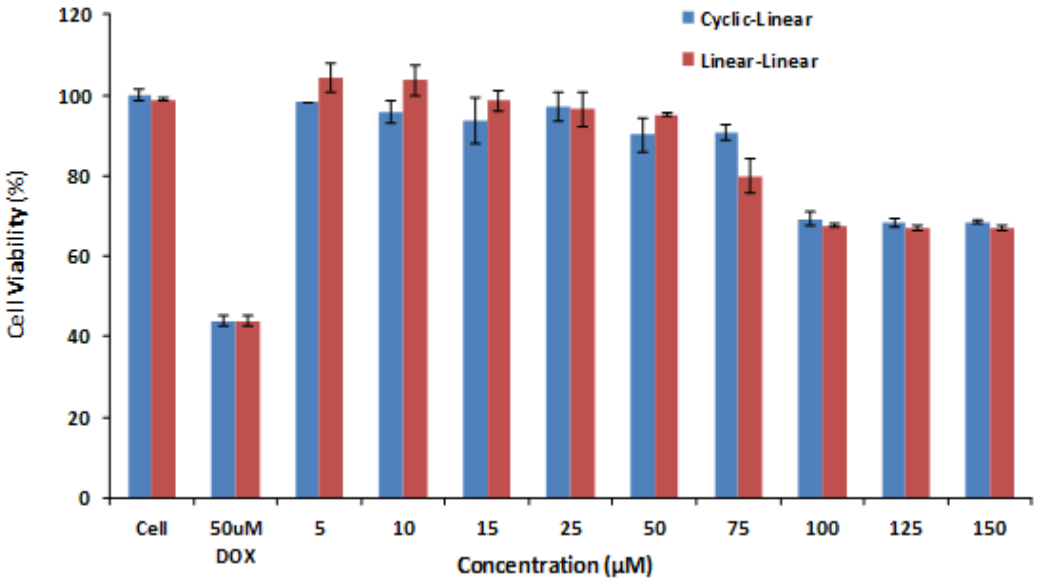
Cyclic-Linear
Linear-Linear
Cell Viability (%)
120
100
80
60
40
20
0
Cell
50uM DOX
5
10
15
25
50
75
100
125
150
Concentration (μM)

Figure 8.

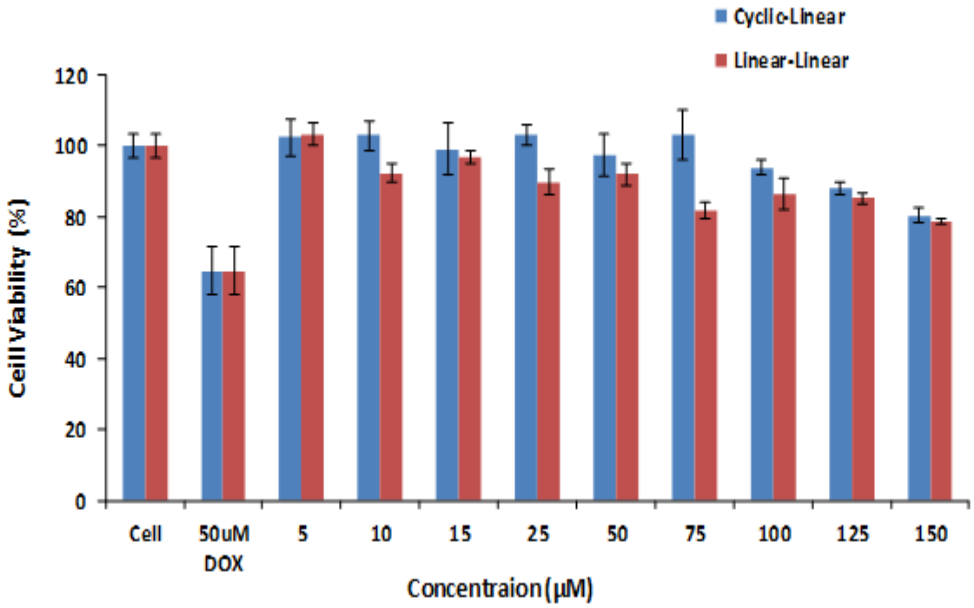
Cyclic-Linear
Linear-Linear
120
100
80
60
40
20
0
Ceill Viability (%)
Cell
50uM DOX
5
10
15
25
50
75
100
125
150
Concentraion (μM)

Figure 9.

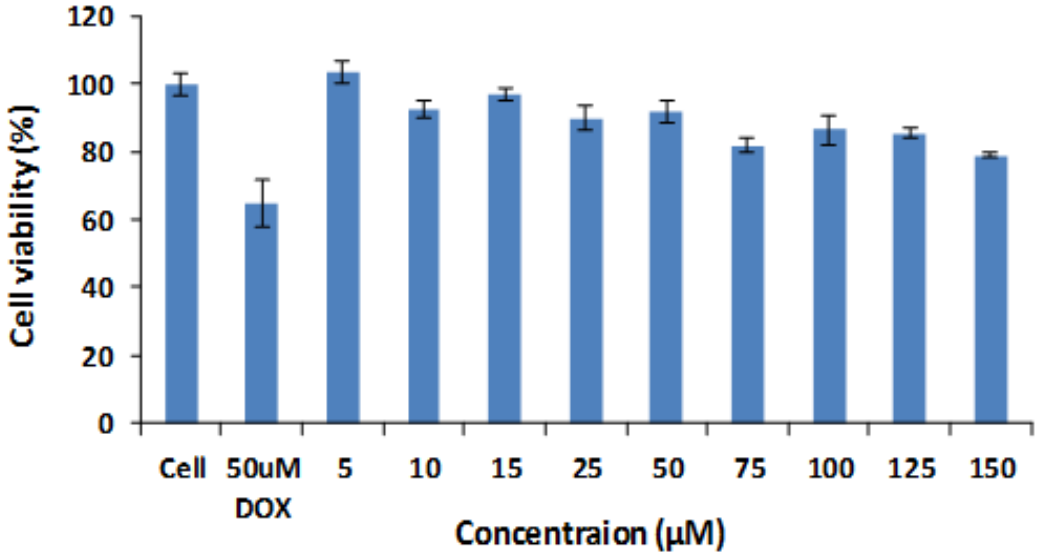
120
100
80
60
40
20
0
Cell viability (%)
Cell
50uM DOX
5
10
15
25
50
75
100
125
150
Concentraion (µM)

Figure 10.

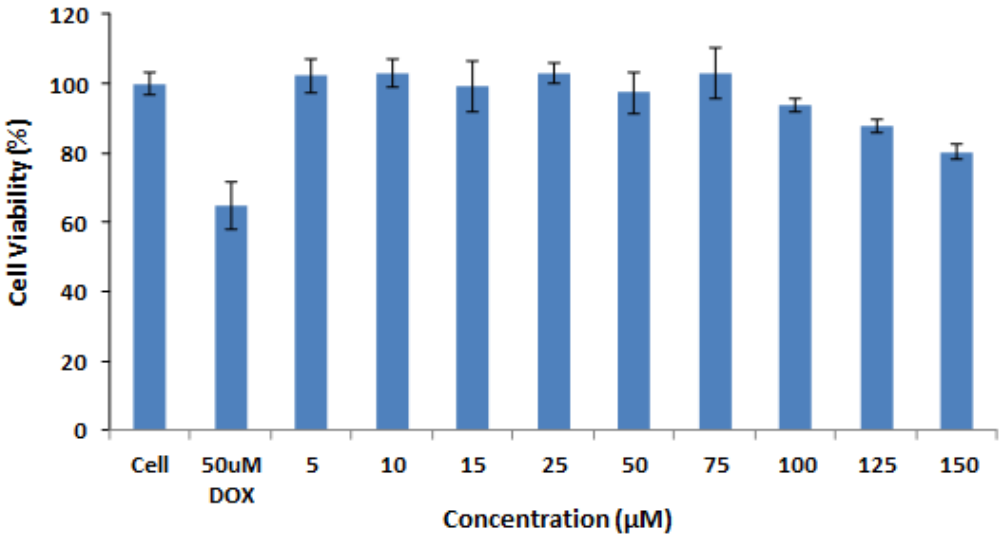
120
100
80
60
40
20
0
Cell Viability (%)
Cell
50uM DOX
5
10
15
25
50
75
100
125
150
Concentration (µM)

Scheme Legends:

Scheme 1. Synthesis of linear $(W(pG))_3$ as the building block.

Scheme 2. Synthesis of cyclic $[W(pG)]_3$ as the building block.

Scheme 3. Synthesis of positively charged peptide containing azide as the building block.

Scheme 4. Synthesis of linear- linear $(WG(triazole\text{-}KR\text{-}NH_2))_3$ and cyclic-linear $[WG(triazole\text{-}KR\text{-}NH_2)]_3$.

Scheme 1.

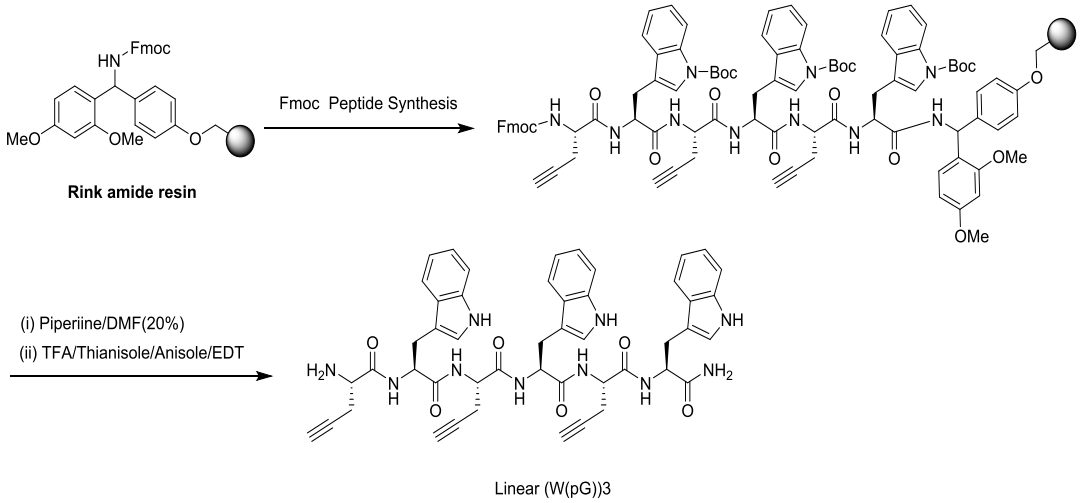
HN
Fmoc
MeO
OMe
O
Rink amide resin
Fmoc Peptide Synthesis
N–Boc
Fmoc
OMe
OMe
(i) Piperiine/DMF(20%)
(ii) TFA/Thianisole/Anisole/EDT
NH
H2N
NH2
Linear (W(pG))3

Scheme 2.

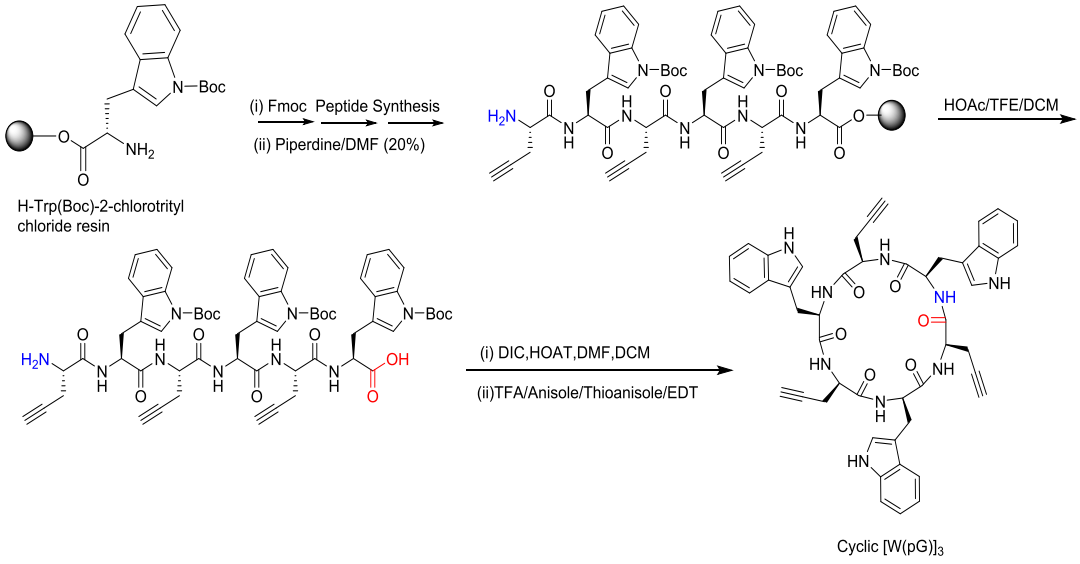
N–Boc
NH2
(i) Fmoc Peptide Synthesis
(ii) Piperdine/DMF (20%)
H-Trp(Boc)-2-chlorotrityl
chloride resin
HOAc/TFE/DCM
OH
(i) DIC,HOAT,DMF,DCM
(ii)TFA/Anisole/Thioanisole/EDT
Cyclic [W(pG)]3

Scheme 3.

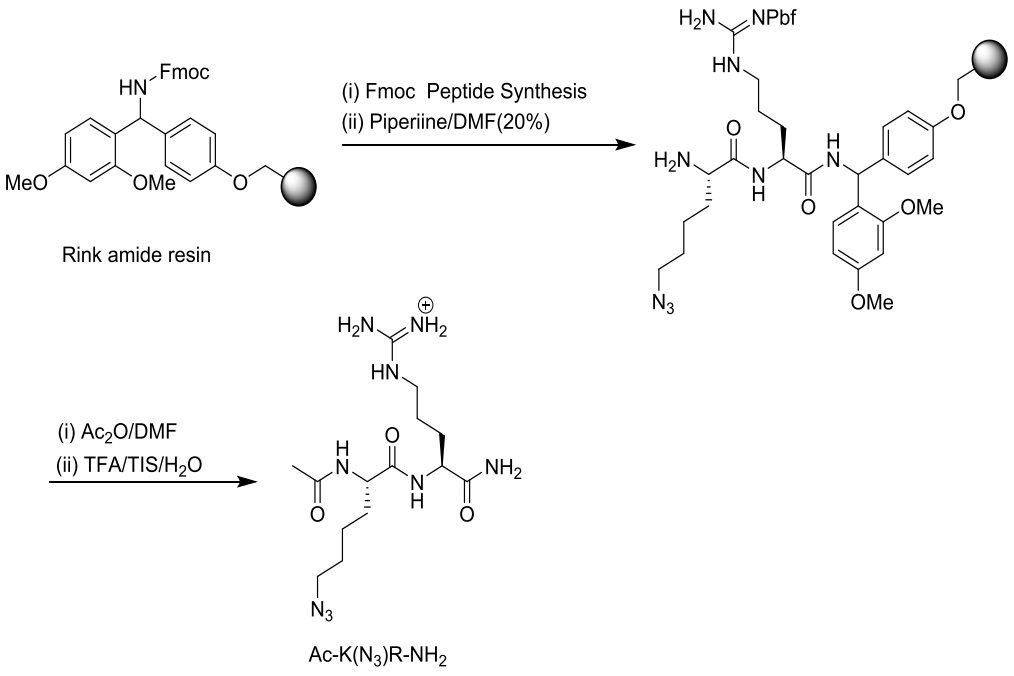
Fmoc
HN
MeO
OMe
O
Rink amide resin
(i) Fmoc Peptide Synthesis
(ii) Piperiine/DMF(20%)
H2N
NPbf
HN
O
H2N
N
H
O
H
N
O
OMe
OMe
N3
(i) Ac2O/DMF
(ii) TFA/TIS/H2O
H2N
NH2
HN
H
N
O
O
N
H
NH2
O
O
N3
Ac-K(N3)R-NH2

Scheme 4.

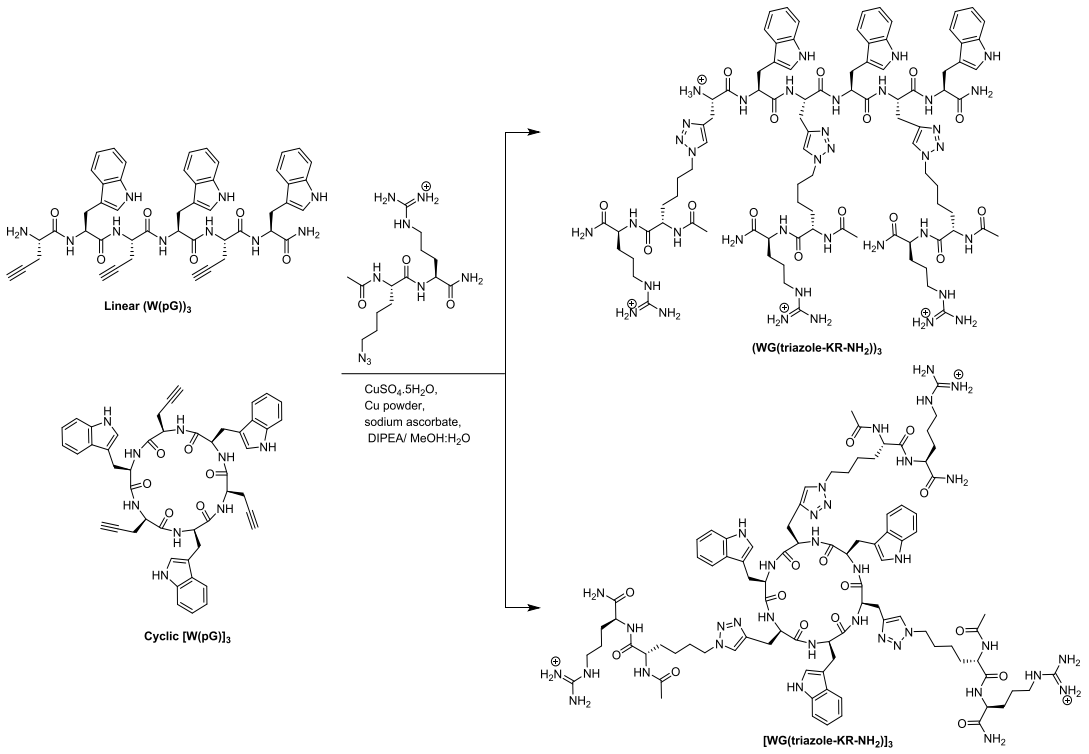
Linear (W(pG))3
Cyclic [W(pG)]3
CuSO4.5H2O,
Cu powder,
sodium ascorbate,
DIPEA/ MeOH:H2O
(WG(triazole-KR-NH2))3
[WG(triazole-KR-NH2)]3

CHAPTER 2

Manuscript II

Submitted to ***Journal of Molecular Modeling***, 2014.

Cyclic Peptide Nanostructures as Drug Delivery Systems: Structural Insights and Dynamical Behavior

Antara Banerjee[a], Nasser Sayeh[b], Amir Nasrolahi Shirazi[b,c], Rakesh Tiwari [b,c], Keykavous Parang[b,c,*], and Arpita Yadav[a,*]

[a]Department of Chemistry, University Institute of Engineering and Technology Chhatrapati Shahuji Maharaj University, Kanpur 208024, India; [b]Department of Biomedical and Pharmaceutical Sciences, College of Pharmacy University of Rhode Island, Kingston, Rhode Island 02881, United States; [c]Chapman University School of Pharmacy, Irvine, CA 92618, United States

Graphical Abstract

Cyclic Peptide Nanostructures as Drug Delivery Systems: Structural Insights and Dynamical Behavior

Antara Banerjee[a], Nasser Sayeh[b], Amir Nasrolahi Shirazi[b,c], Rakesh Tiwari [b,c], Keykavous Parang[b,c,*], and Arpita Yadav[a,*]

[a]Department of Chemistry, University Institute of Engineering and Technology, Chhatrapati Shahuji Maharaj University, Kanpur 208024, India

[b]Department of Biomedical and Pharmaceutical Sciences, College of Pharmacy, University of Rhode Island, Kingston, Rhode Island 02881, United States, [c]Chapman University School of Pharmacy, Irvine, CA 92618, US

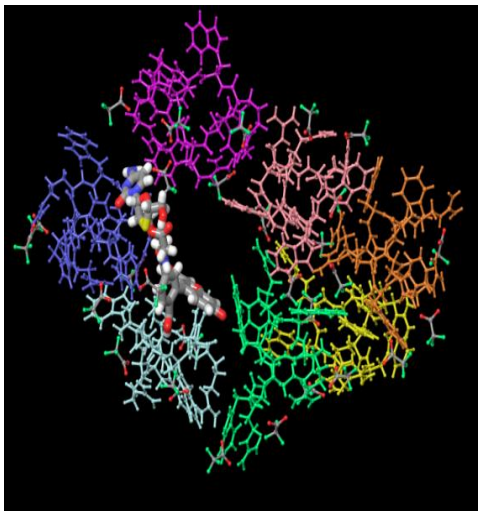

Ab initio molecular orbital calculations alongwith molecular dynamics simulations and experimental results are reported for nanostructure formation by amphiphilic peptides suitable for enhancing drug delivery. It was shown that conformational flexibility, charge environment, and hydrophilicity-lipophilicity balance of these peptides play important roles in determining the nanostructure and its suitability for drug transportation across cell membrane.

Abstract

The objective of this study was to understand the differential behavior of nanostructures formed by cyclic peptides containing tryptophan and arginine residues at the molecular level. $[WR]_4$ was reported to be effective in enhancing cellular delivery of a number of drugs, such as lamivudine (2′,3′-dideoxy-3′-thiacytidine, 3TC) and dasatinib while $[WG(triazole\text{-}KR\text{-}NH_2)]_3$ was found to be an inefficient molecular transporter. Ab initio molecular orbital calculations coupled with molecular dynamics simulation studies along with experimental results showed that nanostructure formation by these cyclic peptides were induced by counterions. Our results showed the suitability of $[WR]_4$ system in enhancing the delivery of fluorescence-labeled drugs (e.g., fluorescence-labeled 3TC (F′-3TC) and fluorescence-labeled daststinib (F′-Das)) were consistent with the experimental results. The conformational flexibility, charge environment, and hydrophilic-lipophilic balance (HLB) of these peptides were found to play important roles in determining their drug delivery capabilities.

Introduction

Bioorganic peptide nanostructure refers to a synthetic peptide molecule that can spontaneously self-assemble to form structures of diameter up to 50 nm. Such self-assembled structures have drawn the attention of scientists in diverse fields due to attractive applications in medicine, material science, biotechnology, and nanotechnology based devices.[1-6] These self-assembled structures are largely held together by non-covalent interactions like hydrogen bonding, electrostatic interactions, and hydrophobic interactions.[7-9] Self-assembling systems have conventionally been of interest to scientists requiring different types of ecofriendly biosurfactants for membrane stabilization.

Peptides surfactants, or pepfactants, have emerged as interesting alternatives forming dynamic nanostructures in pure solution. Cyclic peptides with amphiphilic groups are more stable as compared to their linear counterparts but have remained less studied due to their synthetic complexities.[10] We have recently reported on some amphiphilic cyclic L-peptides forming spontaneous nanostructures acting as stabilizing agents for silver nanoparticles and proteins.[11] Self-aggregation of biosurfactants in the bulk aqueous phase forms different shapes like spherical, bilayer, or cylindrical depending on hydrophilic-lipophilic balance (HLB). It is known that short amphiphilic peptides containing 10–30 amino acid residues (mostly cationic residues like arginine or lysine) possess the ability to penetrate the cell membrane.[12-15] These cell-penetrating peptides (also referred to as CPPs) have been successfully utilized to deliver a large number of macromolecules like proteins, oligonucleotides, and polysaccharides

intracellularly without causing significant toxicity.[16-25] CPPs can exert their effect in vitro and in vivo in micromolar concentrations.[26]

We have reported 27-fold enhancement in the cellular uptake of fluorescence-labelled phosphopeptide F'-PEpYLGLD in presence of 50 μM solution of cyclic peptide $[WR]_4$ (Figure 1) containing tryptophan and arginine residues.[27] Isothermal calorimetry studies confirmed the interaction between the cyclic peptide carrier and the negatively charged cargo phosphopeptides. We have recently designed and reported amphiphilic triazolyl peptides (Scheme 1) synthesized from peptide building blocks containing alkyne and azide functional groups. Cyclic $[W(pG)]_3$ (containing alkyne) (where (pG) = propargylglycine) was conjugated with a peptide functionalized with azide group, Ac-$K(N_3)R$-NH_2, through click chemistry to afford cyclic-linear $[WG(triazole\text{-}KR\text{-}NH_2)]_3$ peptide (Figure 1).[28] The resulting cyclic-linear peptide formed nanostructures and was compared as a drug delivery system with $[WR]_4$.

In the present work, we report on the structural and dynamical aspects of these nanostructures and how these properties govern their drug delivery capabilities. We investigated how the morphology of these systems can be tuned to attain desired nanostructures with desired drug delivery capabilities. Ab initio molecular orbital calculations were used in conjunction with intermolecular interaction studies and molecular dynamics simulations.

Methods

Ab initio molecular orbital calculations [29,] with complete geometry optimizations, were performed at the Hartree Fock level utilizing CEP-31G [30] basis set for the monomer cyclic peptides. Geometry optimizations were performed utilizing Berny's gradient method.[31,32] Self-assembly was explored step by step to determine the possibility of dimer formation, trimer, tetramer, respectively, by repeated interaction energy calculations. Every time a monomer is added interaction energy was calculated as

$$\text{Interaction energy} = E_{\text{complex of n monomers}} - (n.\ E_{\text{monomer}})$$

In this case since the monomers are cationic and repel each other in the absence of counterions, this is the energy consumed in nanoparticulate formation in the absence of counter ions. In the presence of counter ions, energy released in nanoparticulate formation is given as

$$\text{Interaction energy} = E_{\text{complex of n monomers and m counterions}} - (n.\ E_{\text{monomer}} + m\ E_{\text{counterion}})$$

Different possibilities of self-assembly were considered, such as tubular, film formation, and spherical nanoparticulate formation in presence and absence of counterions. Self-aggregation and nanostructure formation were considered in the presence of inducing trifluoroacetate counterions present under experimental conditions. Trifluoroacetic acid (TFA) (2%) was added to water and acetonitrile for HPLC purification.

These calculations were carried out using GAUSSIAN '09[33] software and GAUSSVIEW[34] was used for viewing purposes. After nanostructure formation, its role as drug delivery system was investigated through molecular dynamics simulations. First the cargo drug was docked inside the nanostructure manually. The stability of this loaded nanostructure with time and its dynamical behavior were then studied utilizing molecular dynamics simulation. The containment of drug for a period followed by its delivery was also studied through simulations.

The self-aggregated nanostructure in presence of counterions with drug loaded in core was subjected to relaxation prior to molecular dynamics simulations. System was then subjected to simulated annealing followed by long dynamics at 300K. Shaw's Desmond software[35,] was utilized for the purpose using OPLS force field.[36] NPT (isothermal-isobaric) ensemble was taken using Martyna-Tobias-Klein barostat method.[37] Reversible reference system propagator algorithms (RESPA integrator) was used with 2 fs time step for near and bonded atoms and 6 fs time step for far atoms.[38] Coulombic interaction cutoff was set at 9.0 A. 3.0 ns trajectory was evaluated in each case. Energy analysis and RMSD analysis for all heavy atoms are presented to judge the stability of the system with time. RMSD was taken with reference to frame zero after relaxation of the system.

Cell-based Assays

Cell Culture

Human leukemia cells (CCRF-CEM, ATCC no. CCL-119) were purchased obtained from American Type Culture Collection. Cells were cultured in 75 cm^2 flasks containing RPMI-16 medium. The medium contains supplemental, such as fetal bovine serum (FBS, 10%) as well as penicillin-streptomycin (penicillin: 1%, 10 000 units and streptomycin: 10 mg in 0.9% NaCl) that were used under humidified atmosphere balancing CO_2 (5%) and air (95%) at 37 °C.

Flow Cytometry Studies

CCRF-CEM cells (1×10^7/well) were plated in 6-well plates. Fluorescence-labeled dasatinib (F´-Das) was used as a model drug for this comparative experiment. Thus, F´-Das (5 μM) was added alone and in combination with $[WR]_4$[11b] and $[WG(triazole\text{-}KR\text{-}NH_2)]_3$[28] into wells. All experiments were carried out in triplicate. All plates were kept at 37 °C for 2 h. In this assay, cells with no treatment with F´-Das were employed as negative controls. The treatments were removed after 2 h of incubation. To wash the cell membrane surface, trypsin−EDTA solution was used for 5 min. After that, the cells were twice washed with PBS (5 min each time). To prepare cells for analysis, they were resuspended in flow cytometry buffer and filtered. The analysis of the experiment was performed by FACSVerse flow cytometer using FITC channel. The data for each entry was acquired based on the signal mean fluorescence in 10,000 cells.

All assays were performed in triplicate. A similar procedure was used for flow cytometry studies of the fluorescence-labeled 3TC (F′-3TC) in the presence of the peptides.

Results and Discussion

We have previously shown that peptides containing amino acids with hydrophobic and positively charged residues can form nanostructures at room temperature.[11] The presence of optimized balance between hydrophobicity and charge was determined to be a major driving force for the formation of self-assembled nanostructures through inter and intramolecular interactions.

Initial TEM imaging of $[WR]_4$ showed that this peptide forms nano-spherical particles with the size of 70-85 nm. Multiple forces could be responsible in forming nanosized structure. Hydrophobic segments of the peptide can trigger the supramolecular self-assembly and force the peptide to generate nanospherical structures. Furthermore, TEM investigations on size and morphologies of $[WG(triazole\text{-}KR\text{-}NH_2)]_3$ showed that this peptide can also form spherical structures in the size range of 50-80 nm in aqueous media (Figure 2). Several factors can be involved in the formation of such a structure, including hydrogen bonding and hydrophobic forces.[28] TEM observation revealed that although the structure of $[WG(triazole\text{-}KR\text{-}NH_2)]_3$ and $[WR]_4$ are different, they generated nanoparticles with similar size range and morphologies. Chemical structure of $[WG(triazole\text{-}KR\text{-}NH_2)]_3$ represents a higher degree of flexibility in arginine side chains compared to that of $[WR]_4$.

However, existence of triazole rings could also induce some degree of rigidity to the structure of $[WG(triazole\text{-}KR\text{-}NH_2)]_3$. These data suggest that the orientation of amino acids, such as tryptophan and arginine, can determine the size and morphologies of nanostructures.

Cyclic peptide containing tryptophan and arginine $[WR]_4$ and the amphiphilic triazolyl cyclic-linear peptide $[WG(triazole\text{-}KR\text{-}NH_2)]_3$ were completely optimized utilizing *ab initio* Hartree Fock molecular orbital calculations at the CEP-31G level. The structures of these systems along with their optimized conformations are shown in Figure 1. The molecular electrostatic potential surfaces for both systems are shown in Figure 3. Both systems are cationic in nature, and the data clearly indicate that they require inducing counterions for self-aggregation. However, this became more obvious on a detailed examination of the differences in the potential surfaces of both systems.

In $[WG(triazole\text{-}KR\text{-}NH_2)]_3$ system, the positive charge is located at the ends of the long $KR\text{-}NH_2$ side chains; whereas in $[WR]_4$ system the positive charge is delocalized over the entire system. Because of these differences, the location of counterions in both systems is quite different resulting in a more compact spherical aggregated form in $[WR]_4$ that is more stable. The experimental procedure for purification of both peptides required the use of trifluoroacetate (TFA). Thus, TFA ions were present as the counterions. Considering the availability of these ions, ab initio intermolecular interaction calculations were performed to study counterion-induced self-aggregation of these systems.

As mentioned earlier, self-aggregation may be in different shapes. Therefore, we examined multiple shapes relevant to explain the behavior of these systems at lipid membrane interface and their molecular transporter properties. Results for self-aggregation of cyclic peptide $[WR]_4$ and cyclic-linear peptide $[WG(triazole\text{-}KR\text{-}NH_2)]_3$ are shown in Figures 4 and 5, respectively. Both systems showed formation of spherical nanoparticulates suitable for drug carriage and delivery. The linear or tubular stacking does not generate an inner core sufficiently large enough for the carriage of drugs or molecules. The monomer conformations of cyclic peptides under consideration are not appropriate for tubular structure formation. Overall charge neutrality was maintained in the aggregated form to enable us to study the dynamical behavior utilizing simulation studies. The nanostructure formed by $[WR]_4$ system has the dimensions 7.2 nm x 6.9 nm x 2.0 nm while the nanostructure formed by $[WG(triazole\text{-}KR\text{-}NH_2)]_3$ system has the dimensions 12.0 nm x 10.6 nm x 3.2 nm. These dimensions may vary with variations in aggregated forms but are indicative that the aggregated forms lie in the range of nanostructure.

To compare the transporting ability of $[WG(triazole\text{-}KR\text{-}NH_2)]_3$ and $[WR]_4$, a flow cytometry assay was carried out. Fluorescence-labeled dasatinib (F'-Das) was employed as a model molecular cargo. The intracellular uptake of F'-Das was evaluated in the presence of $[WG(triazole\text{-}KR\text{-}NH_2)]_3$ and $[WR]_4$ and compared with that of the drug alone. As it is shown in Figure 6, the presence of $[WR]_4$ enhanced the cellular uptake of F'-Das by 2.5 fold compared to that of F'-Das alone. However, the results showed that the intracellular uptake of F'-Das was not enhanced in the presence of $[WG(triazole\text{-}KR\text{-}NH_2)]_3$. These data indicated that although both peptides contain

tryptophan and arginine amino acids, they have different transporting abilities for the delivery of F'-Das due to other factors.

Moreover, the intracellular transporting potency of $[WR]_4$ and $[WG(triazole\text{-}KR\text{-}NH_2)]_3$ were compared by using lamivudine (3TC), an anti-HIV drug. The fluorescence-labeled 3TC was prepared based on our previously reported procedure.[11] As expected, the flow cytometry results showed that the cellular uptake of F´-3TC (5 μM) was increased by more than 3-fold when mixed with $[WR]_4$ (50 μM). However, uptake of F´-3TC was reduced in the presence of $[WG(triazole\text{-}KR\text{-}NH_2)]_3$. These data confirmed that $[WR]_4$ is a molecular transporter while $[WG(triazole\text{-}KR\text{-}NH_2)]_3$ is inefficient in improving the cellular delivery.

Molecular modeling and ab intio intermolecular interaction calculation were used to explain the differential behavior of these two cyclic peptides as molecular transporters. The drugs were loaded inside nanostructure to study their carriage and delivery by the peptides. Figures 7 and 8 shows a comparison of solvation energy of fluorescence-labeled 3TC (F′-3TC) and dasatinib and stabilization of drugs inside the nanostructures formed by the two cyclic peptides.

The stabilization of drug inside nanostructures clearly indicates why the drug will be spontaneously encapsulated by the peptides. Figure 9 shows a comparison of solvation energy of fluorescence-labeled dasatinib (F′-Das) and its stabilization inside the nanostructures formed by cyclic peptides. In this case, stabilization offered by peptide nanostructures indicates spontaneous encapsulation of drug. It is also to be noted that the stabilization of drug inside the nanostructure formed by $[WG(triazole\text{-}KR\text{-}NH_2)]_3$ system

is lower than that of $[WR]_4$. This is due to overall lower charge on $[WG(triazole\text{-}KR\text{-}NH_2)]_3$ resulting in less number of counterions and less compact nanostructure due to monomer conformation.

The stability of encapsulated drug and chances of premature expulsion were studied by molecular dynamics simulation studies by evaluating 3ns trajectory. The results for carriage of both the drugs by $[WR]_4$ peptide nanostructure are shown in Figure 10. Snapshot of system during relaxation and root mean square deviations (RMSD) of all heavy atoms throughout simulation are also shown in Figure 10. The RMSD plot clearly shows a reduction in mobility of peptide monomers on nanostructure formation with trifuoroacetate counterions and after loading nanostructure with F′-3TC as well. Encapsulation of F′-Das leads to some instability perhaps due to the larger size of the drug.

Carriage of fluorescence-labeled anti-HIV drug F′-3TC and anticancer drug F′-Das by $[WG(triazole\text{-}KR\text{-}NH_2)]_3$ nanostructure are shown in Figure 11. Snapshots of relaxed system during simulation show a very loosely held nanostructure which has opened up to some extent depicting probability of premature expulsion of both the drugs. Moreover, noticeable is the significant change in monomer conformations with folded ($KR\text{-}NH_2$) side chains. The flexible side chains of this peptide have folded to maximize electrostatic interactions with TFA and intramolecular H-bonding as opposed to interactions with the drug.

This is in contrast to the encapsulation of these drugs by $[WR]_4$ nanostructure which maximizes interactions with drugs to form a compact loaded nanostructure. The

HLB of this system also seems to play a critical role in this reorganization leading to loosely held nanostructures inappropriate for drug delivery. RMSD shows little effect of drug loading perhaps due to opening of nanostructure and expulsion of the drug at the time of relaxation itself during initial stages of the simulation.

This study depicts the suitability of cyclic peptide $[WR]_4$ nanostructures in enhancing the bioavailability of anti-HIV and anticancer drugs of appropriate size. However, cyclic peptides containing cell permeability enhancing arginine residues, but with high mobility of side chains are found to be unsuitable for delivery purposes.

Conclusions

In this study, we have presented ab initio molecular orbital calculations coupled with molecular dynamics simulation studies to show how cyclic amphiphilic peptide $[WR]_4$ forms nanostructures by self aggregation induced by counterions and enhances the cellular delivery of certain nuclear targeted anticancer agents. We have also shown that in $[WG(\text{triazole-KR-}NH_2)]_3$ the cargo-loaded nanostructures were not stable, leading to premature expulsion of the drug and no significant enhancement in cellular delivery. The conformational flexibility of cyclic peptides, their charge environment, and HLB ratio all play important roles in governing the self-aggregation and molecular transporter properties of these amphiphilic cyclic peptides. Molecular dynamics simulation results confirm the experimental cellular assay observations.

Acknowledgements

Dr. Antara Banerjee and Dr. Arpita Yadav gratefully acknowledge financial support (Project no. DST/SR/S1/OC-82/2012) from Science and Engineering Research Board (SERB), Department of Science and Technology, New Delhi. Dr. Antara Banerjee is also thankful to SERB for Senior Research Fellowship. We thank the National Institute of General Medical Sciences of the National Institutes of Health under Grant No. 8 P20 GM103430-12 for sponsoring the core facility.

References

1. Zhang S. Fabrication of novel biomaterials through molecular self-assembly. *Nat. Biotechnol.* **2003**, *21*, 1171-1178.

2. Whitesides, G.M.; Mathias J.P.; Set C.T. Molecular self-assembly and nanochemistry: a chemical strategy for the synthesis of nanostructures. *Science*. **1991,** *254*, 1312-1315.

3. Ghadiri, M.R.; Granja, J.R.; Buehler, L.K. Artificial transmembrane ion channels from self-assembling peptide nanotubes. *Nature*. **1994**, *369*, 301-304.

4. Ellis-Behnke, R.G.; Liang, Y.X.; You, S.W.; Tay, D.K.; Zhang, S.; So, K.F.; Schneider, G.E. Nano neuro knitting: peptide nanofiber scaffold for brain repair and axon regeneration with functional return of vision. *Proc. Natl. Acad. Sci. USA*. **2006**, *103*, 5054-5059.

5. Nuraje, N.; Banerjee, I.A.; MacCuspie, R.I.; Yu, L. Matsui H. Biological bottom-up assembly of antibody nanotubes on patterned antigen arrays. *J. Am. Chem. Soc*. **2004**, *126*, 8088-8089.

6. Yemini, M.; Reches, M.; Rishpon, J.; Gazit, E. Novel electrochemical biosensing platform using self-assembled peptide nanotubes. *Nano Lett.* **2005**, *5*, 183-186.

7. Bryson, J.W.; Betz, S.F.; Lu, H.S.; Suich, D.J.; Zhou, H.X.; O'Neil, K.T.; De Grado, W.F. Protein design: a hierarchic approach. *Science*. **1995**, *270*, 935-941.

8. Dill, K.A. Dominant forces in protein folding. *Biochemistry*. **1990,** *29*, 7133-7155.

9. Brooks, C.L. Protein and peptide folding explored with molecular simulations. *Acc. Chem. Res*. **2002**, *35*, 447-454.

10. Katsara, M.; Selios, T.T.; Deraos, S.; Deraos, G.; Matsoukas, M.T.; Lazoura, E.; Matsoukas, J.; Apostolopoulos, V. Round and round we go: cyclic peptides in disease. *Curr. Med. Chem*. **2006**, *13*, 2221-2232.

11.a) Mandal, D.; Tiwari, R.K.; Shirazi, A.N.; Oh, D.; Ye, G.; Banerjee, A.; Yadav, A.; Parang, K. Self-Assembled Surfactant Cyclic Peptide Nanostructures as Stabilizing Agents. *Soft Matter*. **2013**, *9*, 9465-9475. b) Mandal, D.; Nasrolahi Shirazi, A.; Parang, K. Cell-penetrating homochiral cyclic peptides as nuclear-targeting molecular transporters. *Angewandte Chemie, International Edition*. **2014**, *50*, 9633-9637.

12. Langel, U. in Cell-penetrating peptides: Processes and applications, Boca Raton, *CRC Press*. **2002**.

13. Fischer, P.M.; Krausz, E.; Lane, D.P. Cellular delivery of impermeable effector molecules in the form of conjugates with peptides capable of mediating membrane translocation. *Bioconjugate Chem*. **2001**, *12*, 825-841.

14. Langel, U. in Cell-penetrating peptides: Methods and protocols in molecular biology, *Humana Press, New York*. **2011**.

15. Hansen, M.; Kilk, K.; Langel, U. Predicting cell-penetrating peptides. *Adv. Drug Deliv. Rev*. **2008**, *60*, 572-579.

16. Fawell, S.; Seery, J.; Daikh, Y.; Moore, C.; Chen, L.L.; Pepinsky, B.; Barsoum, J. Tat-mediated delivery of heterologous proteins into cells. *Proc. Natl. Acad. Sci. US.* **1994**, *91*, 664-668.

17. Rojas, M.; Donahue, J.P.; Tan, Z.; Lin, Y.Z. Genetic engineering of proteins with cell membrane permeability. *Nat. Biotechnol*. **1998**, *16*, 370-375.

18. Theodore, L.; Derossi, D.; Chassaing, G.; Llirbat, B.; Kubes, M.; Jordan, P.; Chneiweiss, H.; Godement, P.; Prochiantz, A. Intraneuronal delivery of protein kinase C pseudosubstrate leads to growth cone collapse. *J. Neurosci*. **1995**, *15*, 7158-7167.

19. Allinquant, B.; Hantraye, P.; Mailleux, P.; Moya, K.; Bouillot, C.; Prochiantz, A. Down regulation of amyloid precursor protein inhibits neurite outgrowth in vitro. *J. Cell Biol*. **1995**, *128*, 919-927.

20. Morris, M.C.; Vidal, P.; Chaloin, L.; Heitz, F.; Divita, G. A new peptide vector for efficient delivery of oligonucleotides into mammalian cells. *Nucleic Acids Res*. **1997**, *25*, 2730-2736.

21. Henriques, S.T.; Costa, J.; Castanho, M.A. A new peptide vector for efficient delivery of oligonucleotides into mammalian cells. *FEBS Lett*. **2005**, *579*, 4498-4502.

22. Sawant, R.; Torchilin, V. Intracellular delivery of nanoparticles with CPPs. *Methods Mol. Biol*. **2011**, *683*, 431-451.

23. Torchilin, V.P.; Rammohan, R.; Weissig, V.; Levchenko, T.S. TAT peptide on the surface of liposomes affords their efficient intracellular delivery even at low

temperature and in the presence of metabolic inhibitors. *Proc. Natl. Acad. Sci. USA*. **2001**, *98*, 8786-8791.

24. Jarver, P.; Langel U. Cell-penetrating peptides--a brief introduction. *Biochim. Biophys. Acta*. **2006**, *1758*, 260-263.

25. El-Andaloussi, S.; Holm, T.; Langel, U. Cell-penetrating peptides: mechanisms and applications. *Curr. Pharmaceut. Des*. **2005**, *11*, 3597-3611.

26. Munyendo, W.L.L.; Lv, H.; Ingoula, H.B.; Baraza, L.D.; Zhou, J. Cell penetrating peptides in the delivery of biopharmaceuticals. *Biomolecules*. **2012**, *2*, 187-202.

27. Shirazi A.N.; Tiwari, R.K.; Oh, D.; Banerjee, A.; Yadav, A.; Parang, K. Efficient delivery of cell impermeable phosphopeptides by a cyclic peptide amphiphile containing tryptophan and arginine. *Mol. Pharmaceutics*. **2013,** *10*, 2008-2020.

28. Sayeh, N.; Shirazi, A.N.; Oh, D.; Sun, J.; Rowley, D.; Banerjee, A.; Yadav, A.; Tiwari, R.K.; Parang, K. *Curr. Org. Chem*. **2014,** *18*, 2665-2671.

29. Hehre, W.J.; Radom, L.; Schleyer, P.v.R.; Pple, J.A. in Ab initio molecular orbital theory, John Wiley and Sons Inc., New York, USA. **1986**, 2, 10-42.

30. Stevens, W.J.; Krauss, M.; Basch, H.; Jasien, P.G. Relativistic compact effective potentials and efficient, shared-exponent basis sets for the third-, fourth-, and fifth-row atoms. *Can. J. Chem*. **1992**, *70*, 612-629.

31. Peng, C.; Ayala, P.Y.; Schlegel, H.B.; Frisch, M.J. Using redundant internal coordinates to optimize equilibrium geometries and transition states. *J. Comput. Chem*. **1996**, *17*, 49-56.

32. Peng, C.; Schlegel, H.B. Combining synchronous transit and quasi-Newton methods to find transition states. *Israel J. Chem*. **1993**, *33*, 449-545.

33. Gaussian 09, Revision D.01, Frisch, M. J.; Trucks, G. W.; Schlegel, H. B.; Scuseria, G. E.; Robb, M. A.; Cheeseman, J. R.; Scalmani, G.; Barone, V.; Mennucci, B.; Petersson, G. A.; Nakatsuji, H.; Caricato, M.; Li, X.; Hratchian, H. P.; Izmaylov, A. F.; Bloino, J.; Zheng, G.; Sonnenberg, J. L.; Hada, M.; Ehara, M.; Toyota, K.; Fukuda, R.; Hasegawa, J.; Ishida, M.; Nakajima, T.; Honda, Y.; Kitao, O.; Nakai, H.; Vreven, T.; Montgomery, J. A., Jr.; Peralta, J. E.; Ogliaro, F.; Bearpark, M.; Heyd, J. J.; Brothers, E.; Kudin, K. N.; Staroverov, V. N.; Kobayashi, R.; Normand, J.; Raghavachari, K.; Rendell, A.; Burant, J. C.; Iyengar, S. S.; Tomasi, J.; Cossi, M.; Rega, N.; Millam, M. J.; Klene, M.; Knox, J. E.; Cross, J. B.; Bakken, V.; Adamo, C.; Jaramillo, J.; Gomperts, R.; Stratmann, R. E.; Yazyev, O.; Austin, A. J.; Cammi, R.; Pomelli, C.; Ochterski, J. W.; Martin, R. L.; Morokuma, K.; Zakrzewski, V. G.; Voth, G. A.; Salvador, P.; Dannenberg, J. J.; Dapprich, S.; Daniels, A. D.; Farkas, Ö.; Foresman, J. B.; Ortiz, J. V.; Cioslowski, J.; Fox, D. J. Gaussian, Inc., Wallingford CT, **2009**.

34. GaussView, Version 5, Dennington, R.; Keith, T.; Millam, J. *Semichem Inc.*, Shawnee Mission KS,. Conformational stabilities, infrared, and vibrational dichroism

spectroscopy studies of tris(ethylenediamine) zinc(II) chloride. *J. Mol. Model.* **2009** , *15*, 25-34.

35. Bowers, K.J.; Chow, E.; Xu, H.; Dror, R.O.; Eastwood, M.P.; Gregersen, B.A.; Klepeis, J.L.; Kolossvary, I.; Moraes, M.A.; Sacerdoti, F.D.; Salmon, J.K.; Shan, Y.; Shaw, D.E. Proceedings of the ACM/IEEE conference on Spercomputing (SC06), Tampa, Florida. **2006**, 11-17.

36. Jorgensen, W.L.; Tirado-Rives, J. The OPLS [optimized potentials for liquid simulations] potential functions for proteins, energy minimizations for crystals of cyclic peptides and crambin. *J. Am. Chem. Soc*. **1988**, *110*, 1657-1666.

37. Martyna, G.J.; Tobias, D.J.; Klein, M.L. Constant pressure molecular dynamics algorithms. *J. Chem. Phys*. **1994**, *101*, 4177-4189.

38. Tuckerman, M.; Berne, B.J.; Martyna, G.J. Reversible multiple time scale molecular dynamics. *J. Chem. Phys*. **1992**, *97*, 1990-2001.

Figure Legends:

Figure 1. TEM images of $[WG(triazole\text{-}KR\text{-}NH_2)]_3$ (a,b) and $[WR]_4$ (c,d).

Figure 2. Molecular electrostatic potential surfaces of cyclic peptides.

Figure 3. Self-aggregation of $[WR]_4$.

Figure 4. Self-aggregation of $[WG(triazole\text{-}KR\text{-}NH_2)]_3$.

Figure 5. Cellular uptake of F'-Das in the presence of $[WR]_4$ and $[WG(triazole\text{-}KR\text{-}NH_2)]_3$.

Figure 6. Cellular uptake of F'-3TC in the presence of $[WR]_4$ and $[WG(triazole\text{-}KR\text{-}NH_2)]_3$.

Figure 7. Comparison between stabilization of F′-3TC in aqueous solution and stabilization inside peptide nanostructures of $[WG(triazole\text{-}KR\text{-}NH_2)]_3$.

Figure 8. Comparison between stabilization of fluorescein-labeled dasatinib in aqueous solution and stabilization inside peptide $[WG(triazole\text{-}KR\text{-}NH_2)]_3$ nanostructure.

Figure 9. Carriage of fluorescein labeled lamivudine by $[WR]_4$ nanostructure.

Figure 10. Carriage of fluorescein-labeled dasatinib by peptide $[WG(triazole\text{-}KR\text{-}NH_2)]_3$.

Figure 1.

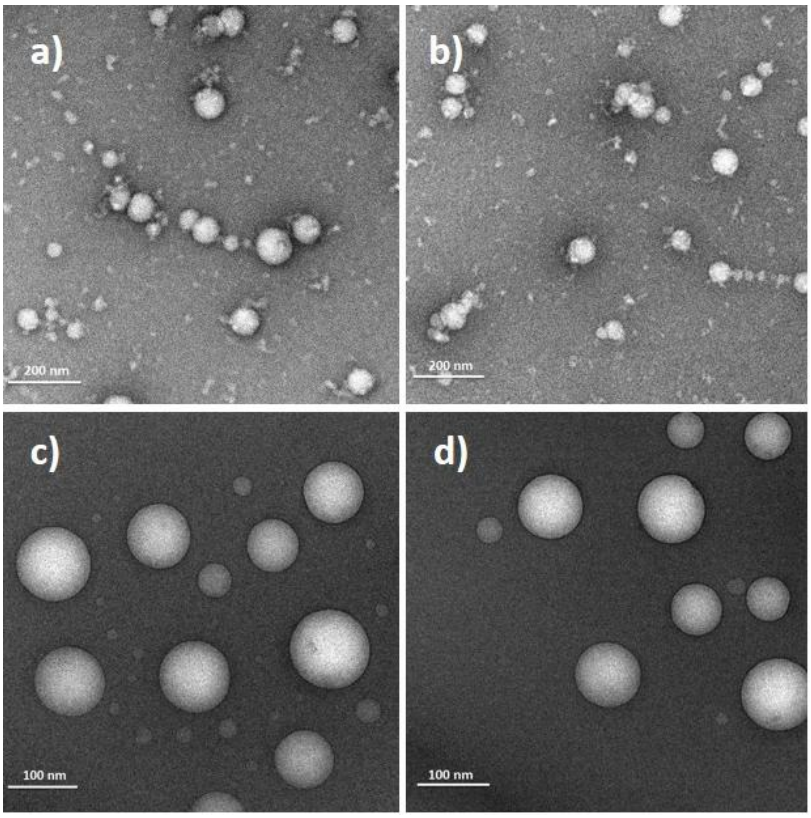

Figure 2.

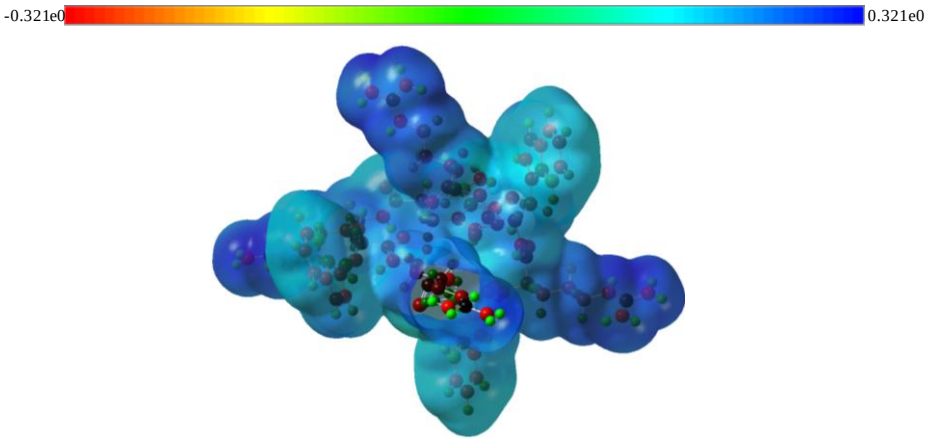

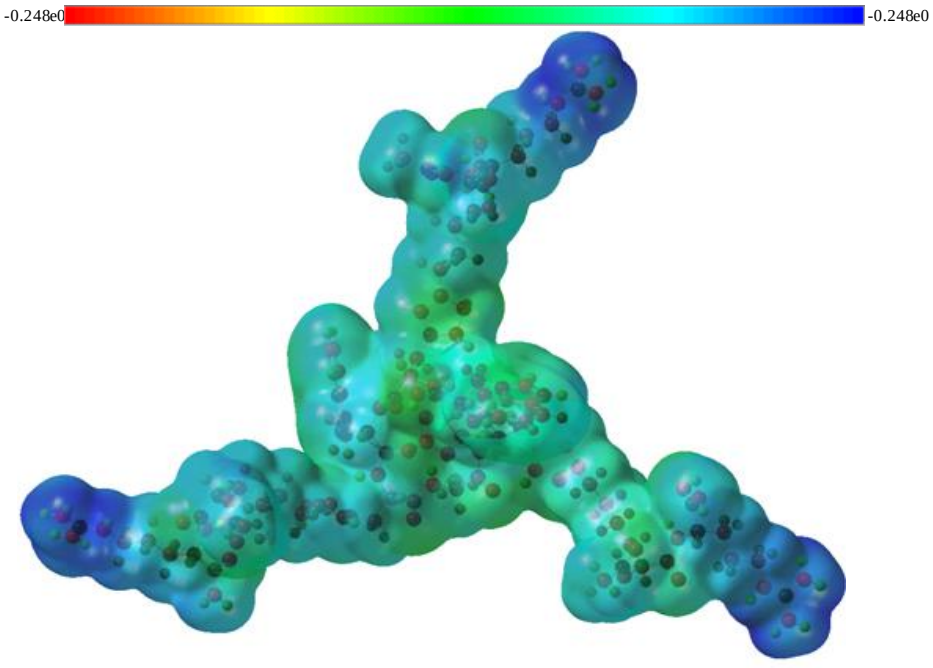

Figure 3.

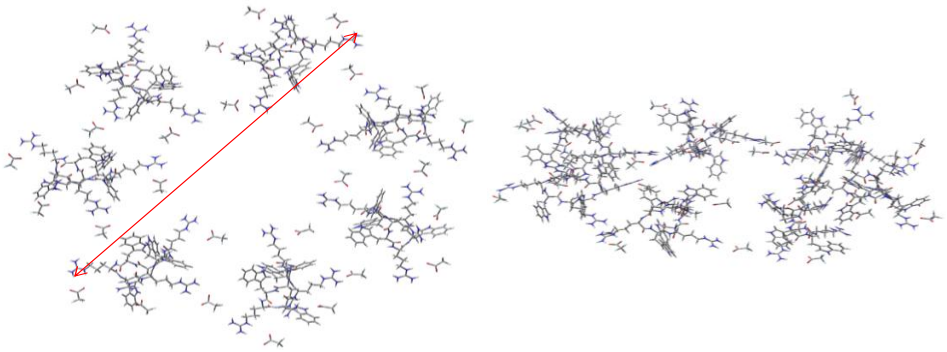

Length ~ 7.2 nm
Breadth ~ 6.9 nm
Height ~2.0 nm

Interaction energy= -2806.14 kCal/mol

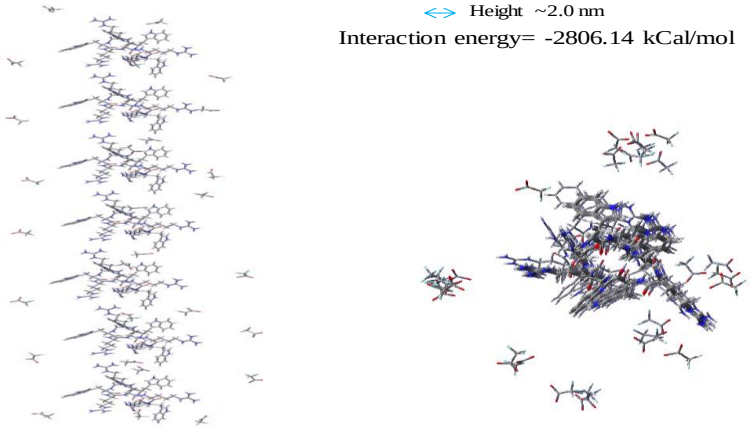

Interaction energy= -1212.93 kCal/mol

Figure 4.

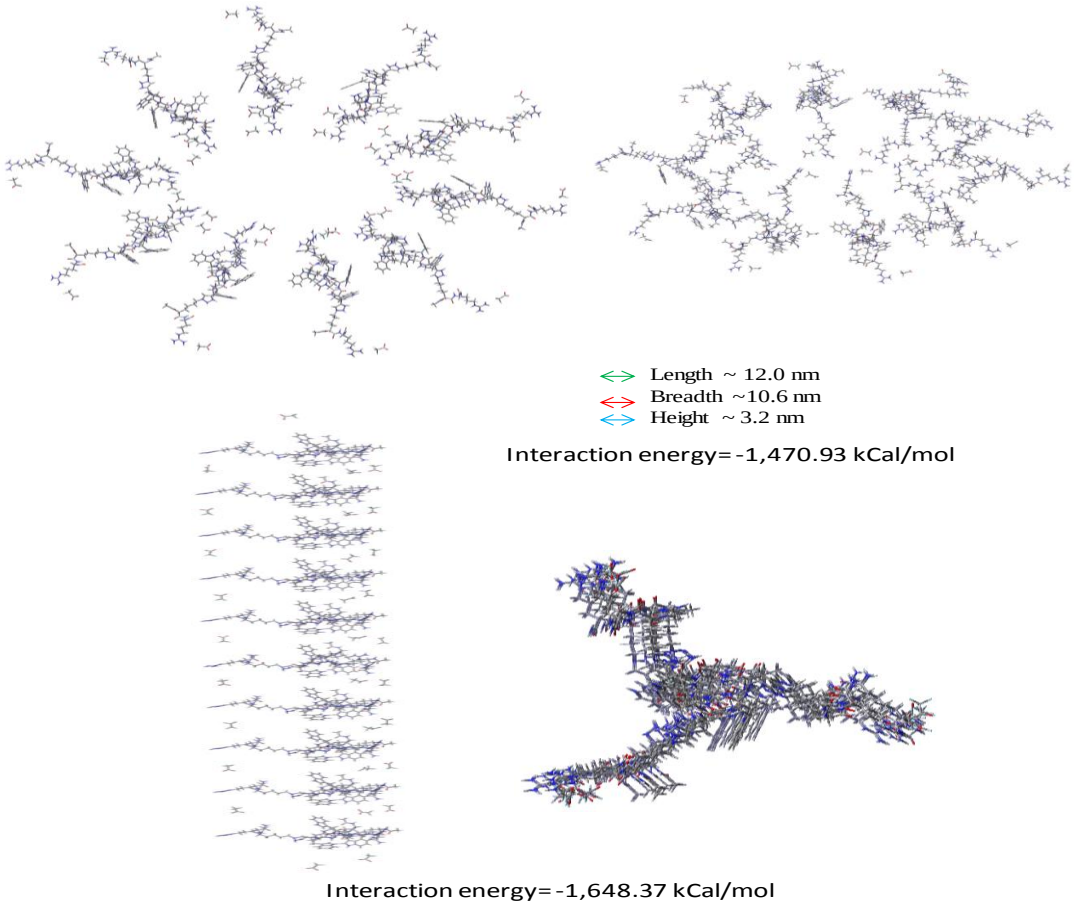
Length ~ 12.0 nm
Breadth ~10.6 nm
Height ~ 3.2 nm
Interaction energy= -1,470.93 kCal/mol
Interaction energy= -1,648.37 kCal/mol

Figure 5.

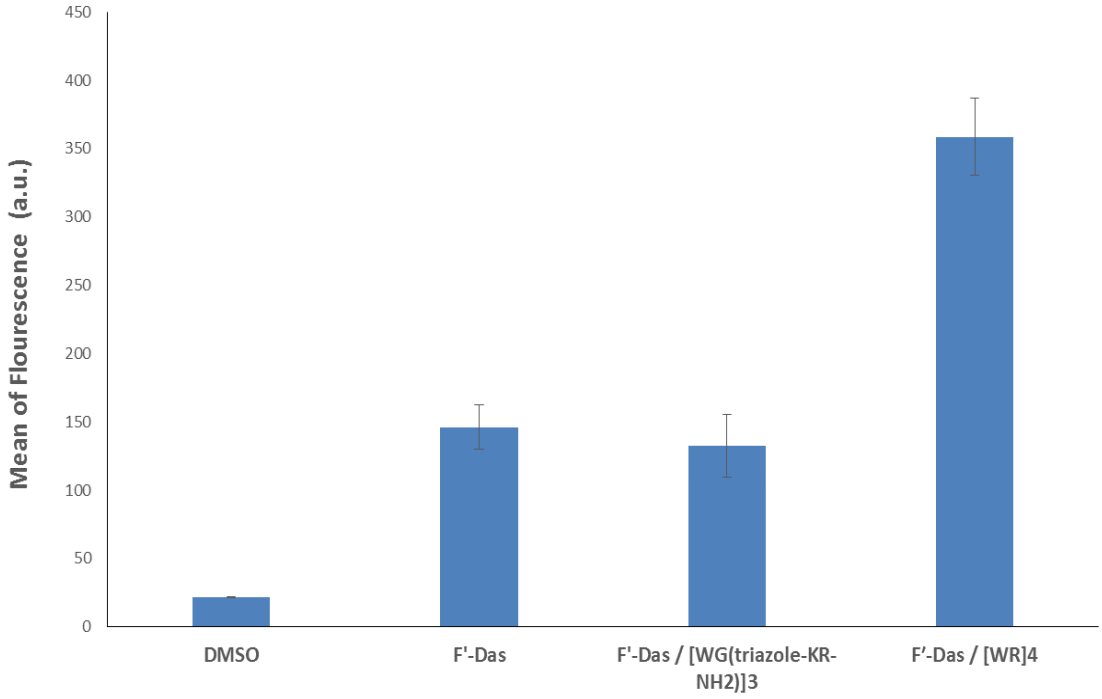
Mean of Flourescence (a.u.)
450
400
350
300
250
200
150
100
50
0
DMSO
F'-Das
F'-Das / [WG(triazole-KR-NH2)]3
F'-Das / [WR]4

Figure 6.

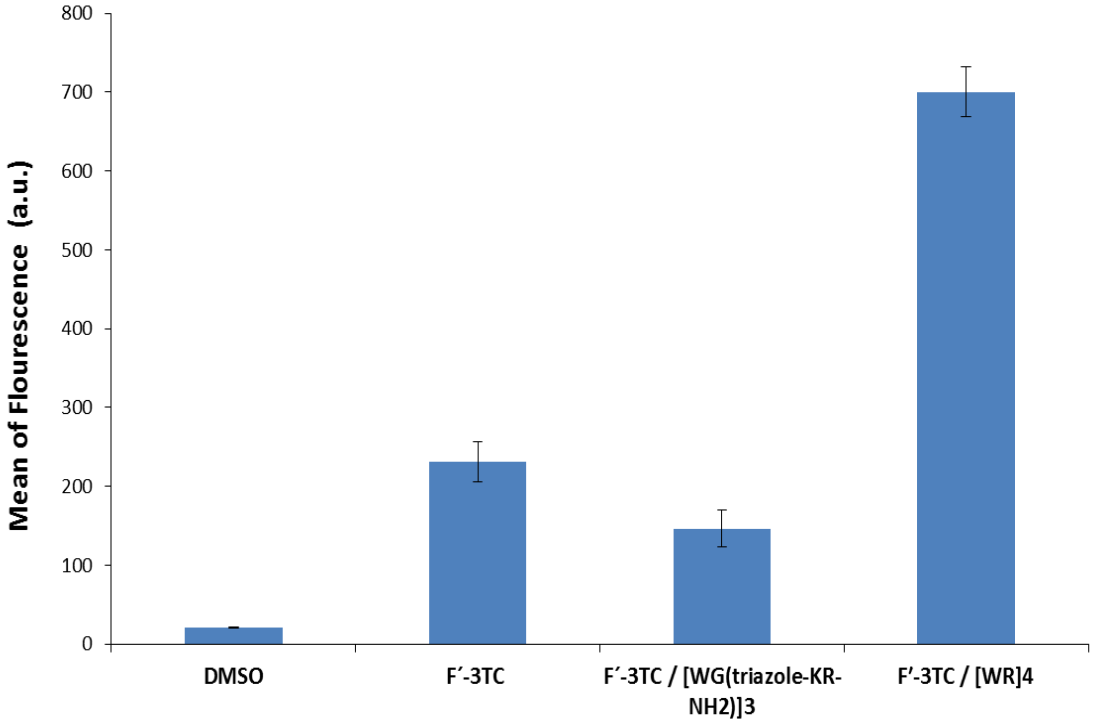
Mean of Flourescence (a.u.)
800
700
600
500
400
300
200
100
0
DMSO
F´-3TC
F´-3TC / [WG(triazole-KR-NH2)]3
F'-3TC / [WR]4

Figure 7.

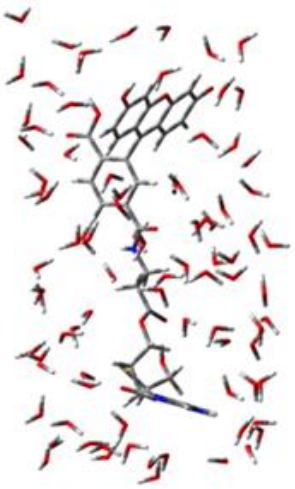

Solvation energy of F'-3TC
a) With 6-31G* -14.97 kCal/mol
b) With CEP-31G -6.62 kCal/mol

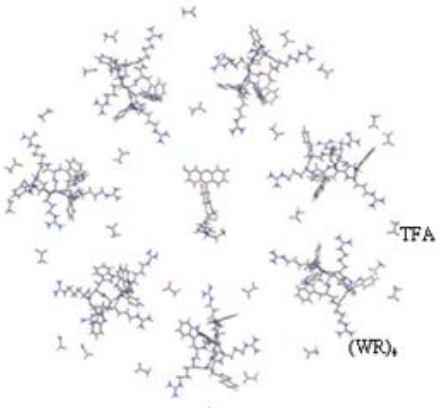

Interaction energy= -1,704.31 kCal/mol

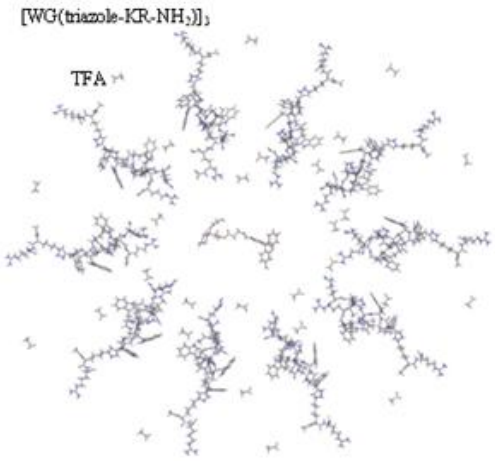

Interaction energy= -934.88 kCal/mol

Figure 8.

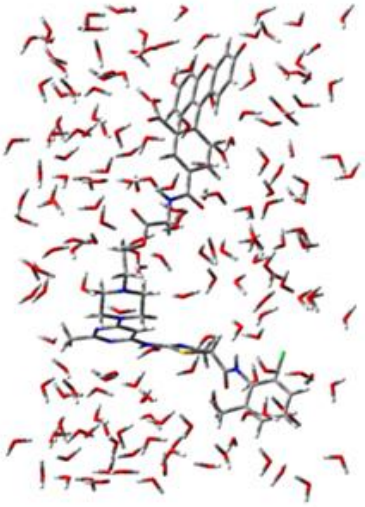

Solvation energy of F'-Das
a) With 6-31G* -16.86 kCal/mol
b) With CEP-31G -8.13 kCal/mol

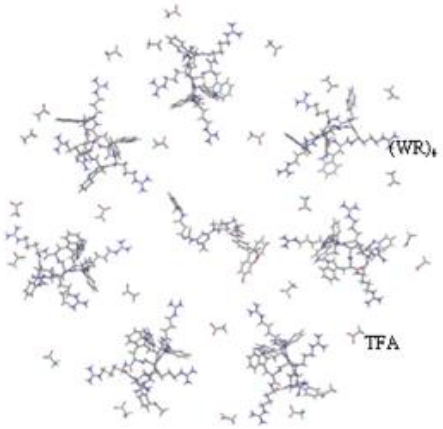

Interaction energy= -2,334.15 kCal/mol

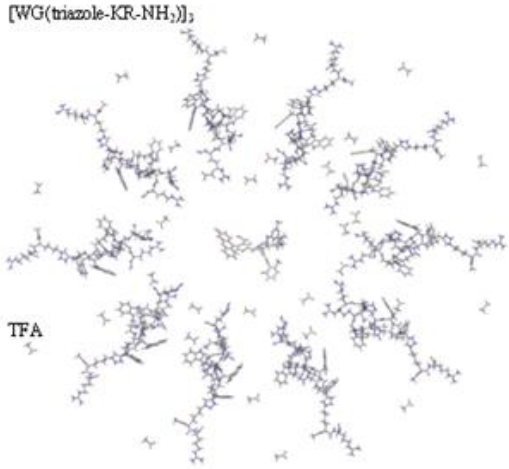

Interaction energy= -1,183.24 kCal/mol

Figure 9.

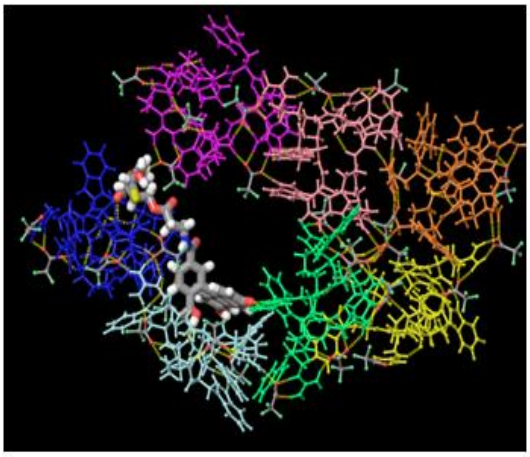

F'-3TC inside $(WR)_4$ nanostructure
(Snapshot of relaxed system during simulation)

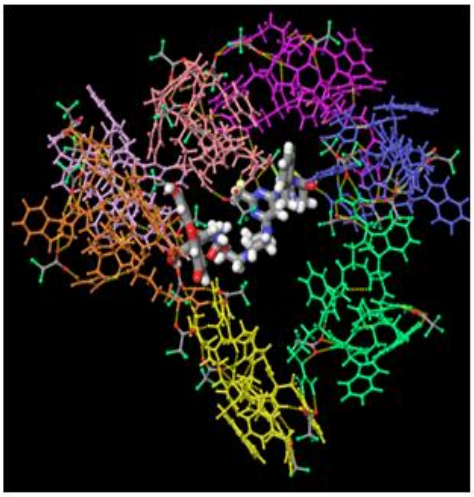

F'-Das inside $(WR)_4$ nanostructure
(Snapshot of relaxed system during simulation)

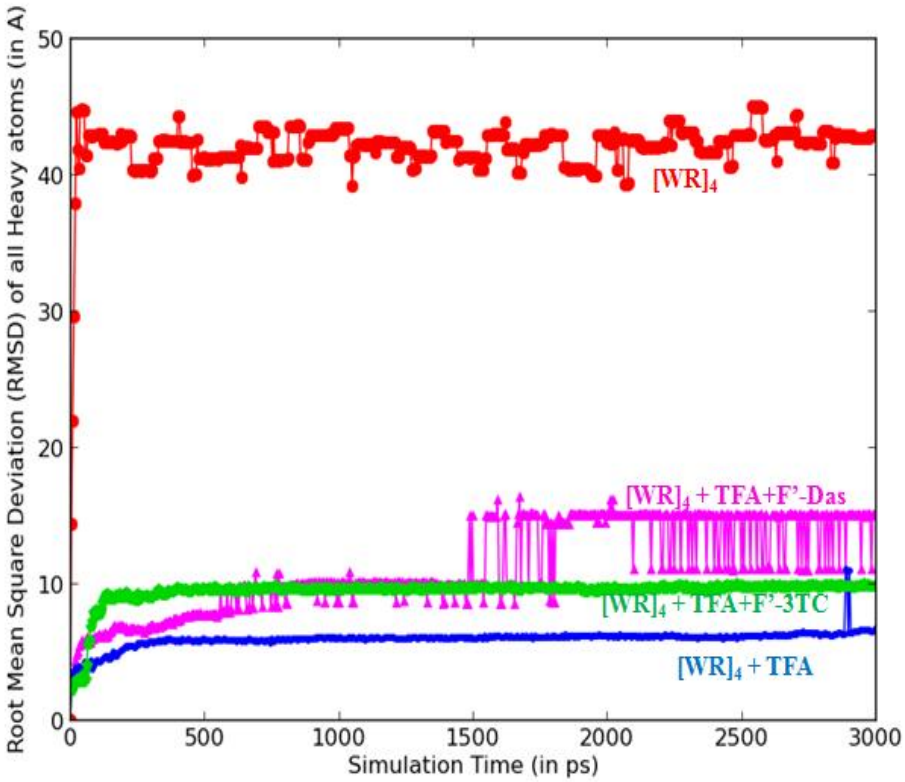

Figure 10.

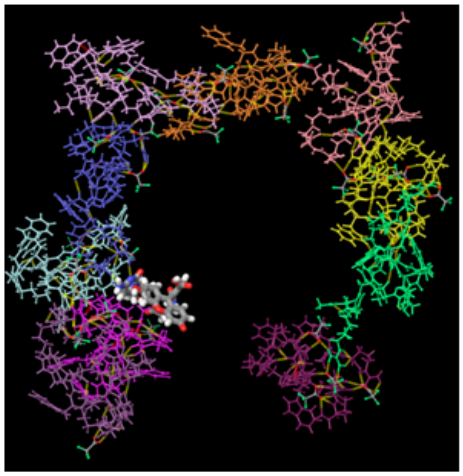

F'-3TC inside [WG(triazole-KR-NH_2)]$_3$ nanostructure
(Snapshot of relaxed system during simulation)

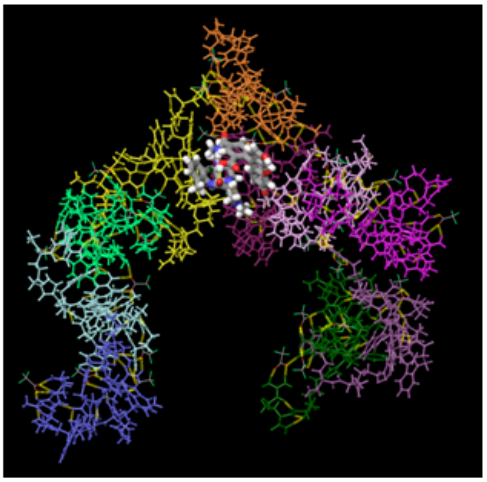

F'-Das inside [WG(triazole-KR-NH_2)]$_3$ nanostructure
(Snapshot of relaxed system during simulation)

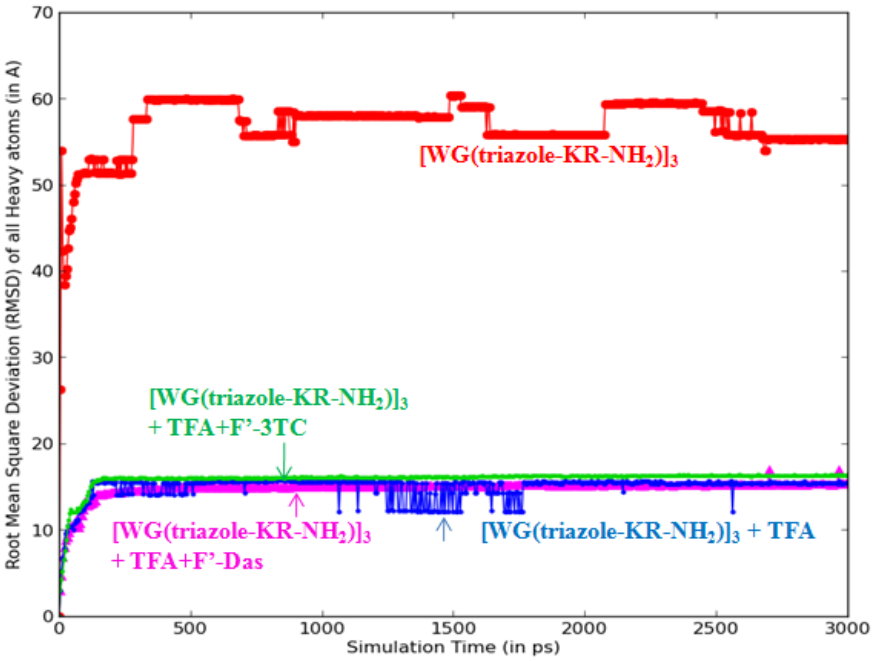

Scheme Legends:

Scheme 1. Structures and optimized conformations of cyclic amphiphilic peptides

Scheme 1.

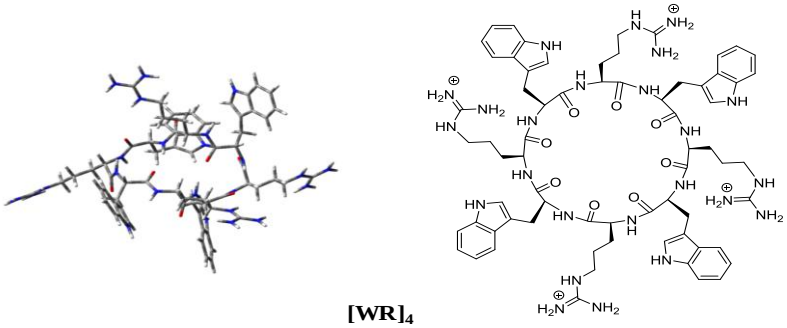

$[WR]_4$

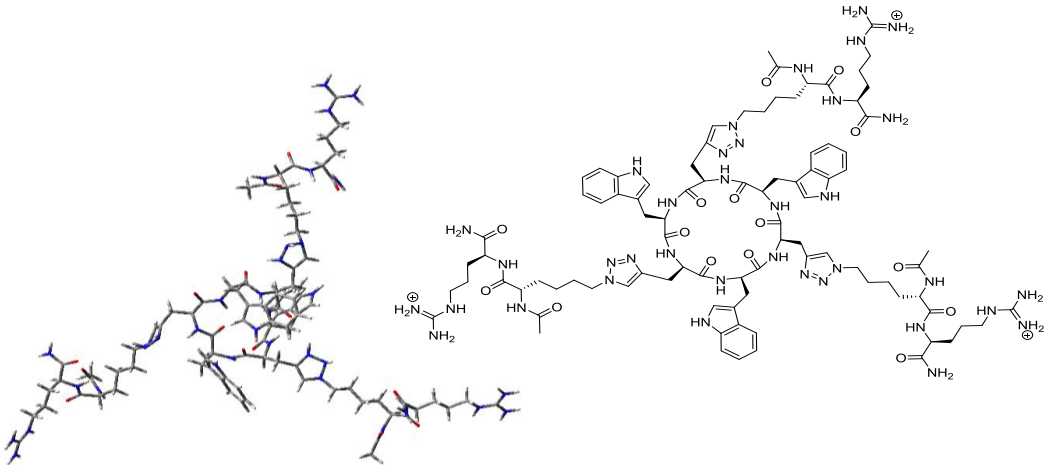

$[WG(triazole\text{-}KR\text{-}NH_2)]_3$

CHAPTER 3

Manuscript III

Synthesis of Derivatives of Amphiphilic Triazolyl Peptides

Naser Sayeh,[a] Rakesh Kumar Tiwari,[a,b,*] Keykavous Parang[a,b,*]

[a]Department of Biomedical and Pharmaceutical Sciences, College of Pharmacy, University Rhode Island, Kingston, Rhode Island, 02881, United States [b]School of Pharmacy, Chapman University, Irvine, CA, 92618, United States

Abstract

Three classes of amphiphilic peptides were synthesized and evaluated as molecular transporters and/or antibacterial agents. Herein we describe the details of the synthesis of the compounds using click chemistry or amide conjugation. The three classes include (a) cyclic-linear $[WG(triazol\text{-}KR\text{-}NH_2)]_4$ and linear-linear $(WG(triazol\text{-}KR\text{-}NH_2))_4$ conjugated through a triazolyl linker, (b) cyclic-linear $[WG(AC\text{-}KR\text{-}NH_2)]_3$ and linear-linear $(WE(AC\text{-}KR\text{-}NH_2))_3$ conjugated through an amide linker, and (c) fatty acyl triazolyl peptides containing myristoyl and stearoyl substituents. The syntheses were accomplished through solid-phase methods followed by click chemistry or amide formation to install the arginine side chains and fatty acyl groups, respectively.

Introduction

Enhanced translocation of drug compounds across plasma membranes is an important strategy to reduce the administered dose and subsequently the side effects of drugs. Among the cell-penetrating peptides (CPPs), arginine-rich peptides have been studied widely and gained much attention due to their efficiency, simplicity, and aqueous solubility.[1] Cationic residues in CPPs, particularly the guanidine moiety in arginine-rich peptides, have been known to play a crucial role for the membrane translocation capability.[2,3]

The critical role of arginine residues in the interaction of CPPs with cell membranes has been described previously by systematic replacement of arginine residues with alanine residues. Such substitutions induced a strong reduction of peptide uptake that was correlated with the number of substituted arginine residues. Thus, the central structural scaffold of the peptides required for cellular uptake was the guanidine head group of arginine.[4] Several studies on the binding affinities of cationic cell penetrating peptides indicate that CPPs strongly bind electrostatically to the negative charges on the cell membranes, including lipid head groups, proteins like nucleolin, and proteoglycans such as heparin sulfate.[5,6] Although electrostatic interactions are known to be important for arginine-rich cell-penetrating peptides, non-electrostatic effects such as hydrophobicity and peptide structural transitions can also contribute to the binding affinity of amphiphilic cell-penetrating peptides to cell membranes.[7]

The successful therapeutic strategies using CCPs has been limited by the poor delivery efficiency of existing synthesized amphiphilic peptides. The development of alternative modified peptides for improved delivery of therapeutic agents and enhanced

biological activity is needed urgently. Parang and coworkers have discovered a new class of amphiphilic peptides, namely $[WR]_4$ that showed the ability to translocate across the cell membrane. Both the positively charged residues and hydrophobic tryptophan contributed in enhancing the cellular uptake property of $[WR]_4$. Fluorescence activated cell sorting (FACS) analysis showed that the cellular uptake of F′-PEpYLGLD in the presence of $[WR]_4$ was increased by 27-fold when compared to F′-PEpYLGLD alone.[8]

Amphiphilic peptides have also become attractive and received attention as potential antibacterial agents. Antimicrobial peptides (AMPs) are produced in nature and are considered the first line of host defense protecting living organisms from pathogenic microorganisms. AMPs are produced at low levels in multi-cellular organisms.[9] Synthetic amphiphilic peptides have been shown to possess a broad spectrum of antitumor, antiviral, and antifungal activities.[10,11] The mechanism of action of antimicrobial peptides involves a non-receptor mediated mechanism whereby the compounds directly target the lipid membrane of the cells.[12] All AMPs tend to share some common characteristics, such as having amphipathic structure containing both hydrophilic and hydrophobic residues that allow binding to the hydrophilic and hydrophobic core of the membrane.[13]

AMPs have nonselective binding since they cannot differentiate between prokaryotic and eukaryotic cells based on hydrophobicity.[14] All AMPs consist of high number of cationic amino acids that result in net positive charge on the peptides, which will bind to the anionic lipids in the bacterial membrane.[15] It has been reported that reducing the positive charge of peptides will lower the activity and subsequently the selectivity of AMPs.[16,17]

Parang et al. (2014) recently reported the synthesis of amphiphilic cyclic CPPs, such as [R_4W_4] that exhibited potent activity against methicillin-resistant *Staphylococcus aureus* (MRSA) with a minimum inhibitory concentration (MIC) of 2.67 μg/mL.[18]

It has been previously reported that addition of fatty acids tail connected to the AMPs can enhance both the activity and selectivity of the peptides [19,20] Matthew and his co-workers reported that conjugation of fatty acid to the AMPs led to increased antibacterial activity of amphiphilic peptides.[21] A new class of peptide amphiphilic (PAs) containing positive charged peptide conjugated with fatty acyl chains showed significant improvement in delivery of different cargo molecules.[22] Studies on the antimicrobial peptide lactoferrin showed that peptide conjugated with twelve carbon fatty acid was able to improve the activity and selectivity of peptide.[23] Other groups have reported that AMPs conjugated to fatty acids with different length ranging from 12 to 18 methylene units improved the activity and selectivity of peptide.[24]

The Parang group recently reported the synthesis of four amphiphilic peptides containing positive charge, namely on arginine and lysine residues, conjugated with C14-palmitic acid and C16- myristic acid.[23] Furthermore, Parang's laboratory synthesized and evaluated fatty acylated cyclic polyarginine peptides (ACPPs), such as octanoyl-[KRRRRR], dodecanoyl-[KRRRRR], and hexadecanoyl-[KRRRRR] as antibacterial agents. All fatty acylated cyclic peptides exhibited more potent antibacterial activity than the non-acylated cyclic peptide [$R]_5$.[18]

Efficient intracellular delivery of biological cargos and/ or improving antibacterial activity requires systematic design of amphiphilic peptides with sufficient number of positively charged amino acids and hydrophobic residues. In continuation of our efforts

to design improved amphiphilic peptides, three class of peptides were synthesized: (1) Modified amphiphilic triazolyl cyclic-linear and linear-linear peptides; (2) Amphiphilic peptide amide derivatives (APADs); and (3) Amphiphilic fatty acyl triazolyl peptides (Figure 1).

The first section of this chapter describes the synthesis of the modified amphiphilic triazolyl peptides (ATPs) using Fmoc solid phase peptides synthesis. The peptides incorporate an increased number of propargyl glycine (pG) and tryptophan (W) residues. The peptides were then conjugated using click chemistry with arginine-lysine (R-K) peptides containing an azide linker to form cyclic-linear $[WG(triazol\text{-}KR\text{-}NH_2)]_4$ and linear-linear $(WG(triazol\text{-}KR\text{-}NH_2))_4$ amphiphilic triazolyl peptides. The biological and physicochemical properties of these peptides will be evaluated and compared with the previously synthesized peptides described in Chapter 2.

The second section of this chapter describes the synthesis of Amphiphilic Peptide Amide Derivatives (APADs). The goal was to compare APADs with the Amphiphilic Triazolyl Peptides (ATPs) described in Chapter 1. APADs with amide bond are presumed to interact with the membrane with more flexibility compared with rigid triazolyl ring of ATPs. By applying Fmoc-based peptide chemistry, APADs were synthesized by coupling of tryptophan (W) residues and glutamic acid (E) with different sequence length. The linear and cyclic peptides were conjugated to arginine lysine (R-K) residues through amide bond. The biological and physicochemical properties of APADS will be evaluated and compared with ATP in future.

Finally, the third group of amphiphilic fatty acyl triazolyl peptides was synthesized as potential antibacterial agents. These peptides consist of fatty acids with different chain lengths of 14 and 18 carbons. We hypothesized that a new class of Amphiphilic Fatty Acyl Triazolyl Peptides (AFTP) with different acyl chain lengths could provide novel antibacterial agents. Two fatty acyl derivatives (myristoyl and stearoyl) were synthesized in this class. Stearic and myristic acids were conjugated with a positively charged peptide containing azide using the click reaction. Their characterization and antibacterial activity for these compounds will be evaluated in the future.

Experimental Section

General

All reactions were carried out in Bio-Rad polypropylene columns by shaking and mixing in Glass-Col small tube rotator under dry conditions at room temperature unless otherwise stated. In general, all peptides in Class I were synthesized and characterized as described in chapter 1. All peptides were synthesized using solid-phase techniques. commercially available Fmoc amino acids, resins were purchased from Sigma-Aldrich Chemical Co. (Milwaukee, WI). The crude peptides were purified by using a reversed-phase Hitachi HPLC (L-2455) on a Gemini C18 column (250 mm × 21.20 cm, 10 µm) and a gradient system. The peptides were separated by eluting the crude peptides at 10.0 mL/min using a gradient of 0-100% acetonitrile (0.1% trifluoroacetic acid (TFA)) and water (0.1% TFA) over 60 min, and then were lyophilized.

Synthesis of Linear-Linear $(WG(triazole\text{-}KR\text{-}NH_2))_4$ and Cyclic-Linear $[WG(triazole\text{-}KR\text{-}NH_2)]_4$

Synthesis of Linear Peptide $(WpG)_4$

The linear peptide was assembled on Rink amide resin (0.59 g, 0.4 mmol, 0.68 mmol/g) by solid-phase Fmoc/*t*Bu peptide synthesis strategy using Fmoc-protected amino acids [Fmoc-Trp(Boc)-OH and Fmoc-L-propargylglycine] (Scheme 1). The linear peptide sequence was assembled on the resin after removing the Fmoc group at the *N*-terminal in the presence of 20% piperidine in DMF (20% v/v) to obtain the sequence NH_2-(pG)W(Boc)(pG)W(Boc)(pG)W(Boc)(pG)W(Boc)-Rink amide resin. The resin was washed with DMF/DCM and dried under vacuum for 24 h. Reagent R cocktail containing trifluoroacetic acid (TFA)/thioanisole/ethandithiol (EDT)/ anisole (90:5:3:2 v/v/v/v, 20.2 mL) was used to cleave the peptide from the resin. The crude peptide was precipitated by adding the filtrates to cold diethyl ether (200 mL, Et_2O). The solution was centrifuged at 4000 rpm for 5 min followed by decantation to obtain the solid precipitate. The peptide was lyophilized and purified by reversed-phase HPLC using a gradient system as described above to yield solid white coloured linear peptide $(W(pG))_4$ (Scheme 1). MALDI-TOF (m/z) $[C_{64}H_{62}N_{12}O_9]$: calcd, 1142.4763 ; found, 1143.3317 $[M + H]^+$, 1181.3810 $[M + K]^+$.

Synthesis of Cyclic Peptide $[W(pG)]_4$

The linear protected peptide sequence was assembled using H-Trp(Boc)-2-chlorotrityl resin (0.51 g, 0.4 mmol, 0.78 mmol/g). The resin was swelled using DMF (3

× 30 mL, 10 min) followed by coupling with appropriate amino acids (Fmoc-Trp(Boc)-OH and Fmoc-L-propargylglycine) and deprotection with piperidine in DMF (20% v/v). The final *N*-terminal Fmoc group was removed to assemble the sequence on the peptidyl resin, NH_2-(pG)W(Boc)(pG)W(Boc)(pG)W(Boc)(pG)W(Boc)-2-chlorotrityl resin (Scheme 2). The resin was washed with DMF (3 × 15 mL) and DCM (3 × 15 mL) to remove any traces of piperdine. Side chain-protected peptides were cleaved from the resins by agitating the peptidyl resin with the cleavage cocktail, acetic acid/ 2,2,2-trifluoroethanol (TFE)/dichloromethane (1:2:7, v/v/v, 50 mL), for 1 h at room temperature followed by filtration and washing the resin with TFE:DCM (2:8 v/v, 20 mL). The collected filtrate was evaporated to reduce the volume. Hexane (2 × 25 mL) and DCM (1 × 25 mL) were added to the residue to remove the acetic acid. The solvents were evaporated to yield a fluffy white solid compound that was dried overnight under vacuum. The cyclization of the protected crude solid peptide was carried out in the presence of a mixture of coupling reagents, 1-hydroxy-7-azabenzotriazole (HOAt) (162 mg, 0.4 mmol) and *N*,*N*′-diisopropylcarbodiimide (DIC) (310 µL, 0.4 mmol), in anhydrous DMF:DCM (60/200 mL) for 24 h. The solvent was evaporated under reduced pressure and the residue was deprotected with reagent R. The cyclization was confirmed by mass spectrometry. All the solvents were removed under reduced pressure that generated a high viscous liquid.

The final peptide cleavage to remove the side chain protection was carried out by shaking the residue with cleavage cocktail, reagent R, TFA/thioanisole/anisole/EDT (90:5:2:3 v/v/v/v, 15 mL), for 2 h at room temperture. The crude peptide was precipitated by the addition of cold diethyl ether (200 mL, Et_2O) and centrifuged at 4000 rpm for 5

min followed by decantation to obtain the solid precipitate. The solid material was further washed with cold ether (2 × 100 mL). The crude peptide was lyophilized and purified by reversed-phase HPLC as described above to yield cyclic peptide $[W(pG)]_4$ (Scheme 2). MALDI-TOF (m/z) $[C_{64}H_{60}N_{12}O_8]$: calcd, 1124.4657; found 1147.3156 $[M + Na]^+$, 1163.3579 $[M + K]^+$.

Synthesis of Azide Functionalized Positively Charged Peptide (Ac-K(N_3)R-NH_2)

The peptide was assembled on Rink amide resin (294 mg, 0.2 mmol, 0.68 mmol/g) by solid-phase peptide synthesis using Fmoc-protected amino acids, Fmoc-Arg(Pbf)-OH and Fmoc-Lys(N_3)-OH. The Rink amide resin was swelled with DCM (50 mL, 10 min) followed by DMF (50 mL, 2 × 10 min). The Fmoc group on the resin was deprotected by piperidine in DMF (20%, v/v, 25 mL, 2 × 10 min) followed by washing with DMF (3 × 30 mL). Fmoc-Arg (pbf)-OH (389 mg, 0.2 mmol/g) was then coupled to the peptidyl resin in the presence of coupling reagents HBTU (228 mg, 0.2 mmol/g) and DIPEA (210 µL) in *N*,*N*-dimethylformamide (DMF, 10 mL). The mixture was agitated at room tempertuare for 1 h. The resin was then washed with DMF (3 × 10 mL) for 5 min.

The Fmoc group was deprotected using using piperidine in DMF (20% v/v, 25 mL, 2 × 10 min) followed by washing with DMF (3 × 20 mL). The Fmoc-Lys (N_3)-OH (173 mg, 0.2 mmol) was coupled using HBTU (228 mg, 0.2 mmol) and DIPEA (210 µL) in DMF for 1 h. The resin was washed with DMF (3 × 20 mL), and the Fmoc group was removed using piperdine in DMF (20% v/v, 25 mL, 2 × 10 min). The resin was washed with DMF followed by reacting the the amino group with acetic anhdyride (Ac_2O, 95 µL, 1 mmol) and DIPEA (174 µL, 1 mmol) in anhdyrous DMF (3 mL) for 30 min.

The resin was washed with DMF (3 × 30 mL), DCM (3 × 30 mL), and was dried in vaccum overnight before the final cleavage. A freshly prepared cleavage cocktail, TFA/triisopropylsilane/water (95:2.5:2.5 v/v/v, 10 mL), was added to the resin and shaken at room temperature for 1.5 h. The resin was filtered and evaporated to reduce the volume under dry nitrogen. The crude peptide was precipitated by adding cold diethyl ether (200 mL, Et_2O) and centrifuged at 4000 rpm for 5 min followed by decantation to obtain the solid precipitate. The peptide was purified by reversed-phase HPLC using a gradient system as described above, and the HPLC fractions were collected, evaporated and lyophilized to obtain dry product (Scheme 3). ESI-TOF (m/z) [$C_{14}H_{27}N_9O_3$]: calcd, 369.2237; found, 370.2144 $[M + H]^+$.

Synthesis of Amphiphilic Triazolyl Peptides by Click Chemistry of Peptides (Linear or Cyclic) with Azide-Functionalized Positively Charged Linear Peptide

The click reaction was carried out in a 20 mL glass vial with small magnetic stir bar by adding the alkyne linear peptide (7.46 mg, 8.68 µmol) or cyclic peptide (7.25 mg, 8.68 µmol)), $CuSO_4.5H_2O$ (6.5 mg, 0.026 mmole), Cu powder (16.5 mg, 0.26 mmol), sodium ascorbate (51.5 mg, 0.26 mmol), and azide-functionalized peptide, Ac-K(N_3)R-NH_2 (10 mg, 0.026 mmol) in methanol:water (2:1v/v, 5 mL) followed by addition of DIPEA (9 µL, 0.052 mmol). The mixture was stirred at room temperature for 24-48 h. The completion of the reaction was confirmed by MALDI mass spectroscopy. The reaction mixture was filtered, and the solvent was evaporated under reduced pressure to afford the crude product. The crude product was further purified by HPLC using a gradient system as described above, and the HPLC fractions were collected, evaporated

and lyophilized to obtain solid compounds (Schemes 4 and 5). Cyclic-linear [WG(triazole-KR-NH_2)]$_4$, MALDI-TOF (m/z) [$C_{120}H_{168}N_{48}O_{20}$]: calcd, 2601.3605; found 2621.1569 [M + H + H_2O]$^+$; Linear-linear (WG(triazole-KR-NH_2))$_4$ MALDI-TOF (m/z) [$C_{120}H_{170}N_{48}O_{21}$]: calcd, 2619.3710; found 2621.1569 [M + 2]$^+$, 2637.5587 [M + H_2O]$^+$.

Amphilphilic Peptide Amide Derivatives

Synthesis of Linear Peptide (WE)$_3$

The linear peptide was assembled on Rink amide resin (425 mg, 0.47 mmol, 1.1 mmol/g) by solid-phase Fmoc/*t*Bu peptide synthesis strategy using Fmoc-protected amino acids [Fmoc-Trp(Boc)-OH (315 mg, 0.2 mmol) and Fmoc-L-glutamic acid (225 mg, 0.2 mmol) (Scheme 6). The linear peptide sequence was assembled on the resin after removing the Fmoc group at the *N*-terminal in the presence of 20% piperidine in DMF (v/v) to obtain the sequence NH_2-(E)W(Boc)(E)W(Boc)(E)W(Boc)-Rink amide resin. The resin was washed with DMF/DCM and dried under vacuum for 24 h. Reagent R was used to cleave the peptide from the resin. The crude peptide was precipitated by adding filtrates to cold diethyl ether (200 mL, Et_2O). The resulting solution was centrifuged at 4000 rpm for 5 min followed by decantation to obtain the solid precipitate. The peptide was lyophilized and purified by reversed-phase HPLC using a gradient system as described above to yield solid white colored linear peptide (WE)$_3$ (Scheme 6). MALDI-TOF (m/z) [$C_{48}H_{54}N_{10}O_{12}$]: calcd, 962.3923 ; found, 986.6340 [M + Na]$^+$, 1002.6207 [M + K]$^+$.

Synthesis of Cyclic Peptide $[WE]_3$

The linear protected peptide sequence was assembled using H-Trp(Boc)-2-chlorotrityl resin (512 mg, 0.78 mmol, 1.5 mmol/g). The resin was swelled in DMF (3 × 30 mL, 10 min) followed by coupling with appropriate amino acids (Fmoc-Trp (Boc)-OH (632 mg, 0.4 mmol) and Fmoc-L-glutamic acid (638.25 mg, 0.4 mmol) and deprotection cycle with piperidine in DMF (20% v/v). The final *N*-terminal Fmoc group was removed to assemble the desired sequence NH_2-(E)W(Boc)(E)W(Boc)(E)W(Boc)-2-chlorotrityl resin (Scheme 7). The resin was washed with DMF (3 × 15 mL) and DCM (3 × 15 mL) to remove any traces of piperdine. Side chain-protected peptides were cleaved from the resins by agitating the peptidyl resin with cleavage cocktail, acetic acid/ 2,2,2-trifluoroethanol (TFE)/dichloromethane (1:2:7, v/v/v, 50 mL), for 1 h at room temperature followed by filtration and washing the resin with TFE:DCM (2:8 v/v, 20 mL). The collected filtrate was evaporated to reduce the volume. Hexane (2 × 25 mL) and DCM (1 × 25 mL) were added to the residue to remove the acetic acid from the residue. The solvents were evaporated to yield a fluffy white solid compound that was dried overnight.

The cyclization of the protected crude solid peptide was carried out in the presence of a mixture of the coupling reagents 1-hydroxy-7-azabenzotriazole (HOAt) (162 mg, 0.4 mmol) and *N,N′*-diisopropylcarbodiimide (DIC) (310 µL, 0.4 mmol) in anhydrous DMF:DCM (60/200 mL) for 24 h. The solvent was evaporated from a sample solution (5 mL) under reduced pressure. Mass spectrometry confirmed the cyclization in the residue.

Thus, all the solvents were removed under reduced pressure that generated a high viscous liquid. The final peptide cleavage to remove the side chain protection was carried out by shaking the residue with cleavage cocktail, reagent R, TFA/thioanisole/anisole/EDT (90:5:2:3 v/v/v/v, 15 mL) for 2 h at room temperature. The crude peptide was precipitated by the addition of cold diethyl ether (200 mL, Et_2O) and centrifuged at 4000 rpm for 5 min followed by decantation to obtain the solid precipitate. The solid material was further washed with cold ether (2 × 100 mL). The crude peptide was lyophilized and purified by reversed-phase HPLC (Hitachi L-2455) as described above to yield cyclic peptide $[WE]_3$ (Scheme 7). MALDI-TOF (m/z) $[C_{48}H_{51}N_9O_{12}]$: calcd, 945.3657; found 968.1992 $[M + Na]^+$.

Synthesis of Amino Functionalized Positively Charged Peptide (Ac-KR-NH_2)

The peptide was assembled on Rink amide resin (294 mg, 0.2 mmol, 0.68 mmol/g) by solid-phase peptide synthesis using Fmoc-protected amino acids, Fmoc-Arg(Pbf)-OH and Fmoc-Lys-OH. The Rink amide resin was swelled with DCM (50 mL, 10 min) and then DMF (50 mL, 2 × 10 min). The Fmoc group on the resin was deprotected by piperidine in DMF (20%, v/v, 25 mL, 2 × 10 min) followed by washing with DMF (3 × 30mL). Fmoc-Arg (pbf)-OH (389 mg, 0.2 mmol/g) was then coupled to the peptidyl resin in the presence of HBTU (228 mg, 0.2 mmol/g) and DIPEA (210 µL) in *N*,*N*-dimethylformamide (DMF, 10 mL). The mixture was agitated at room temperature for 1 h. The resin was then washed with DMF (3 × 10 mL) for 5 min. The Fmoc group was deprotected using using piperidine in DMF (20% v/v, 25 mL, 2 × 10 min) followed by washing with DMF (3 × 20 mL).

The Fmoc-Lys-OH (173 mg, 0.2 mmol) was coupled by using HBTU (228 mg, 0.2 mmol), DIPEA (210 µL) in DMF for 1 h. The resin was washed with DMF (3 × 20 mL), and Fmoc group was deprotected by using piperdine in DMF(20% v/v, 25 mL, 2 × 10 min). The resin was washed with DMF, and the amino group was acetylated by reaction with acetic anhdyride (AC_2O, 95 µL, 1 mmol) and DIPEA (174 µL, 1 mmol) in anhdyrous DMF (3 mL) for 30 min. The resin was again washed with DMF (3 × 30 mL), DCM (3 × 30 mL), and then dried in vaccum overnight before the final cleavage. A freshly prepared cleavage cocktail, TFA/ triisopropylsilane/ water (95:2.5:2.5 v/v/v, 10 mL), was added to the resin and shaken at room temperature for 1.5 h.

The resin was filtered and the filtrate was evaporated to reduce the volume under dry nitrogen. The crude peptide was precipitated by adding cold diethyl ether (200 mL, Et_2O) and centrifuged at 4000 rpm for 5 min followed by decantation to obtain the solid precipitate. The peptide was purified by reversed-phase HPLC using a gradient system, and lyophilized to obtain the desired product (Scheme 8). ESI-TOF (m/z) [$C_{14}H_{29}N_7O_3$]: calcd, 343.4320; found, 343.2140 $[M]^+$.

Coupling of Amphiphilic Peptides $(WE)_3$ and $[WE]_3$ with Amino-Functionalized Positively Charged Peptide (Ac-KR-NH_2) via an Amide Bond.

The reaction was carried out in 20 mL round flask with small magnetic stir bar by adding the amphiphilic peptide linear peptide $(WE)_3$ (10 mg, 0.01 mmol) or cyclic peptide $[WE]_3$ (7.0 mg, 0.01 µmol), HOBT (1.8 mg, 0.01 mmole), benzotriazol-1-yloxy) tripyrrolidino-phosphonium hexafluorophosphate (PyBOP, 14 mg, 0.1 mmol), DIPEA (14 µL, 0.01 mmol), and amino-functionalized peptide, Ac-KR-NH_2 (10.85

mg, 0.01 mmol) in 2 mL of DMF. The mixture was stirred at room temperature for 1-2 h. The completion of the reaction was confirmed by MALDI mass spectroscopy. The reaction mixture was filtered, and the solvent was evaporated under reduced pressure to afford the crude product. The crude product was further purified by HPLC using a gradient system, and the desired compound was lyophilized to dryness (Scheme 9). Linear-linear $(WE(AC\text{-}KR\text{-}NH_2))_3$, MALDI-TOF (m/z) ($C_{90}H_{138}N_{31}O_{18}$): Calcd, 1938.0601; found 1954.1202 $[M + H_2O]^+$. Cyclic-linear $[WG(AC\text{-}KR\text{-}NH_2)]_3$ MALDI-TOF (m/z) [$C_{90}H_{132}N_{30}O_{18}$]: Calcd, 1921.0336; found 1925.0213 $[M + 4H]^+$.

Amphiphilic Fatty Acyl Triazolyl Peptides

Synthesis of Stearic Propargyl Amide

Stearic acid (284.48 mg, 2.48 mmol) and hydroxybenzotriazole (HOBT, 544 mg, 0.4 mmol) were dissolved in 20 mL of anhydrous tetrahydrofuran (THF). Propargylamine (160 µl, 2.50 mmol) was then added to the reaction at room temperature and the mixture was cooled to 0 °C. A solution of dicyclohexylcarbodiimide (DCC) (511 mg, 2.48 mmol) in 15 mL of anhydrous THF was added, and the mixture was stirred for 2 days at room temperature. The reaction was monitored by TLC with hexane/ ethyl acetate 7:3 v/v as the mobile phase. The reaction was filtered and the solvent was removed under reduced pressure. Dichloromethane (250 mL) was added and the organic phase was washed three times with 1 M of $KHSO_4$ solution followed by three times with 1 M $NaHCO_3$. The organic layer was separated, and the solvent was removed under reduced pressure. The resulting white solid was purified by recrystallization from ethanol (yield 75%), a white

solid *N*-propargyl stearic amide (Scheme 10). MALDI-TOF (m/z) ($C_{21}H_{39}NO$): Calcd, 321.3032; found 322.2315 $[M + H]^+$.

Synthesis of Myristic Propargyl Amide

Myristic acid (228.37 mg, 0.043 mmol) and hydroxybenzotriazole (HOBT, 654 mg, 4.3 mmol) were dissolved in 40 mL of anhydrous tetrahydrofuran (THF). Propargylamine (275 µl, 2.50 mmol) was added to the reaction and the mixture was then cooled to 0 °C. A solution of DCC (888 mg, 4.3 mmol) in 25 mL of anhydrous THF was added, and the mixture was stirred for 2 days at room temperature. The reaction was monitored by TLC with hexane/ethyl acetate 7:3 v/v as the eluent. The mixture was then filtered, and the solvent was removed under reduced pressure. Dichloromethane (250 mL) was added, and the organic phase was washed three times with 1 M of $KHSO_4$ solution followed by three times with 1 M $NaHCO_3$. The organic layer was concentrated under reduced pressure and the resulting white solid was purified by recrystallization from ethanol (yield around 75%), a white solid *N*-propargyl myristic amide (Scheme 10). MALDI-TOF (m/z) ($C_{17}H_{31}NO$): Calcd, 265.2406; found 266.2345 $[M + H]^+$.

Synthesis of Protected Positively Charged Peptidyl Resin Functionalized with Azide

The peptide was assembled on Rink amide resin (294 mg, 0.2 mmol, 0.68 mmol/g) by solid-phase peptide synthesis using Fmoc-protected amino acids, Fmoc-Arg(Pbf)-OH and Fmoc-Lys(N_3)-OH.The Rink amide resin was swelled with DCM (50

mL, 10 min) and then DMF (50 mL, 2 × 10 min). The Fmoc group on the resin was deprotected by piperidine in DMF (20%, v/v, 25 mL, 2 × 10 min) followed by washing with DMF (3 × 30 mL). Fmoc-Arg (Pbf)-OH (389 mg, 0.2 mmol/g) was then coupled to the peptidyl resin in the presence of HBTU (228 mg, 0.2 mmol/g) and DIPEA (210 µL) in *N*,*N*-dimethylformamide (DMF, 10 mL). The mixture was agitated at room temperature for 1 h. The resin was then washed with DMF (3 × 10 mL) for 5 min. The Fmoc group was deprotected using piperidine in DMF (20% v/v, 25 mL, 2 × 10 min) followed by washing with DMF (3 × 20 mL). Fmoc-Lys (N_3)-OH (173 mg, 0.2 mmol) was coupled using HBTU (228 mg, 0.2 mmol), DIPEA (210 µL) in DMF for 1 h. The resin was washed with DMF (3 × 20 mL), and Fmoc group was deprotected by using piperdine in DMF (20% v/v, 25 mL, 2 × 10 min). The resin was washed with DMF followed by acetylating the amino group in the presence of acetic anhdyride (Ac_2O, 95 µL, 1 mmol) and DIPEA (174 µL, 1 mmol) in anhdyrous DMF (3 mL) for 30 min. The resin was washed with DMF (3 × 30 mL), DCM (3 × 30 mL), and was dried under vaccum overnight before the final cleavage. The peptide-attached resin remained protected for coupling with fatty propargyl stearyl and myristoyl amide (Scheme 11). MALDI-TOF (m/z) ($C_{43}H_{58}N_9O_9S$): Calcd, 876.4078; found 877. 0532 $[M + H]^+$.

Click Reaction of Fatty Propargyl Amide with Positively Charged Arginine Azide

Click reaction was carried out in 50 mL round bottom flask with small magnetic stir bar. Protected arginine azide (530 mg, 0.25 mmol) was swelled in DMF (50 mL × 3 for 10 min). Next, CuBr (18 mg, 0.13 mmol), sodium ascorbate (75 mg, 0.13 mmol),

DIPEA (218 µl, 0.13 mmol), 2,6-lutidine (145µl, 0.13 mmol), stearic propargyl peptide (120 mg, 0.125 mmol) or myristic propagyl peptide (99 mg, 0.125 mmol) were added. The mixture was stirred at room temperature for 24-48 h. The completion of the reaction was confirmed by MALDI mass spectroscopy. The reaction mixture was filtered, and the solvent was evaporated under reduced pressure to afford the crude product. The crude product was further purified by HPLC using a gradient system as described above, and the HPLC fractions were collected, evaporated and lyophilized to obtain solid compounds. Stearic Acyl Triazolyl peptide MALDI-TOF (m/z) [$C_{35}H_{66}N_{10}O_4$]: calcd, 690.5612; found 691.1710 $[M + H]^+$ (Scheme 11); Myristic Acyl Triazolyl peptide MALDI-TOF (m/z) [$C_{31}H_{58}N_{10}O_4$]: calcd, 634.8725; found 635.0931 $[M + H]^+$.

Results and Discussion

We reported the synthesis of amphiphilic linear and cyclic peptides containing tryptophan (W) and arginine (R) connected through trizaole ring with proparglyglycine (PG) in Chapter I. The compounds were characterized and evaluated for their potential role as drug delivery tools. The peptides did not show any efficiency in improving the cellular uptake possibly because of the limited number of three positively charged amino acids in each peptide. Thus, there is a need to optimize amphiphilic peptides by increasing the number of positive charged residues and hydrophobic residues to improve the cell penetrating property of the peptides and to enhance the intracellular delivery of bioactive compounds.

To address the above issue, three classes of compounds were synthesized. In Class I, linear-linear $(WG(triazole\text{-}K(N_3)R\text{-}NH_2))_4$ and cyclic-linear $[WG\ (triazole\text{-}K(N_3)R\text{-}NH_2)]_4$ containing L-amino acids were synthesized using Fmoc-based peptide chemistry. The linear peptide sequence $(WpG)_4$ was assembled on the Fmoc-Rink amide resin using solid-phase synthesis strategy. The last Fmoc group on the *N*-terminal was deprotected by piperidine (20% v/v, DMF). Then the resin was dried, washed, and cleaved to afford the linear peptide, which was purified by reversed-phase HPLC (Scheme 1). Synthesis of cyclic peptide was accomplished by assembling of the linear protected peptide (WpG) on the H-Trp (Boc)-2-chlorotrityl chloride resin. The side chain protected group was removed, and the peptide was again purified using HPLC (Scheme 2). The synthesis of azide-functionalized positively charged peptide building block ($Ac\text{-}K(N_3)R\text{-}NH_2$) was performed on Rink amide resin. The Fmoc group was deprotected, and amino group was acetylated using acetic anhydride in DMF. The peptide was cleaved from the resin and purified by HPLC to afford $Ac\text{-}K(N_3)R\text{-}NH_2$ (Scheme 3).

Click chemistry reactions were performed by coupling linear-linear and cyclic-linear peptides containing alkyne, $(W(pG))_4$ and $[W(pG)]_4$, and the azide-functionalized linear peptide $Ac\text{-}K(N_3)R\text{-}NH_2$ in solution phase using $CuSO_4{\cdot}5H_2O$, Cu powder, sodium ascorbate, and *N*,*N*-diisopropylethylamine (DIPEA) in methanol:water for 24-48 h. The formation of the conjugated products was confirmed by MALDI-TOF mass spectroscopy (Schemes 4 and 5).

In Class II, new amphiphilic peptides amide derivatives were synthesized. The purpose was to compare the triazole peptides derivatives with the corresponding amide peptides for their role as molecular transporter. Linear and cyclic tryptophan and glutamic

acid containing peptides were connected through amide bonds with the lysine residue in Ac-KR-NH_2. Linear-linear $(WE(AC\text{-}KR\text{-}NH_2))_3$ and cyclic-linear $[WE(AC\text{-}KR\text{-}NH_2)]_3$ peptides were again synthesized using Fmoc-based peptide chemistry. The linear peptide sequence $(WE)_4$ was assembled on the Fmoc-Rink amid resin using solid-phase synthesis strategy. The last Fmoc group on the *N*-terminal was deportected by piperidine (20% v/v, DMF). Then the resin was dried, washed, and cleaved to afford the linear peptide which was purified by reversed-phase HPLC (Scheme 6). Synthesis of cyclic peptide was accomplished by assembly of the linear protected peptide $(WE)_4$ on the H-Trp(Boc)-2-chlorotrityl chloride resin. The side chain protected group was removed, and the peptide was purified using HPLC (Scheme 7).

The synthesis of functionalized positively charged peptide building block (Ac-KR-NH_2) was performed on Rink amide resin. The Fmoc group was deprotected, and amino group was acetylated using acetic anhydride in DMF. The peptide was cleaved from the resin and purified by HPLC to afford Ac-KR-NH_2 (Scheme 8). The coupling reaction was performed by adding $(WE)_3$ and $[WE]_3$, and an amino-functionalized peptide, Ac-KR-NH_2, in DMF in the presence of the coupling reagents HOBT, PyBOP, DIPEA. After HPLC purification, the formation of the product was confirmed by MALDI-TOF mass spectroscopy (Scheme 9).

In Class III, two Amphiphilic Fatty Acyl Triazolyl Peptides (AFTP) derivatives were synthesized using peptides containing arginine and lysine azide (AC-K(N_3)R-NH_2). Myristic acid and stearic acid were coupled to propagylamine in the presence of HOBT in THF. Positively charged peptidyl resin functionalized with an azide group was synthesized by assembling the peptide on Rink amide resin using Fmoc-Arg(Pbf)-OH

and Fmoc-Lys(N_3)-OH. After Fmoc removal and capping of the peptides by acetic anhdyride, click chemistry was used to react the myristic propargyl and stearic propargyl amides in the presence of CuBr, sodium ascorbate to afford the stearic triazolyl peptide and myristic triazolyl peptides (Schemes 10 and 11).

Conclusion

In conclusion, three classes of amphiphilic peptides were synthesized to be evaluated as molecular transporters and antibacterial agents. Fmoc-based peptide synthesis, click chemistry, and amide bond formation were used in the synthesis of compounds. In the future, the physicochemical properties, cytotoxicity, nanostructure formation, molecular transporter efficiency, and antibacterial activity of these compounds will be evaluated and compared with linear-linear $(WG(triazole\text{-}KR\text{-}NH_2))_3$ and cyclic-linear $[WG(triazole\text{-}KR\text{-}NH_2)]_3$ in Manuscript I.

Acknowledgments

We thank National Center for Research Resources, NIH, and Grant Number 1 P20 RR16457 for sponsoring the core facility.

References

1. Delaroche, D.; Ausseda, B.; Aubry, S.; Chassaing, G.; Burlina, F.; Clodic, G.; Bolbach, G.; Lavielle, S.; Sagan, S. Tracking a new cell-penetrating (W/R) nonapeptide, through an enzyme-stable mass spectrometry reporter tag. *Anal Chem*. **2007**, *79*, 1932–1938.
2. Wender, PA.; Mitchell, DJ.; Pattabiraman, K.; Pelkey, ET.; Steinman, L.; Rothbard; JB. The design, synthesis, and evaluation of molecules that enable or enhance cellular uptake: Peptoid molecular transporters. *Proc Natl Acad Sci USA.* **2000**, *97*, 13003–13008.
3. Mitchell, DJ.; Kim, DT.; Steinman, L; Fathman, CG.; Rothbard, JB. Polyarginine enters cells more efficiently than other polycationic homopolymers. *J Pept Res.* **2000**, *56*, 318–325.
4. Ziegler, A. Thermodynamic studies and binding mechanisms of cell-penetrating peptides with lipids and glycosaminoglycans. *Adv. Drug Deliv Rev.* **2000**, *60*, 580–597.
5. Ziegler, A.; Blatter, X.; Seelig, A.; Seelig, J. Protein transduction domains of HIV-1 and SIV TAT interact with charged lipid vesicles. Binding mechanism and thermodynamic analysis. *Biochemistry.* **2003**, *42*, 9185–9194.
6. Nasrolahi Shirazi, A.; Tiwari, R. K.; Oh, D.; Banerjee, A.; Yadav, A.; Parang, K. Efficient delivery of cell impermeable phosphopeptides by a cyclic peptide amphiphile containing tryptophan and arginine. *Molecular Pharmaceutics.*

2013, *10*, 2008-2020.

7. Goncalves, E.; Kitas, E.; Seelig, J. Binding of oligoarginine to membrane lipids and heparan sulfate: structural and thermodynamic characterization of a cell-penetrating peptide. *Biochemistry.* **2005**, *44*, 2692–2702.
8. Zasloff M. Antimicrobial peptides of multicellular organisms. *Nature.* **2002**, *15*, 389-339.
9. Hwang, PM.; Vogel, HJ. Structure-function relationships of antimicrobial peptides. *Biochem Cell Biol*. **1998**, *76*, 235–246.
10. Hoskin, D.W.; and Ramarmoorthy A. Studies on anticancer activities of antimicrobial peptides. *Biochim. Biophys*. **2008**, *1778*, 357–375.
11. Wade, D.; Boman, A.; Wåhlin, B.; Drain, CM.; Andreu, D.; Boman, HG.; Merrifield, RB. All-D amino acid-containing channel-forming antibiotic peptides. *Proc Natl Acad Sci USA.* **1990**, *87*, 4761–4765.
12. Matsuzaki, K. Why and how are peptide-lipid interactions utilized for self-defense? Magainins and tachyplesins as archetypes. *Biochim Biophys.* **1999**, *1462*, 1–10.
13. Shai, Z. Y. Oren From "carpet" mechanism to de-novo designed diastereomeric cell-selective antimicrobial peptides. *Peptides.* **2001**, *22*, 1629–1641.
14. Dathe, M.; Wieprecht, T. Structural features of helical antimicrobial peptides: their potential to modulate activity on model membranes and biological cells. *Biochim Biophys Acta*. **1999**, *1462*, 71–87

15. Wieprecht, T.; Dathe, M.; Beyermann, M.; Krause, E.; Maloy, WL.; MacDonald, DL.; Bienert, M. Peptide hydrophobicity controls the activity and selectivity of magainin 2 amide in interaction with membranes. *Biochemistry*. **1997**, *36*, 6124–6132.

16. Brogden, K. A. Antimicrobial peptides: pore formers or metabolic inhibitors in bacteria. *Nat. Rev. Microbiol*. **2005**, *23*, 25010-25038.

17. Oh, D.; Sun, J.; Nasrolahi Shirazi, A.; LaPlante, K. L.; Rowley, D. C.; Parang, K. Antibacterial activities of amphiphilic cyclic cell-penetrating peptides against multidrug resistant pathogens. *Mol. Pharmaceutics*. **2014,** *11*, 3528-3536.

18. Avrahami, D.; Shai, Y. Conjugation of a magainin analogue with lipophilic acids controls hydrophobicity, solution assembly, and cell selectivity. *Biochemistry*. **2002**, *41*, 2254–2263.

19. Thennarasu, S.; Lee; D. K.; Tan, A.; Prasad Kari, U.; and Ramamoorthy; A. Antimicrobial activity and membrane selective interactions of a synthetic lipopeptide MSI-843. *Biochim. Biophys*. **2005**, *1711*, 49–58.

20. Chu-Kung, A.F.; Bozzelli, K.N; Lockwood, N.A.; Haseman, J. R.; Mayo, K.H.; Tirrell, M. V. "Promotion of peptide antimicrobial activity by fatty acid conjugation," *Bioconjugate Chemistry*. **2004**, *15*, 530-536.

21. Chu-Kung, A. F.; Nguyen, R.; Bozzelli, K. N.; Tirrell, M. Chain length dependence of antimicrobial peptide–fatty acid conjugate activity. *Journal of Colloid and Interface Science.* **2010**, *345*, 160-167.

22. Nasrolahi Shirazi, A.; Oh, D.; Tiwari, R. K.; Sullivan, B.; Gupta, A.; Bothun, GD;Parang,K;peptide amphiphile containing arginine and fatty acyl chains as molecular transporters. *Journal of Molecular pharmaceutics*. **2013**, *10* , 4717-4727.

23. Lockwood, N. A.; Haseman, J. R.; Tirrell, M. V.; Mayo, K. H. Acylation of SC4 dodecapeptide increases bactericidal potency against Gram-positive bacteria, including drug-resistant strains. *Biochem. J.* **2004**, *378*, 93–103.

24. Majerle, A.; Kidric, J; and Jerala, R. Enhancement of antibacterial and lipopolysaccharide binding activities of a human lactoferrin peptide fragment by the addition of acyl chain. *J. Antimicrob. Chemother*. **2003**, *51***,** 1159-1165.

Figure legends.

Figure 1. Chemical structures of three classes of amphiphilic peptides.

Figure 1.

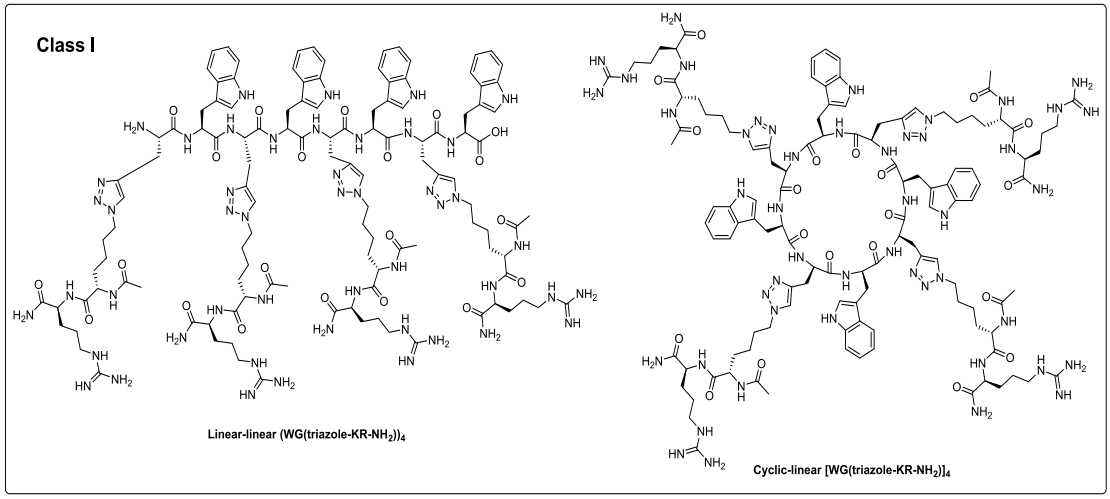
Class I
Linear-linear (WG(triazole-KR-NH2))4
Cyclic-linear [WG(triazole-KR-NH2)]4

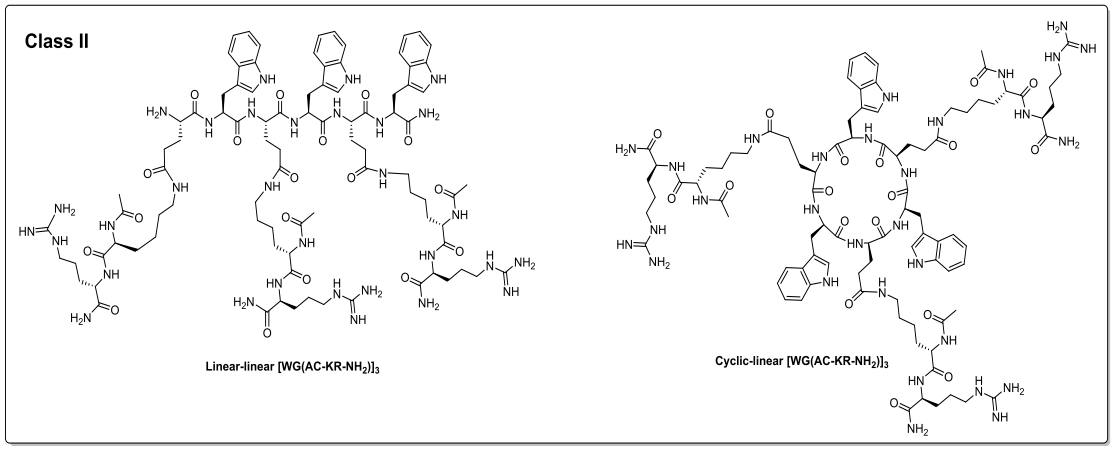
Class II
Linear-linear [WG(AC-KR-NH2)]3
Cyclic-linear [WG(AC-KR-NH2)]3

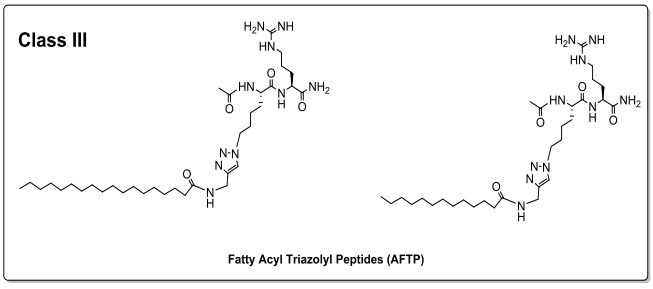
Class III
Fatty Acyl Triazolyl Peptides (AFTP)

Scheme Legends:

Scheme 1. Synthesis of linear $(W(pG))_4$.

Scheme 2. Synthesis of cyclic $[W(pG)]_4$.

Scheme 3. Synthesis of positively charged peptides containing an azide.

Scheme 4. Click Chemistry of to react the propargyl groups on a linear peptide with azides on a positively charged peptide.

Scheme 5. Click Chemistry of to react the propargyl groups on a cyclic peptide with azides on a positively charged peptide.

Scheme 6. Designing of linear $(WE)_3$ amide derivatives of amphiphilic peptides.

Scheme 7. Designing of cyclic $[WE]_3$ amide derivatives of amphiphilic peptides.

Scheme 8. Synthesis of positively charged peptides with arginine and lysine residues.

Scheme 9. Coupling of cyclic amphiphilic peptides by creation of an amide bond.

Scheme 10. Synthesis of stearyl propargyl amide and myristyl propargyl amide building blocks.

Scheme 11. Synthesis of positively charged protected peptidyl resin functionalized with azide and click chemistry to react fatty acyl propargyl amides with azides on arginine containing units.

Scheme 1.

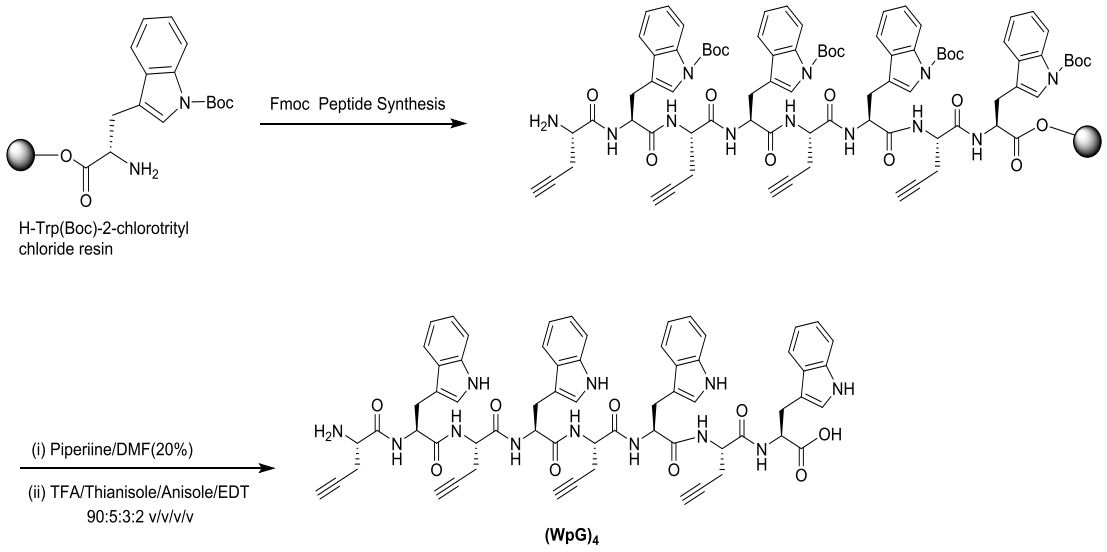
Fmoc Peptide Synthesis
H-Trp(Boc)-2-chlorotrityl chloride resin
(i) Piperiine/DMF(20%)
(ii) TFA/Thianisole/Anisole/EDT 90:5:3:2 v/v/v/v
(WpG)4

Scheme 2.

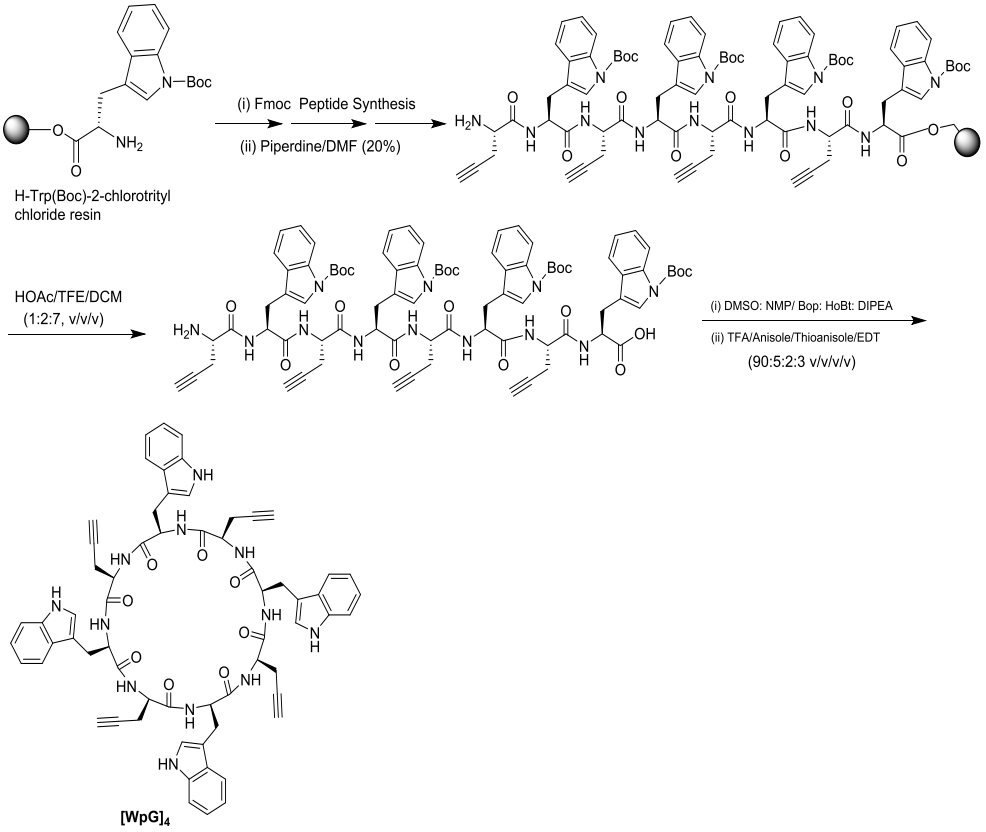
(i) Fmoc Peptide Synthesis
(ii) Piperdine/DMF (20%)
H-Trp(Boc)-2-chlorotrityl chloride resin
HOAc/TFE/DCM (1:2:7, v/v/v)
(i) DMSO: NMP/ Bop: HoBt: DIPEA
(ii) TFA/Anisole/Thioanisole/EDT
(90:5:2:3 v/v/v/v)
[WpG]4

Scheme 3.

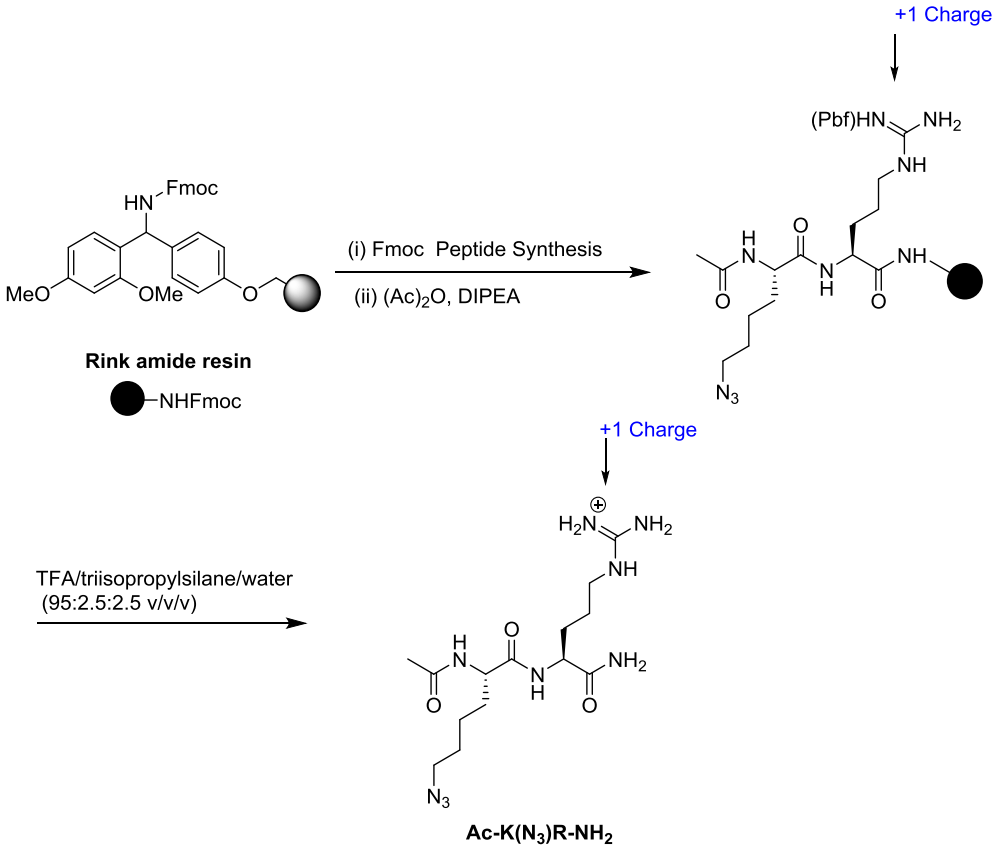
+1 Charge
(Pbf)HN
NH2
NH
Fmoc
HN
MeO
OMe
O
(i) Fmoc Peptide Synthesis
(ii) (Ac)2O, DIPEA
Rink amide resin
NHFmoc
N3
+1 Charge
TFA/triisopropylsilane/water
(95:2.5:2.5 v/v/v)
Ac-K(N3)R-NH2

Scheme 4.

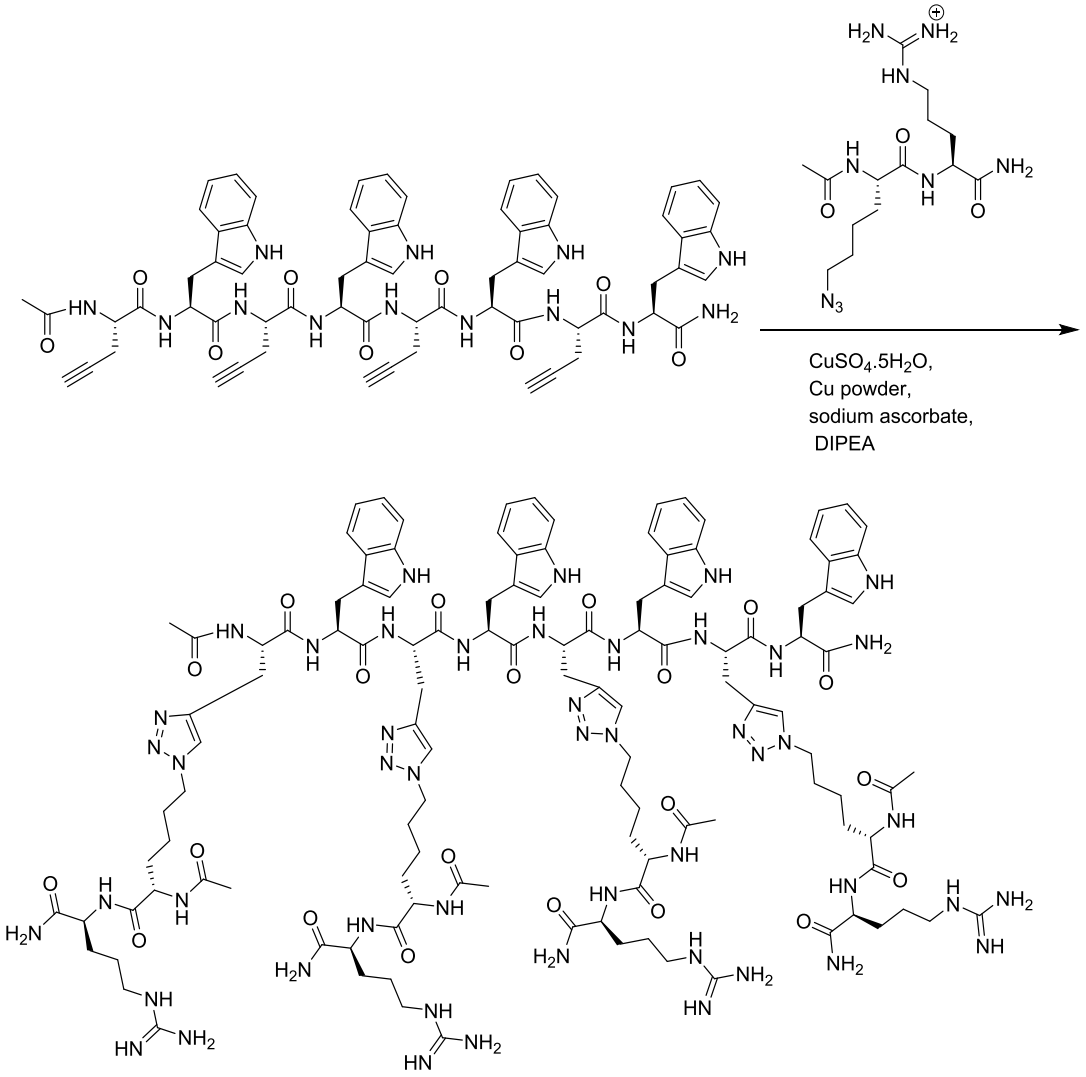

Linear-linear (WG(triazole-KR-NH_2))$_4$

Scheme 5.

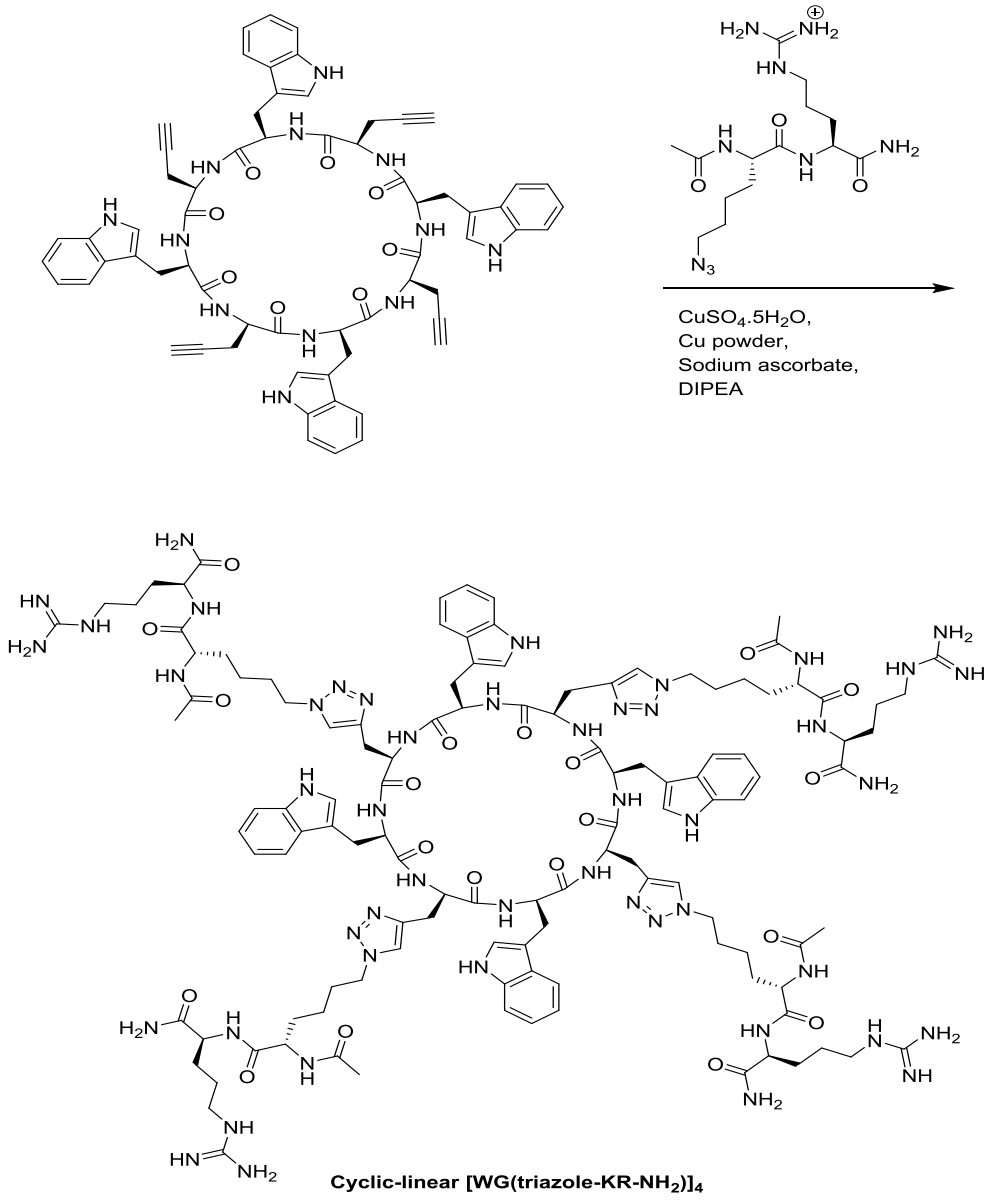
CuSO4.5H2O,
Cu powder,
Sodium ascorbate,
DIPEA
Cyclic-linear [WG(triazole-KR-NH2)]4

Scheme 6.

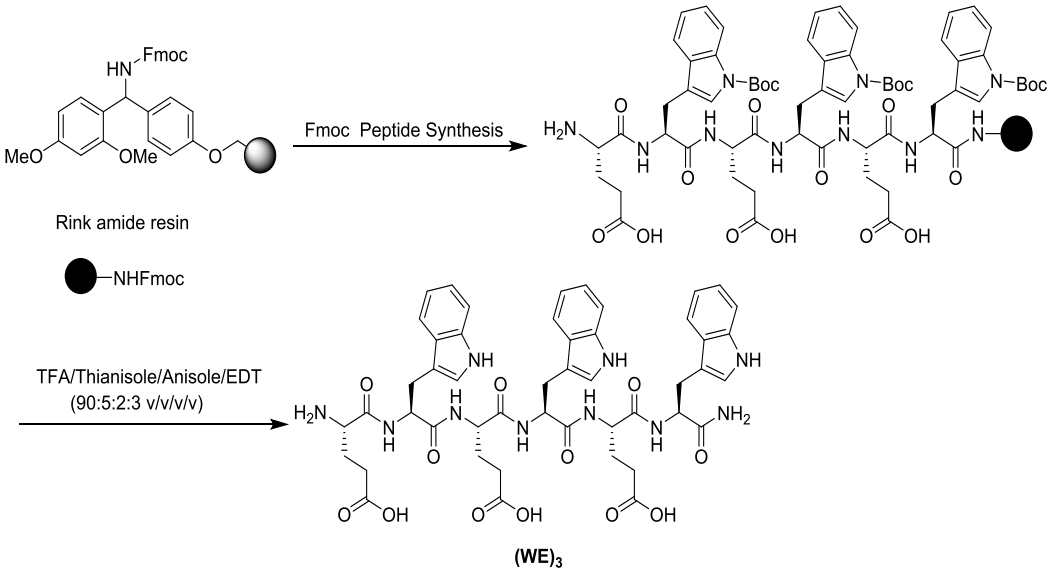
HN
Fmoc
MeO
OMe
O
Rink amide resin
NHFmoc
Fmoc Peptide Synthesis
N–Boc
TFA/Thianisole/Anisole/EDT
(90:5:2:3 v/v/v/v)
NH
H_2N
NH_2
OH
$(WE)_3$

Scheme 7.

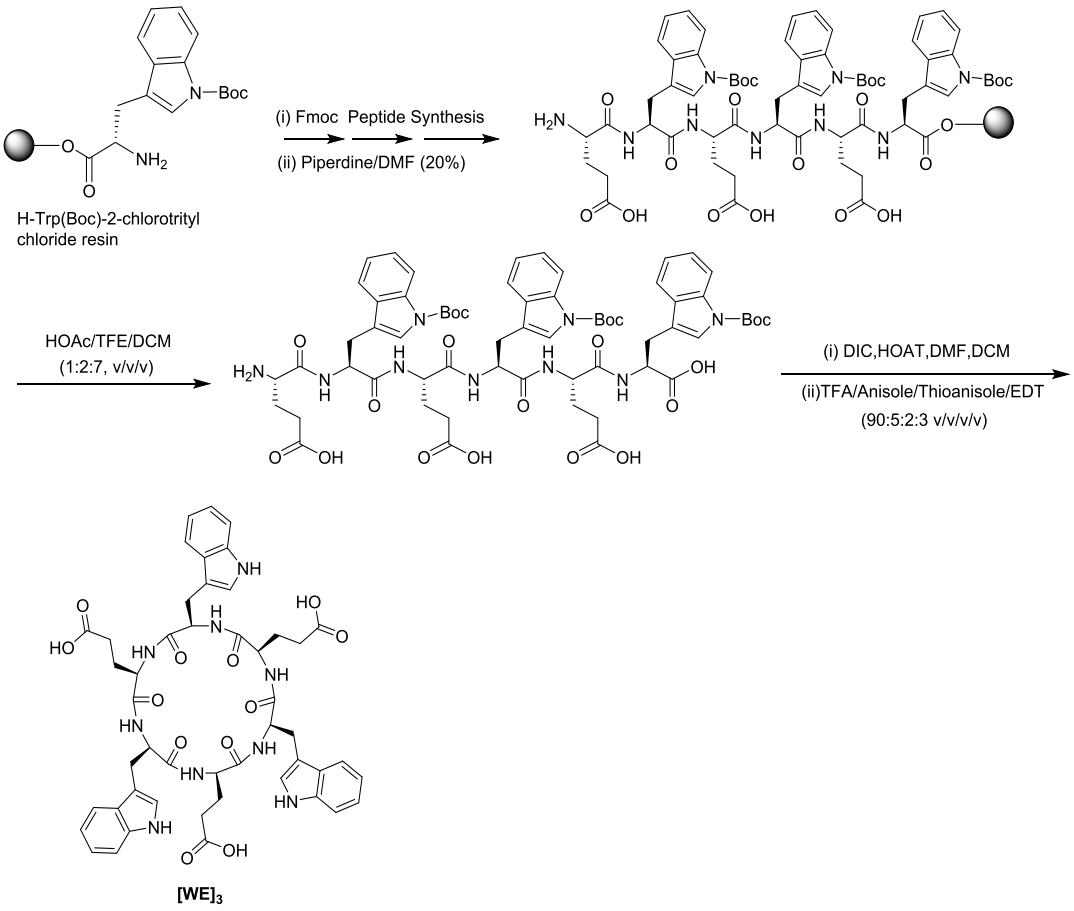
(i) Fmoc Peptide Synthesis
(ii) Piperdine/DMF (20%)
H-Trp(Boc)-2-chlorotrityl chloride resin
HOAc/TFE/DCM
(1:2:7, v/v/v)
(i) DIC,HOAT,DMF,DCM
(ii)TFA/Anisole/Thioanisole/EDT
(90:5:2:3 v/v/v/v)
[WE]3

Scheme 8.

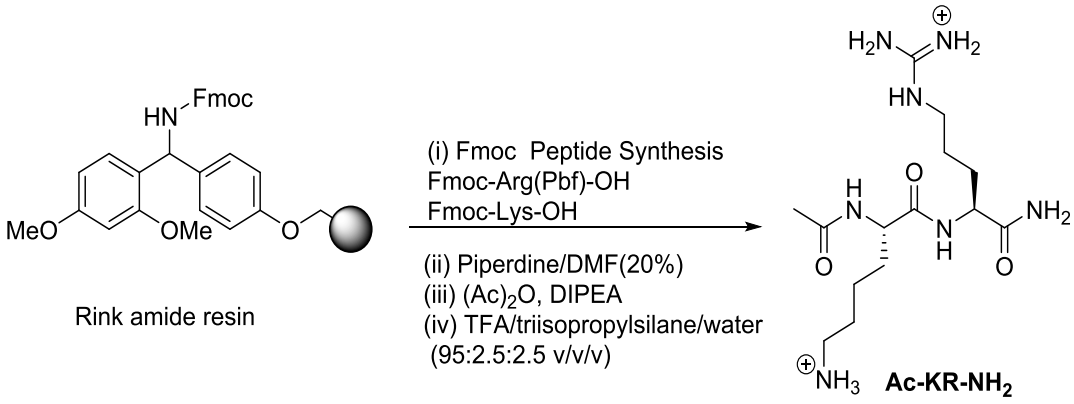
HN
Fmoc
MeO
OMe
O
Rink amide resin
(i) Fmoc Peptide Synthesis
Fmoc-Arg(Pbf)-OH
Fmoc-Lys-OH
(ii) Piperdine/DMF(20%)
(iii) (Ac)2O, DIPEA
(iv) TFA/triisopropylsilane/water
(95:2.5:2.5 v/v/v)
H2N
NH2
HN
H
N
O
N
H
NH2
O
O
NH3
Ac-KR-NH2

Scheme 9.

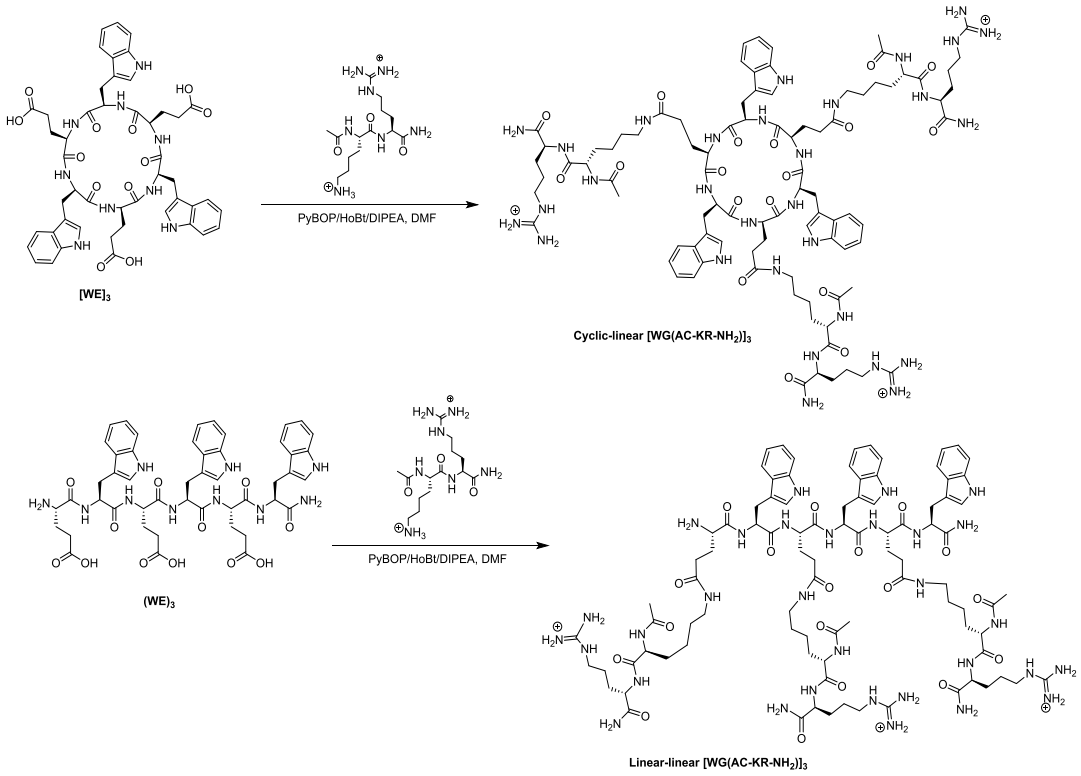
[WE]3
PyBOP/HoBt/DIPEA, DMF
Cyclic-linear [WG(AC-KR-NH2)]3
(WE)3
PyBOP/HoBt/DIPEA, DMF
Linear-linear [WG(AC-KR-NH2)]3

Scheme 10.

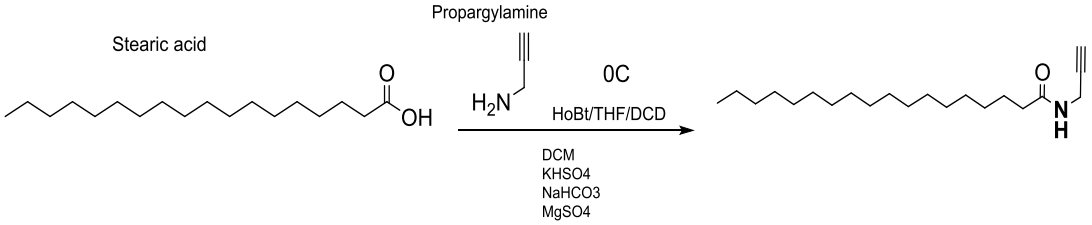
Propargylamine
Stearic acid
O
OH
H_2N
0C
HoBt/THF/DCD
DCM
KHSO4
NaHCO3
MgSO4
O
N
H

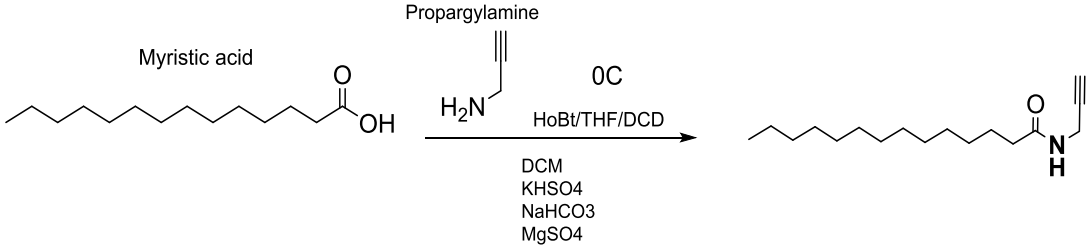
Propargylamine
Myristic acid
O
OH
H_2N
0C
HoBt/THF/DCD
DCM
KHSO4
NaHCO3
MgSO4
O
N
H

Scheme 11.

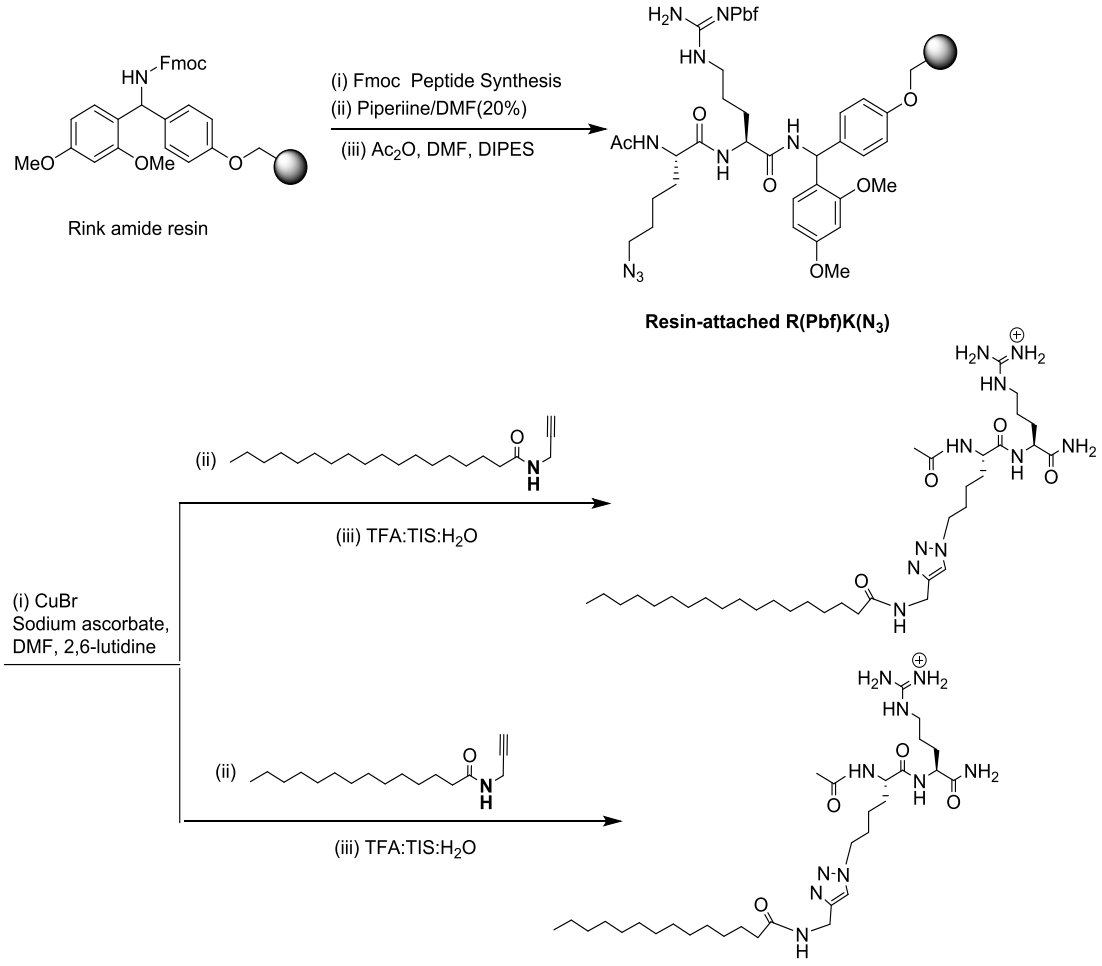
Fmoc
HN
MeO
OMe
O
Rink amide resin
(i) Fmoc Peptide Synthesis
(ii) Piperiine/DMF(20%)
(iii) Ac2O, DMF, DIPES
H2N
NPbf
HN
AcHN
N3
OMe
Resin-attached R(Pbf)K(N3)
(i) CuBr
Sodium ascorbate,
DMF, 2,6-lutidine
(ii)
(iii) TFA:TIS:H2O
(ii)
(iii) TFA:TIS:H2O